Gypsum efflorescence on clay brick masonry

Jacek CHWAST

Supervisors:
Prof. Dr. J. Elsen
Prof. Dr. Ir. H. Janssen

Members of the Examination Committee:
Dr. H. De Clercq (KIK-IRPA)
Prof. Dr. P. Degryse
Prof. Dr. Ph. Muchez
Prof. Dr. R. Swennen
Ir. H. Van Wijck (TCKI)
Ir. L. Vasseur (Wienerberger)

Dissertation presented in partial fulfilment of the requirements for the degree of Doctor of Science: Geology

June 2017

Acknowledgements

Abstract

Persistent efflorescence on ceramic brick masonry is on the rise, with progressively more buildings in Belgium being affected every year. This results in a growing number of consumer complaints, as the bricks fail to provide the desired appealing facade appearance. Even though persistent efflorescence has been observed for more than three decades, neither a method for its assessment nor a solution for the surface blemish is available. Those deficiencies stem from the limited understanding of its cause and mechanism, which puts brick manufacturers in an uneasy situation, as they are helpless in preventing this growing flaw. Consequently, persistent efflorescence is now perceived as a considerable threat for the ceramic brick industry.

Regardless of the alarming scale of the problem, little is known about the specifics of the Belgian cases. This motivated the first step of this project: a field survey wherein 28 affected constructions were subjected to a systematic on-site investigation. Facades exposed to wind-driven rain were most affected, demonstrating the critical role of moisture transfer in the efflorescence development. At the same time, the efflorescence affected bricks regardless of their moisture properties, thus showing their negligible impact. The mineralogical analysis of collected samples allowed establishing the composition of the persistent efflorescence – gypsum in most cases –, while the moisture influences indicated that its source was either a brick or mortar joint. The latter was the main departure point for the next step: a tailored experiment demonstrating gypsum formation upon cement paste carbonation. The obtained expertise formed the backbone for developing a fast and versatile test method, which allowed assessing the risk of efflorescence in a relatively short period of time. Its application to the masonry components combined with the field survey and cement carbonation studies shed light on the genesis of persistent gypsum efflorescence and indicated possible solutions.

The test results have confirmed the complex nature of gypsum efflorescence and the underlying processes leading to its formation. Gypsum under ordinary conditions exhibits an intrinsic propensity towards precipitation just below the surface, leading to pore clogging, hindering any further gypsum accumulation. This typically results in negligible intergrain efflorescence, and moreover, it appears to prevent the formation of other types of efflorescence. Gypsum accumulation at the surface can nevertheless be triggered by the presence of surfactant-based mortar admixtures, which modify the gypsum crystallisation behaviour. Their implementation in the test was manifested by a formation of abundant gypsum accumulation, reminiscent of the field survey cases. Moreover, their increased use on construction sites coincides with the reported onset of gypsum efflorescence cases, further proving their major role.

Both bricks and carbonated cement paste may contain considerable gypsum sources, in the form of anhydrite and gypsum, respectively. However, the tested brick types were deficient in anhydrite and did not yield abundant gypsum efflorescence, demonstrating that it is possible to limit the brick's contribution to the gypsum efflorescence risk considerably. The selected commercial cements yielded substantial gypsum source formation upon carbonation of prepared pastes, but they nevertheless solely produced slight efflorescence, owing to gypsum's subflorescing propensity. In contrast, a test applied to the binder fraction from a premixed mortar generated abundant efflorescence formation, proving that a mortar joint can contribute both as a gypsum source and through admixtures triggering gypsum accumulation on the surface.

The results of this research indicate that elimination of surfactant based admixtures may solve the gypsum efflorescence problem. It requires finding a substitute, and as an initial approach a single superplasticizer product was tested. The tested product yielded promising results in the benchmarking tests, but showed unsatisfactory results in combination with cement paste due to an interaction effect. It needs to be noted though, that superplasticizers cannot be considered as replacement for air-entraining agents, while a lack of the latter may result in insufficient freeze-thaw durability of hardened mortar. Regardless of the apparent complexity of the problem, the efflorescence free old masonry buildings demonstrate that this problem can be avoided, and this project provides the required tools and also sets the direction for achieving this goal.

List of minerals

α-quartz	SiO_2
AFm	$Ca_2(Al,Fe)(OH)_6X \cdot xH_2O$ X is an anion (Cl^-, OH^-, $0.5SO_4^{2-}$, $0.5CO_3^{2-}$, ...)
AFt	$Ca_6(Al,Fe)_2X_3(OH)_{12} \cdot 26H_2O$ X is a doubly charged anion (SO_4^{2-}, CO_3^{2-})
Alite M3	Ca_3SiO_5
Anhydrite	$CaSO_4$
Aragonite	$CaCO_3$
Belite β	Ca_2SiO_4
C3A orthorhombic	$Ca_3Al_2O_6$
Calcite	$CaCO_3$
Calcium langbeinite	$K_2Ca_2(SO_4)_3$
Ettringite	$3CaO \cdot Al_2O_3 \cdot 3CaSO_4 \cdot 32H_2O$
Ferrite	$Ca_2(Al,Fe)_2O_5$
Gypsum	$CaSO_4 \cdot 2H_2O$
Hemicarboaluminate	$Ca_4Al_2O_7(CO_2)_{0.5} \cdot 12H_2O$
Hemihydrate	$CaSO_4 \cdot 0.5H_2O$
Labile salt	$2Na_2SO_4 \cdot CaSO_4 \cdot 2H_2O$
Monocarboaluminate	$Ca_4Al_2O_7(CO_2) \cdot 11H_2O$
Monosulphate	$3CaO \cdot Al_2O_3 \cdot CaSO_4 \cdot 12H_2O$
Portlandite	$Ca(OH)_2$
Pyrite	FeS_2
Syngenite	$K_2Ca(SO_4)_2 \cdot H_2O$
Vaterite	$CaCO_3$
Zincite	ZnO

Abbreviations

A	surface area
A_{cap}	capillary absorption coefficient
a.u.	arbitrary unit
AICc	corrected Akaike information criterion
ANOVA	analysis of variance
ATM	accelerated test method
C3A	aluminate phase ($Ca_3Al_2O_6$)
CE	cumulative evaporation
CH	portlandite, lime ($Ca(OH)_2$)
CSH	calcium silicate hydrate phase ($CaO\text{-}SiO_2\text{-}H_2O$)
DR	drying rate
DTG	first TG derivative
GE	gypsum efflorescence
H	height
IA	non-normalized efflorescence coverage
ICP-OES	inductively coupled plasma–optical emission spectrometry
IRA	initial rate of absorption
LOI	loss on ignition
m	mass
mol%	molar percentage
NA	not analysed
OPC	ordinary Portland cement
PDF	powder diffraction file
QPA	quantitative phase analysis
RH	relative humidity
RSD	relative standard deviation
S	south
SCM	supplementary cementitious materials
SD	standard deviation
SEM-EDS	scanning electron microscope equipped with an energy dispersive X-ray detector

SW	southwest
t	time
TG	thermogravimetric analysis
W	west
w/c	water-cement ratio
w_{cap}	capillary water content
WD-XRF	wavelength-dispersive X-ray fluorescence spectrometry
WF	waalformat (brick format)
Wj(n)	weight fraction of the phase j after n-days
w_{sat}	vacuum water content
wt%	weight percentage
XRD	X-ray powder diffraction
ZAF	atomic number (Z), absorption (A) and fluorescence (F)
%E	normalized efflorescence coverage
Δm_{abs}	mass of water absorbed by a brick sample
Δm_{TS}	mass of water evaporated from a test solution
Δt_{abs}	duration of the wetting water wick
Δt_{wick}	duration of the total wick phase
ρ	density

x

Table of contents

1 Introduction and research objectives

1.1 Introduction

Over the last two decades Belgian ceramic brick masonry constructions are getting increasingly affected by persistent stains developing on their facades (Figure 1.1). These are referred to as efflorescence i.e. a mineral deposit accumulating on the surface of a porous material. Such efflorescence requires the presence of water, a mineral source, and drying conditions, where water plays the role of both the dissolution and the transport medium. The efflorescence formation is driven by the solution evaporating at the exposed surfaces, which induces salt precipitation as well as sustains the liquid transport. Masonry constructions definitely fulfil the conditions promoting efflorescence growth. Both brick and mortar joint are porous and contain water soluble mineral components. In bricks they originate from the clay mix, and they can additionally be generated upon their interaction with fumes during the firing process. The main soluble mineral source in mortars is the binder fraction, which nowadays is mostly Portland cement, produced from clinker, interground with calcium sulphate(s), and often mixed with industrial residues (such as fly ash). Water can be easily sourced from natural rainfall, and the walls are continuously exposed to the external conditions, which to varying degrees promote the drying process. The combination of these conditions is optimally met in spring, when wet walls are regularly exposed to mild drying conditions. This is reportedly often the first moment when the owners are surprised with the disappointing new appearance of their dwelling.

Figure 1.1 Belgian cases of persistent efflorescence

Efflorescence on masonry is not uncommon, as it is frequently found on newly erected constructions. However, this early efflorescence is of temporary nature, since it is composed of well soluble salts and washes off quickly with natural rainfall. In contrast, the above-mentioned recent cases of efflorescence concern persistent stains, developing only after a couple of years, which are moreover not removed by natural rainfall. Instead, once formed on the masonry surface, they stay and permanently spoil the facade appearance. Even though this problem relates solely to the aesthetic aspect of a construction, and does not pose any risk of damage to the material, it creates a considerable threat for the brick manufacturing industry. Nowadays clients pay more attention to the visual presentation of a building, and their choice of the facade product is often mainly conditioned by its appealing appearance. In Belgium, facing clay bricks are the most common material used in facades. Along with a growing number of complaints regarding the formation of such unsightly stains, the brick manufacturers are facing a perspective of losing their market share and thus a considerable drop in income. This type of persistent efflorescence develops predominantly on the brick surface, in most cases leaving the surrounding masonry joint untouched. For that reason the brick producers are being blamed for delivering a product of mediocre quality, and in some cases are even obliged to clean the facade, typically a costly measure.

While there is much literature available on efflorescence in general (MacGregor Miller and Melander, 2003), far less work has been expressly devoted to persistent efflorescence on masonry. The available reports address recent cases identified in the UK (Bowler and Winter, 1996; Bowler and Winter, 1997; Bowler and Sharp, 1998) and in the Netherlands (Brocken and Nijland, 2004), which appear to share the typical features of the Belgian cases. While these reports do shed some light on the mechanism of formation, at the same time they reveal the extraordinary complexity of the underlying processes, and consequently raise many unsolved research questions.

1.2 Research objectives and strategy

The Belgian brick manufacturers are in a critical situation, as the number of persistent efflorescence cases is growing in an alarming pace, calling for an urgent solution. The producers are helpless in preventing the problem, as there is no method available for predicting the performance of masonry components with respect to the risk of persistent efflorescence. This stems from a lack of understanding about the source, the cause and the mechanism of formation for this type of efflorescence. Besides this, more fundamental questions about the phenomenon, like the factors that favour and/or inhibit the development of this type of efflorescence, also remain unanswered. The main aims of this project are hence to reveal the mechanism of persistent efflorescence development and to develop an efficient and versatile test method capable of assessing the risk of its occurrence. This will consequently allow for optimizing the quality of masonry components and eliminating this problem in future. A first and necessary step, before addressing the above more specific research questions, is to gather general information on the characteristic appearance and composition of efflorescence in Belgian cases, as well as on the types of affected materials.

Indeed, persistent efflorescence in Belgium has not been addressed in a systematic investigation up till now. This problem was investigated in much more detail e.g. in the UK and the Netherlands, and a similar view emerges from the analysed cases therein. Persistent efflorescence is a recent phenomenon affecting constructions erected within approximately the last three decades, contrasting with the older spotless buildings. It is reported to develop with a delay of a few years, to exclusively affect the wind-driven rain exposed facades, and in most cases to be composed of gypsum and/or syngenite. This naturally raises the question whether the Belgian problem is of the same nature, and what is the cause for these specific characteristics.

The field survey established that gypsum ($CaSO_4 \cdot 2H_2O$) was found in most occurrences of persistent efflorescence, which brings up the question what gypsum sources are present in masonry, or whether it could have formed upon interaction with air pollution. Bricks may contain varying levels of anhydrite ($CaSO_4$), but according to the Belgian experience also bricks that are particularly deficient in calcium sulphate are found in constructions affected with gypsum efflorescence. This suggests that gypsum can be possibly derived from the mortar as well, e.g. through the addition of calcium sulphate(s) to control the setting of cement. Nevertheless, during the hydration of cement, these are typically turned into virtually insoluble ettringite and monosulphate phases. A hypothesis was proposed indicating that gypsum may be released back form mortar upon its carbonation (Brocken and Nijland, 2004). Several papers were published indicating that synthetic ettringite and monosulphate phases indeed decompose back to gypsum upon carbonation (Grounds *et al.*, 1988; Nishikawa *et al.*, 1992; Xiantuo *et al.*, 1994), and that this process can be possibly hindered (Pajares *et al.*, 2003). However, these phenomena have not been yet reported for complex cementitious materials. While these indicate that brick and mortar may possibly contain the sources of gypsum efflorescence, determining their actual contribution requires a method which allows establishing precisely the effect of the masonry component quality (e.g. the gypsum source content) on the risk of gypsum efflorescence. This could be potentially achieved by adapting the existing salt crystallisation test protocols. Commercially available bricks and cements contain varying levels of gypsum source(s), and such method could aid in identifying products which contribution to gypsum efflorescence is negligible.

However, even though gypsum efflorescence has been observed for more than three decades, neither a method for its assessment nor a solution for this deficiency is available. Salt crystallisation tests are widely applied to porous materials, but when adapted to gypsum efflorescence reproduction they often fail (Franke and Grabau, 1994), or take far too much time (Bowler and Winter, 1997). Calcium sulphate(s) are ubiquitous components of many natural and artificial building materials, including brick and anhydrous cement used for masonry mortar preparation. In the UK the efflorescence components could have been possibly derived from bricks, as these are often considerably rich in anhydrite. However, such bricks have been in use for more than a century without evidence of any surface blemish (Bowler and Fisher, 1989). This fact may possibly stem from the specific crystallisation behaviour of gypsum i.e. its tendency for a subsurface crystallisation (Franke and Grabau, 1994), but it has not yet been demonstrated on commercial hand moulded bricks. Bowler *et al.* (1997, 1998) linked the persistent efflorescence outbreak in the UK with the introduction of surfactant based mortar admixtures, and experimentally demonstrated that these substances may indeed trigger the formation of gypsum efflorescence. A wide range of mortar admixtures

is used on Belgian construction sites, however up to now these have not been evaluated as a possible gypsum efflorescence trigger, nor a substitute for them is available.

Addressing these research questions requires developing a versatile efflorescence test method, thus easily adaptable for testing (i) brick and cement as gypsum efflorescence (GE) sources, (ii) the effect of brick moisture properties and (iii) mortar admixtures as potential factors triggering this surface blemish. On top of this, such method should yield results within a reasonable period of time, to be considered for practical application.

This industrial PhD project was conceived as a cooperation between KU Leuven's Department of Earth and Environmental Sciences and the Belgian Brick Federation within the framework of a VLAIO Baekeland grant. It needs to be noted that at the start of this project there were many preconceptions in the brick industry regarding persistent efflorescence. While the Belgian persistent efflorescence cases had not been yet investigated, these were suspected to be composed of gypsum as the industry was aware of similar Dutch cases (Brocken and Nijland, 2004). It was questioned though whether gypsum efflorescence can be formed upon gypsum dissolution, transport and precipitation, because of its very low solubility (as compared to alkali sulphates which commonly form early efflorescence). Instead, air pollution and wall insulation were often suspected for triggering this surface blemish. The impact of mortar admixtures was generally neglected, since these are added at very low levels to masonry mortars and their influence is not evident. Masonry mortar was suspected as a potential efflorescence source, since persistent efflorescence affected also masonry constructed of bricks which were characterised by exceptionally low content of water soluble sulphates.

The main emerging research questions and aims can be summarised as follows:

1. **GE characteristics, mechanism and sources**
   1.1. *What is the composition of persistent efflorescence in Belgium? What are its characteristic features and how do they relate to the British and Dutch cases?*
   1.2. *Are the GE components derived from internal or external sources?*
2. **Aim: development of a fast and versatile efflorescence test method**
3. **GE genesis**
   3.1. *Why did GE not occur before 80-90's and what triggered its formation later on?*
4. **GE risk**
   4.1. *Can brick provide a sufficient amount of the GE source?*
   4.2. *Can mortar provide a sufficient amount of the GE source?*
   4.3. *Is it possible to limit the brick contribution to the GE risk by limiting its GE source?*
   4.4. *Is it possible to limit the brick contribution to the GE risk by optimizing its moisture properties?*
   4.5. *Is it possible to limit the mortar contribution to the GE risk by reducing the calcium sulphate(s) addition to cement?*
   4.6. *Is it possible to limit the mortar contribution to the GE risk by inhibiting gypsum formation in a cement paste?*
   4.7. *Is it possible to limit the GE risk by eliminating the surfactant-based mortar admixtures?*

The research questions are addressed in four dedicated studies. First, Belgian constructions affected by persistent efflorescence were thoroughly analysed. Secondly, gypsum formation upon cement carbonation was investigated experimentally. Thirdly, an accelerated test method allowing for fast and versatile gypsum efflorescence risk assessment was gradually developed. Finally, the developed method was applied to evaluate the contribution of brick, cement and mortar admixtures to the gypsum efflorescence risk.

Field survey

Selected cases of persistent efflorescence in Belgium were investigated on-site. Efflorescence was sampled and subjected to a qualitative X-ray powder diffraction (XRD) analysis to reveal its composition. The constructions were carefully examined and documented with photographs. When possible the owners were interviewed and in many cases this yielded information on the age of construction, the onset of the efflorescence and the brick type used for construction.

Experimental cement paste carbonation

The hypothesis of gypsum formation upon ettringite and monosulphate decomposition in cement paste was investigated by monitoring phase development and water soluble sulphate evolution upon its carbonation. The former was realised with quantitative phase analysis (QPA) and thermogravimetric analysis (TG), while the latter was implemented by a leaching experiment followed by leachate analysis with inductively coupled plasma–optical emission spectrometry (ICP-OES). The carbonation process was accelerated by reducing the size of hardened cement paste to a powder and by ensuring optimal carbonation conditions. Moreover, a simple dissolution monitoring experiment was designed to demonstrate gypsum formation and to quantify its amount.

Accelerated gypsum efflorescence

The efflorescence test method was developed based on a basic wick test setup, where a brick core sample (transport medium) stays in continuous contact with a test solution containing the source of efflorescence (e.g. brick or carbonated cement sample). However, the preliminary efflorescence test setup suffered from numerous flaws and was progressively improved, what included (i) a selection of an inert adhesive, (ii) leaching brick core samples, (iii) optimisation of test conditions (temperature and relative humidity), (iv) implementation of frequent wetting phases, (v) setting up a procedure for collecting high quality efflorescence photographs and efflorescence quantification, (vi) investigating the effect of brick surface quality, and (vii) setting up a protocol for analysis of efflorescence composition (XRD and HCl test).

Gypsum efflorescence factors

Application of the developed efflorescence test procedure to masonry components required adapting it separately to each independent variation addressed to assessing (i) the effect of brick moisture properties, (ii) brick and carbonated cement paste as GE sources, and (iii) the effect of mortar admixtures. As the tests were realised on small brick cores, for each test setup the amount of tested sample was calculated to reflect the ratio of components in an actual masonry wall. In case of cement evaluation, a cement paste was prepared and carbonated based on the developed accelerated carbonation protocol.

1.3 Manuscript outline

The thesis is subdivided into nine chapters and starts with introduction (Chapter 1). Chapter 2 presents the state of the art and provides the context for the gypsum efflorescence problem. The methods used throughout this project are described in detail in Chapter 3. Chapter 4 focuses on the on-site investigations carried out during the field survey, and on the analysis of the Belgian persistent efflorescence cases. The hypothesis of gypsum formation upon cement carbonation is experimentally assessed in Chapter 5, which also discusses possibilities of limiting contribution of cement towards the risk of gypsum efflorescence formation. Chapter 6 explains how the efflorescence test method was designed, illustrating each improvement with a set of experimental results, and gives first insights on the genesis of gypsum efflorescence. The latter is addressed in more detail in Chapter 7, where the developed efflorescence test method is applied to evaluation of masonry components, i.e. brick, cement and mortar admixtures. The thesis is summarised in the conclusions (Chapter 8) followed by appendices (Chapter 9).

2 State of the art

2.1 Introduction

While the literature specifically dedicated to gypsum efflorescence is relatively limited, there are a number of studies from various other fields which can enhance the understanding of the underlying processes. These primarily relate to calcium sulphate sources, transport and crystallisation. This background knowledge allows interpreting the field survey observations, which is crucial in defining a strategy for the subsequent chapters (each addressing a dedicated study). Gypsum efflorescence cases have been reported before on masonry in the UK and Netherlands (Section 2.2). Both masonry components can contain gypsum sources: anhydrite is not an uncommon component of ceramic bricks (Section 2.3.1), while there is a hypothesis suggesting gypsum formation upon mortar joint carbonation (Section 2.3.2). Apart from the presence of internal calcium sulphate sources, gypsum efflorescence necessitates their transport. Sections 2.4 and 2.5 corroborate the possibilities for dissolution of calcium sulphate in masonry and its crystallisation at the surface in the form of gypsum. However, the available knowledge indicates that gypsum exhibits a propensity for subsurface accumulation, and the factors which lead to the recent cases of gypsum efflorescence remain unexplained. As its occurrence is restricted in Belgium to the last two decades only, contrasting thus with the older unaffected buildings, the recent changes in brick (Section 2.6.1) and mortar composition (Section 2.6.2), and also in the use of wall insulation (Section 2.6.3) are analysed. The main aim of this research project is to develop a fast and versatile efflorescence test method, which can be designed by adapting the existing protocols (Section 2.7.1). Even though the impregnation and drying test (Bowler and Winter, 1997) reproduced gypsum efflorescence formation, it suffered from many flaws, and particularly from a long duration (Section 2.7.2). Section 2.8 discusses on how its shortcomings can be addressed and solved with the wick test protocol, while the chapter is summarised in Section 2.9.

2.2 Reported cases of gypsum efflorescence on masonry

Bowler and Winter (1996) were the first to communicate on a new type of efflorescence occurring in the UK. The persistent deposits were observed between 1985 and 1995, exclusively on recently built houses, constructed only down to 1980. Older brickwork, on the other hand, was free from such staining. The affected buildings were found in different locations spread over the UK. Various brick types were involved, ranging from bricks with very low salt content to the bricks of the Fletton type, typically containing 3.4 wt% of calcium sulphate in its least active form – anhydrite. Interestingly, some brick types traditionally used for more than 100 years with no history of such staining were also affected. Most manufacturers observed the same problem with their products. The mortars used for construction covered various mortar formulations and cement types. Many of the reported houses had insulated cavity walls.

White or greyish deposits developed on the façade side exposed to the action of wind-driven rain, typically facing the south-west direction. These stains were mostly very thin and invisible when masonry was wet, but occasionally also some encrustation was found. They proved to be very persistent, and instead of being washed away with natural weathering, as for primary efflorescence, they often exacerbated with time. The discoloration often became apparent only after two years or more after construction, whereas some cases were reported already after a few months. Samples of the deposits were analysed with X-ray powder diffraction methods, which revealed that the main component was gypsum, syngenite, or both. Very often efflorescence was found not only on bricks but also on mortar joints, which were moreover surrounded with white halo staining, indicating transport of soluble salts from the mortar joint to the brick.

Persistent efflorescence occurrence was also reported in the Netherlands (Brocken and Nijland, 2004). The cases were very similar to those reported in the UK, exhibiting almost all their characteristics. These permanent deposits were found as well on the external leaf of an insulated masonry wall. A specific delay in development was also observed, ranging from several months to a couple of years, and the discoloration was becoming more intense with time. On the other hand, no white 'halo' surrounding the mortar joint was noticed and only gypsum and no syngenite was identified in the deposits.

2.3 Calcium sulphate sources

Calcium sulphate occurs in three distinct mineral forms: gypsum, bassanite and anhydrite, which are respectively the dihydrate ($CaSO_4 \cdot 2H_2O$), hemihydrate ($CaSO_4 \cdot 0.5H_2O$) and anhydrous ($CaSO_4$) forms. Both gypsum and anhydrite can be present in masonry, and it is hence important to distinguish between these two mineral forms. Under normal conditions gypsum is the stable calcium sulphate mineral form, explaining its presence in efflorescence. The conversion to anhydrite occurs at temperatures above 350°C (Kuntze, 2008).

2.3.1 Brick as a calcium sulphate source

Calcium sulphate in ceramic bricks may originate from the initial calcium sulphate in the clay mix, or may stem from high-temperature reactions taking place during brick firing. In the former case the calcium sulphate persists during firing, since the typical brick firing temperatures of 900–1050°C are below the calcium sulphate decomposition temperature of 1200–1300°C. In the latter case it is formed due to the reaction between calcium, bound as carbonate or more reactive oxide, with sulphates, formed by sulphide oxidation (e.g. pyrite decomposition) or directly available from the flue gasses (Vogt and Tatarin, 2013). Independent of the reaction path, the final calcium sulphate mineral form present in the ceramic brick is anhydrite, given the high firing temperatures.

2.3.2 Mortar as a calcium sulphate source

Calcium sulphate is present in Portland cement, where it primarily reacts with tricalcium aluminate (C3A) (to control the setting properties). The calcium sulphate and C3A interaction occurs in two stages: initially ettringite is formed, which then further reacts to monosulphate. Originally, such added calcium sulphate was not considered as an efflorescence trigger, because ettringite and monosulphate are virtually insoluble (MacGregor Miller and Melander, 2003). Synthetic ettringite does however undergo carbonation when exposed to CO_2, decomposing back to gypsum and other minerals (Grounds *et al.*, 1988). Monosulphate is even less stable than ettringite, and hence more prone to decomposition (Gabrisová *et al.*, 1991). Carbonated mortar is therefore a potential source of calcium sulphate, a hypothesis initially proposed by Brocken and Nijland (2004), but actual gypsum formation upon mortar carbonation has not been yet demonstrated.

The chemistry of cement

The usual commercial cements are composed of cement clinker interground with calcium sulphate(s), and optionally blended with supplementary cementitious materials (SCM). A cement composed of the former two ingredients is called an ordinary Portland cement (OPC). The SCMs are mineral additives, the most common being fly ash, blastfurnace slag, natural pozzolanas and limestone. The three former components exhibit pozzolanic activity.

Portland cement clinker is composed of four main mineral phases (names are provided in cement chemist notation): alite (tricalcium silicate $3CaO \cdot SiO_2$), belite (dicalcium silicate $2CaO \cdot SiO_2$), aluminate (tricalcium aluminate $3CaO \cdot Al_2O_3$) and ferrite (tetracalcium alumino ferrite $4CaO \cdot Al_2O_3 \cdot Fe_2O_3$). We will refer to the latter two as aluminate phases. All four components react with water, upon which the cement paste sets and hardens. Alite and belite hydrate to semi-amorphous calcium-silicate hydrate (CSH) and calcium hydroxide (CH). The latter can be partially consumed in reaction with SCMs exhibiting pozzolanic activity (Snellings *et al.*, 2012). Aluminate is the most reactive cement phase, and its hydration needs to be controlled by addition of calcium sulphate(s). Ferrite is less reactive, but it follows similar reaction paths as aluminate. In presence of calcium sulphate(s), hydration of aluminates leads to the formation of AFt (Al_2O_3-Fe_2O_3-tri) and AFm (Al_2O_3-Fe_2O_3-mono) phases, where the most common members are ettringite and monosulphate, respectively.

The hydrated cementitious material is exposed to external conditions during the construction's service life, during which it progressively reacts with CO_2 from air. The most sensitive phase is CH which carbonates to calcium carbonate. At later stages of carbonation CSH decomposes to i.a. silica gel, while ettringite and monosulphate convert to i.a. gypsum.

Calcium sulphate(s) addition

The role of calcium sulphate(s) addition to cement is covered in the book of Taylor (1997). It plays an important role during cement hydration and its content needs to be optimised in order to achieve desirable material properties. It affects the setting time, strength development and volume stability. Optimising each property may require different additions of calcium sulphate(s), and the optimal content varies also for different materials: cement paste, mortar or concrete. Adding too little calcium sulphate(s) yields rapid stiffening called a 'flash set', which induces irreversible poor strength development and shortens the workability period. Calcium sulphate(s) addition is governed by the amount, reactivity and availability of the aluminate phases, but also the reactivity of calcium sulphate, the latter being mainly controlled by choosing the proper proportions of calcium sulphate species (anhydrite, hemihydrate, and gypsum). Moreover, both calcium and sulphate ions can be also supplied from the clinker phases or from deliberate addition of alkali sulphate(s) or calcium langbeinite, what may reduce the required calcium sulphate(s) addition.

Carbonation effect on pore solution

The major products of ordinary Portland cement hydration are CH (20-25 wt%) and CSH (60-70 wt%) (Spence, 1992). Dissolution of CH controls the chemistry of pore water by its buffering capacity (Garrabrants et al., 2004), as its content is far higher than needed to saturate the pore solution (Anstice, 2000). Saturated solution of CH yields a pH of 12.45 at 25°C (Taylor, 1997). However, carbonation of cement paste progressively removes CH, leading eventually to a drop of the pore solution's pH to a level as low as 7-8 (Anstice et al., 2005; Šavija and Luković, 2016).

Ettringite formation and stability

The reaction of aluminate with calcium sulphate(s) occurs in two stages: initially ettringite ($3CaO \cdot Al_2O_3 \cdot 3CaSO_4 \cdot 32H_2O$) is formed, which then reacts further with aluminate and transforms to monosulphate ($3CaO \cdot Al_2O_3 \cdot CaSO_4 \cdot 12H_2O$). Their extent depends on the ratio of calcium sulphate(s) to aluminate (Taylor, 1997), while the presence of calcium carbonate hampers the transformation to monosulphate (Kuzel and Pöllmann, 1991). While both phases are virtually insoluble, synthetic ettringite decomposes upon carbonation (Nishikawa et al., 1992; Xiantuo et al., 1994; Grounds et al., 1988):

$3CaO \cdot Al_2O_3 \cdot 3CaSO_4 \cdot 32H_2O$ (ettringite) + $3CO_2$ →

→ $3(CaSO_4 \cdot 2H_2O)$ (gypsum) + $3CaCO_3$ + $Al_2O_3 \cdot xH_2O$ (alumina gel) + $(26-x)H_2O$ (Equation 1.1)
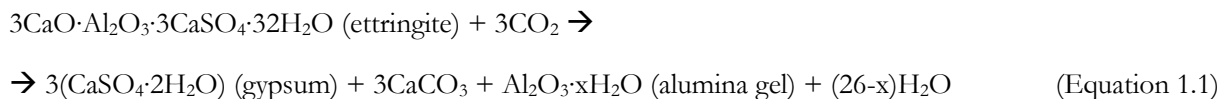
However, a high pH stabilises ettringite - synthetic ettringite stays stable above a pH of 10.7 (Myneni et al., 1998) - while monosulphate already decomposes below a pH of 11.6 (Gabrisová et al., 1991). Fresh cement paste provides a high pH of 13-14 (Taylor, 1997). Since CH mainly contributes to the high pH of the pore solution, its content in the cement phase determines the ettringite and monosulphate stability. This effect has been demonstrated for ettringite formed upon cement hydration in mortar (Brocken et al., 2000) as well as for the synthetic mineral (Pajares et al., 2003). Nevertheless, CH is consumed upon carbonation leading to a pH drop below the stability threshold of ettringite and monosulphate. This also finds confirmation in a study on cement paste carbonation (Anstice et al., 2005), where a considerable increase in water soluble sulphate was found only for samples where the pore solution's pH had dropped below 10.7. An increase of water soluble sulphate was also reported upon cementitious mortar carbonation (Brocken and Nijland, 2004; Kraus and Droll, 2009). It indicates gypsum formation upon ettringite and monosulphate decomposition as already reported for synthetic phases (Grounds et al., 1988; Nishikawa et al., 1992), but nevertheless this has not been yet demonstrated for complex cementitious materials.

2.4 Solubility and dissolution of calcium sulphate

Contrary to other salts typically present in masonry, gypsum is soluble at 0.015 mol/kg at 25°C, which furthermore varies only minimally in the temperature range 0–25°C. The solubility of anhydrite, on the other hand, is somewhat higher at 0.019 mol/kg at 25°C, decreasing strongly with increasing temperature. In relation to dissolution, however, the reverse holds: in identical conditions, the dissolution rate of

anhydrite is roughly two orders of magnitude smaller than the dissolution rate of gypsum (Jeschke and Dreybrodt, 2002).

The presence of other solutes significantly alters the solubilities of gypsum and anhydrite: unlike ions (not related to gypsum e.g. Na^+, K^+, Cl^-) may increase it up to four times, whereas like ions (related to gypsum: Ca^{2+} and SO_4^{2-}) decrease it (Charola et al., 2006). While the dissolution of anhydrite, and its hydration to gypsum, is kinetically hindered, it does accelerate in the presence of specific salts (Freyer and Voigt, 2003). The most effective hydration accelerators are alkali sulphates, which convert anhydrite to gypsum via an intermediate step of the double salt formation process (e.g. syngenite $K_2Ca(SO_4)_2 \cdot H_2O$ or labile salt $2Na_2SO_4 \cdot CaSO_4 \cdot 2H_2O$) (Conley and Bundy, 1958; Singh, 2005). The dissolved calcium sulphate is then transported by diffusion (movements of ions within the solution) and advection (bulk transport of solution), like any other salt. For exposed facade orientations the yearly wind-driven-rain load can go up to 100's of litres per square meter (Janssen et al., 2007), providing sufficient 'solution' to allow for continuous diffusion and advection throughout the depth of the outer brick leaf.

2.5 Calcium sulphate crystallisation

Calcium sulphate exhibits somewhat particular crystallisation behaviour. Typically, the location of salt crystallisation in a porous material is determined by the location of the drying front: drying at the surface is stated to result in crystallisation at the surface (efflorescence), while a drying front below the surface is said to lead to crystallisation within the material (subflorescence). This would lead one to expect that the same experimental conditions should result in the same crystallisation locations for different salts. The inverse is often observed in actual salt damage cases though, and this observation is further upheld by laboratory experiments demonstrating salt-specific crystallisation behaviour under well-defined laboratory conditions. For instance, Cardell et al. (2008) reported that efflorescence develops on limestone samples immersed in various salts solutions and their mixtures, but not for the gypsum solution for which only a limited subflorescence was identified. Based on field measurements, Charola et al. (2006) similarly concluded that gypsum tends to accumulate just below the surface for non-calcareous materials. Gypsum accumulation under the surface and resulting pore clogging are also currently addressed in computer simulation studies, which may shed more light in future on the underlying physico-chemical mechanisms (Todorović and Janssen, 2014, 2015).

2.6 Recent changes in masonry materials

Up to this point, the available knowledge offers some first insights into the physico-chemical processes underlying gypsum efflorescence. A first and the most important blow to the argumentation formulated above is that both the sources and the transports have been active in ceramic-brick-and-Portland-cement-based masonry since its original application, which does not allow explaining the only recent occurrence of gypsum efflorescence. Moreover, the tendency of gypsum to crystallise under the surface further impairs the aforementioned reasoning chain. The general validity of the latter can however be questioned, due to limited data. Gypsum efflorescence has sprung up during the last three decades, what apparently coincides with a number of major changes in material composition and construction technology. These mainly concern the chemical composition of cements and the use of mortar admixtures. This section therefore investigates the recent changes in masonry components and construction technology, to shed further light on the cause of this problem.

2.6.1 Brick composition evolution

To the authors' knowledge, the brick production technology in Belgium (and Europe) has not experienced significant changes over the last few decades. Bowler and Winter (1996) do indeed state a similar remark in relation to the UK. They verify this observation with an example of old and new constructions applying brick types that have been in use for over 100 years. Only the recent constructions are affected by gypsum efflorescence, while the older constructions do not suffer from such staining.

2.6.2 Mortar composition evolution

Masonry mortar composition, on the other hand, has evolved substantially over the last three decades, both in Belgium and in the UK. These changes mostly relate to the quality of binder and to the use of admixtures. In the UK cement/lime mortars have been gradually replaced by cement/air entrainer mixes. The presence of lime delays ettringite carbonation (Brocken et al., 2000; Pajares et al., 2003), and such shift

to cement only-based mortars might therefore facilitate the release of sulphate due to mortar carbonation. In Belgium, cement-based mortar came into use in the 1950's owing to the availability of very fine sand ('papzand') which was sufficient to provide the desired workability to the mortar mix. Its application did however lead to frost damage, whereto the introduction of plasticizers and air entrainers came as a solution, by allowing for using coarser sand types. Consequently the cement mortars containing admixtures are preferred by masons nowadays (Hendrickx, 2009).

Cement composition

Bowler and Winter (1996) provide a thorough analysis of the more recent changes in the British cement industry. They conclude that the changes in fuel composition and production technology may lead to increased levels of sulphate in cement clinker. Nevertheless, the sulphate content is limited by national standards, and an analysis of their recent changes can benefit the evaluation. Bowler and Winter (1996) state that the sulphate level limits increased from 3% to 3.5% in the UK. It was accompanied by reducing and finally removing constraints for the C3A content. They hypothesize that, all in all, these changes might have led to a higher availability of sulphate in fresh mortar, which in turn could potentially be absorbed by bricks, to finally crystallise as the persistent efflorescence. To the knowledge of the author, the sulphate limits in Belgium in the last three decades have been fluctuating between 3.5% and 4.5%, with no constraints on the C3A content for ordinary cements. A more recent trend is the addition of fly ash to Portland cement. Its presence results in faster and deeper carbonation, due to a lower content of portlandite, and formation of more carbonation-prone hydrates (McPolin *et al.*, 2009).

Use of admixtures

Ettringite and monosulphate decomposition cannot solely explain the recent occurrences of gypsum efflorescence in Belgium. Both cement hydrates have been present in masonry mortars as long as cement has been used for their preparation, and in the case of Belgium pure cement mortars have been commonly used since the 1950's. Bowler and Winter (1996) thus considered the use of admixtures as one of the potential triggers for gypsum efflorescence. Gypsum efflorescence started to occur from the 1980's onwards, which according to them coincides with the introduction of surfactant-based mortar admixtures, such as dedicated air entrainer and plasticizer products but also simple domestic detergents (Bowler and Winter, 1996, 1997). Butterworth reported already in 1957 though that air-entraining agents were frequently used in the UK, criticising the use of domestic detergents. In Belgium the first reports of GE stem from the 1990's, while industrial plasticizers and air entrainers were introduced in respectively the 1970's and 1980's already. The use of mortar admixtures in Belgium is nowadays well appreciated, which sometimes leads to the use of non-officially certified products, dosed according to the user's experience (Hendrickx, 2009).

Bowler and Winter (1997) conducted a series of wetting–drying tests on individual Fletton bricks to examine the influence of admixtures on gypsum efflorescence, including aqueous solutions of air entrainers and washing-up liquids. They noted that persistent efflorescence occurred only on the admixture-treated samples, contrasting with the unaffected reference samples. Since the bricks were known to contain elevated levels of anhydrite and the used substances did not contain soluble salts, they concluded that gypsum must have been derived from the bricks only. Similar results were obtained from experiments on masonry bins exposed to natural weathering for several years (Bowler and Sharp, 1998). Bowler's experiments actually demonstrate that even anhydrite, being often considered as immobile and thus inert, can be activated as the source of gypsum efflorescence by admixtures. This generally confirms the experience of the British brick industry, as before 1980s no cases of persistent efflorescence were reported even though bricks with high anhydrite content were commonly used (Butterworth, 1957; Bowler and Fisher, 1989). The composition of the tested admixtures was based on surfactants, which can influence the formation of efflorescence in a number of ways. Bowler and Winter (1997) explained their observations through the surfactants effect on the pore solution mobility. Surfactants accumulate at the liquid–gas interface, modifying the wettability by reducing the liquid-stone contact angle, in turn enhancing liquid capillary transport and hence efflorescence formation (Rodriguez-Navarro *et al.*, 2000). Surfactants can also modify gypsum crystal growth, due to the preferential adsorption on crystal faces (Badens *et al.*, 1999). Finally, one can also reason that the Bowler and Winter (1997) experiments indicate

an effect of surfactants on the dissolution and solubility of anhydrite in brick. The application of admixtures might therefore possibly explain the recent occurrence of gypsum efflorescence.

2.6.3 Use of insulation

Besides these internal changes in material composition and production, over the last few decades, modifications in the wall composition form an important external change. As reported by Bowler and Sharp (1998), the use of thermal insulation inside the cavity of masonry walls has significantly increased. It is assumed that walls become colder and wetter, hence potentially enhancing the risk of gypsum efflorescence. On the other hand, gypsum efflorescence was found on both insulated and non-insulated cavity walls. The ways in which insulation may affect gypsum efflorescence, via impacts on the gypsum formation, transport and/or crystallization, remain unknown.

2.7 Efflorescence test methods

Efflorescence formation requires fulfilling four conditions simultaneously, which are: presence of (i) an efflorescence source, (ii) a porous transport medium, (iii) water, and (iv) drying. The efflorescence source is a water soluble compound which can supply ion components of efflorescence salts. In masonry, the brick and mortar play the role of being both the efflorescence source and porous transport medium. However, it is commonly observed that efflorescence affects mostly the brick's surface. Water presence is necessary, as it serves as the medium allowing for salt dissolution, transport and precipitation. The latter two are induced by water evaporation at the surface, a process which is highly dependent on the drying conditions. Water is primarily supplied by rainfall, while the drying conditions are governed by temperature, humidity, and air speed at the masonry surface.

2.7.1 Salt crystallisation tests

The common tests used for simulating salts crystallisation in porous materials are mostly realised by providing a test solution to a porous material and exposing it to drying conditions. The test solution can be supplied to a porous material in two ways: either by its impregnation, or by continuous immersion in a test solution (wick test) (Steiger and Asmussen, 2008). In the former case, the sample is often subjected to additional cycles of impregnation and drying. Both types of tests have been widely applied in research on salt crystallisation (Scherer, 2004; Steiger and Asmussen, 2008) as well as specifically for assessing the tendency towards efflorescence. The impregnation and drying protocol was prescribed by British normatives, while the wick test by the US and Russian standards (Chin and Behie, 2010).

Impregnation and drying test applied to GE

Bowler and Winter (1997) applied an impregnation and drying test based on a British normative (Chin and Behie, 2010), where a brick impregnated with water was sealed from all sides with the exception of the stretcher, to dry under room conditions. Each brick was subjected to several cycles of drying and water impregnation, for a duration of one year at least. The effect of admixtures was investigated by adding them to the water used for the first impregnation episode. In parallel, field tests were realised on masonry wallettes, but these took more than 2.5 years, and required much space and labour (Bowler and Winter, 1997; Bowler and Sharp, 1998).

Wick test applied to GE

The wick test setup (Figure 2.1) is based on an experimental concept wherein a porous transport medium (here a brick sample) stays in contact with a test solution. The exemplary setup consists of a container closed with a lid, the latter is perforated and sealed with the brick sample by an adhesive. During the test, the medium is uninterruptedly impregnated with the test solution, while evaporation takes place only over the exposed medium's surfaces, promoting continuous efflorescence formation. Wick test variations have been widely applied to the research of damage upon salt crystallisation (Goudie, 1986; Rodriguez-Navarro and Doehne, 1999; Scherer, 2004; Steiger and Asmussen, 2008) and efflorescence formation (ASTM C67-07, 2007; Sanders and Brosnan, 2010; Eloukabi *et al.*, 2013).

Franke and Grabau (1994, 1998) have applied a wick test setup to study gypsum crystallisation on a historic brick sample. In their study, the container served as a reservoir of water or efflorescence source in form of a salt solution. This approach solved a shortcoming of Bowler and Winter's (1997) setup, as it

allowed for separating the transport medium from the efflorescence source. Besides applying it to a salt solution, the wick test design can be also conveniently adjusted for testing solid efflorescence sources. Sanders and Brosnan (2010) used a similar test setup as Franke and Grabau (1994, 1998), but applied it for evaluating bedding materials as potential efflorescence sources on paver bricks. Crushed bedding material topped up with water served as the test solution, while a paver brick staying in touch with the test solution played a role of the transport medium. The latter did not yield efflorescence when tested alone and hence did not interfere with the test result. The leached salts accumulated on the brick sample surface, indicating the propensity towards efflorescence of the tested bedding material.
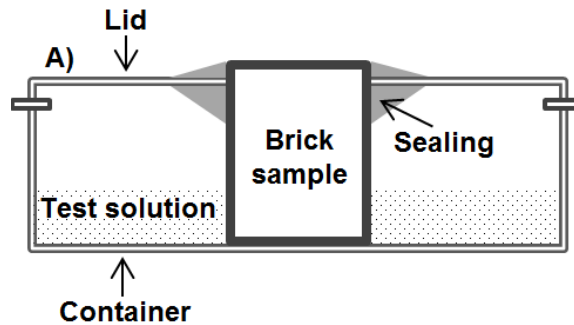
Figure 2.1 An example of a wick test setup.

2.7.2 Long duration of the impregnation and drying test

GE formation under field conditions is reported to take a couple of years. It is also reflected in the duration of efflorescence tests, which took a year or a couple of years to develop GE for the impregnation and drying tests on bricks and field tests on masonry wallettes, respectively (Bowler and Winter, 1997; Bowler and Sharp, 1998).

The long duration is likely the result of (i) the low solubility of calcium sulphate compared to the common effloresing salts (e.g. sodium sulphate and chloride), (ii) the interrupted nature of the Bowler's impregnation and drying test procedure, (iii) the slow drying conditions (laboratory room or field climate), and (iv) the delayed formation of GE source in a cement paste. Because of the first, more water is required for sufficient GE source dissolution and in consequence more time for the drying process yielding gypsum accumulation at the sample surface.

2.8 Discussion

Both brick and mortar may be the source of gypsum efflorescence. The source is either in the form of anhydrite contained within the brick or can be formed via carbonation of the mortar joint. For the former, anhydrite as the source of gypsum efflorescence is questionable, since it is characterised by an exceptionally low dissolution rate. The carbonation of mortar, on the other hand, does not seem to be a limiting factor and actually supports the observed delay in gypsum efflorescence. Gypsum efflorescence then proceeds through the processes of dissolution inside the masonry and transport to the surface of the masonry, the former induced by moisture ingress supplied by wind-driven rain, the latter resulting from moisture drainage by surface evaporation.

These processes can be simulated by impregnation and drying tests, and by wick test procedures. The impregnation and drying test procedure applied by Bowler and Winter (1997) suffered from numerous disadvantages, though. Firstly, a transport medium and efflorescence source were combined both in the same brick, which did not allow assessing their impact separately. Secondly, the test was not suitable for testing masonry mortar. Finally, the test duration of (at least) 1 year was far too long for practical applications. Each of these shortcomings can be addressed by adjusting the wick test protocol.

Wick test design enables testing separately masonry components (mortar constituents and brick) against GE risk, by virtue of separating the transport medium (brick core) from the test solution (e.g. mortar component with water), similarly as done by Sanders and Brosnan (2010) for the bedding material evaluation.

Efflorescence tests have been previously applied to testing cement mortars as e.g. test wallettes components (Bettzieche, 1994; de Bueger *et al.*, 2005). Nevertheless, GE is a recent problem and carbonated cement paste has not been yet addressed in an efflorescence test protocol. The carbonated sample can be prepared beforehand and then subjected to a wick test by inserting it into the test container together with water (both forming the test solution), what is further addressed in Chapter 7.

Acceleration of the test duration can be addressed in multiple ways at the same time. First, the wick test protocol promotes uninterrupted efflorescence growth making thus the test more efficient. Second, the test setups can be exposed to the climate conditions accelerating the drying process, by increasing temperature, decreasing humidity or enhancing air circulation over the drying surface. Last, gypsum formation in cement paste is delayed, as it requires its substantial carbonation. Full carbonation of masonry joint made of cement mortar is reported to take 2 years (Brocken *et al.*, 2000), hence carbonation of test wallettes under ordinary conditions would be too long for practical applications. It requires hence accelerating the carbonation process by e.g. reducing the sample size and optimizing the carbonation conditions (Section 3.2) while a powdered sample can be conveniently tested using the wick test setup. On the downside, the separation of carbonated mortar (or cement paste) from the brick sample does not account for the effect of the interfacial zone formed between the brick and mortar.

2.9 Summary

Gypsum efflorescence is a recent phenomenon affecting masonry components. Its mechanism may seemingly appear simple, as it involves source dissolution, transport and crystallisation, processes which are considered well understood for the other common efflorescing salts. However, this impression proves superficial, as the available data reveals a complex interplay of the underlying processes as well as crucial knowledge gaps related to the mechanism of GE formation. While research dedicated to gypsum efflorescence in particular is limited, a literature review of publications related to the sources, transport and crystallisation of gypsum has offered a number of insights.

Both masonry components can serve as a gypsum source: anhydrite can be found in considerable amount in bricks, while according to a recent hypothesis gypsum may be formed upon mortar joint carbonation. Although the low solubility of calcium sulphate(s) does not appear sufficient to hinder substantially GE formation, the literature review did reveal some puzzling bottlenecks. The processes related to the dissolution, transport and crystallisation should be equally feasible in the older spotless masonry, what contrasts with gypsum efflorescence affecting constructions erected exclusively within the last three decades only. What is more, the apparent propensity of gypsum for subsurface accumulation adds to the GE intricacy. The analysis of the recent changes in masonry components quality reveals some fluctuations in the sulphate levels in cement and a considerably new and currently common practice of mortar admixture application. Nonetheless, many of the inferences articulated above remain hypothetical, which led to initiation of this research project. Its main aim is to design an experimental method allowing for reproducing gypsum efflorescence formation under laboratory conditions. The method may be based on the existing wick test design commonly used for salts crystallisation tests. However, the standard procedures do not appear adequate for practical application due to the too long duration of the test and its non-versatile nature. A wick test setup design can be possibly easily adjusted for both accelerating the test and addressing different research questions. A validated method could be adapted for evaluating brick and carbonated mortar as an efflorescence source, addressing the effect of brick moisture properties, and investigating the effect of admixtures or other parameters.

3 Methodology

3.1 Introduction

This chapter addresses technical aspects of this research project: from sample preparation, over storage conditions, to the measurement settings and a strategy for data analysis. Section 3.2 discusses different aspects related to the preparation of carbonated cement paste, while brick sample preparation is explained in the subsequent Section 3.3. Various techniques were used to analyse mineral composition of cement and efflorescence samples, and these are described in Section 3.4. These were often complemented by chemical analysis, and the employed techniques are presented in Section 3.5. Sections 3.6.1 and 3.6.2 address the characterisation of brick moisture properties, while the surface tension measurements were determined according to the procedure explained in Section 3.6.3. Note that this chapter does not comprise the efflorescence test methodology, which is treated in Chapters 6 and 7.

3.2 Cement paste carbonation

3.2.1 Preparation and carbonation

Cement paste was prepared with a water-cement ratio w/c = 0.5. First, cement powder and water were mixed with a spatula until a uniform paste was obtained. This was then further mixed with a Hobart N50 mixer equipped with a wire whip in the following order: 1min at speed 1 (136 RPM), 30s at speed 2 (281 RPM), scraping the sides and mixing with a spatula for 1min, and final mixing at speed 2 for 1min. Next, the cement paste was cast into plastic moulds (0.5L), closed with a lid and additionally sealed with tape. Curing was carried out during 28 days at 20°C and 90% relative humidity (RH).

Once the samples were demoulded, the samples were crushed to a coarse powder and exposed to conditions favourable for carbonation. The hardened cement paste was first crushed in a jaw crusher and then the powder fraction of 0.5-2mm (Chapter 7) or 2-4mm (Chapter 5) was separated by sieving with a Vibratory Sieve Shaker AS 200, set at amplitude of 4mm and duration of 10min. The optimal RH range for carbonation lies within 50-70% (Hewlett, 2004), while increasing CO_2 concentration over 5% does not increase further the effectiveness of carbonation (Parrott, 1987). The selected fraction was spread on flat plastic dishes and placed in a carbonation cabinet Sanyo MCO-17AIC, set at 25°C and 5% CO_2. The humidity was controlled by a NaBr salt solution (RH of approx. 53% after equilibration). The temperature and relative humidity in the cabinet were additionally recorded by a HOBO Pro v2 Data Logger.

3.2.2 Sampling during carbonation

To monitor the carbonation progress, 10g samples were taken from the carbonating cement paste powder. This allows for averaging the carbonation progress on approximately 510 grains (deduced from the average number of 51 grains counted in 5 subsamples, each weighing 1g). The sample was subsequently ground with mortar and pestle, until the whole sample passed through a 500μm sieve. For each characterisation technique a specific sample preparation procedure was further followed, see Sections 3.4.2, 3.4.3, and 3.5.1.

3.2.3 Storage conditions

All cement paste samples were stored, until further sample preparation or analysis, in a desiccator under conditions adapted for arresting carbonation. It was achieved by providing low RH conditions ($CaCl_2$ salt solution, 35% RH) and by CO_2 removal (soda-lime CO_2-scrubber) from the desiccator. The former was chosen as it has been reported to prevent ettringite dehydration (Renaudin et al., 2010).

3.2.4 Normalisation to dry mass

The hydrated and carbonated cement pastes were characterised by means of mineralogical (Sections 3.4.2 and 3.4.3) and chemical (Section 3.5.1) analyses, while the results were normalised to anhydrous cement (g or mmol/100g anhydrous). No dedicated free water removal procedure was applied to the samples,

normalisation of the component's content to dry mass was based on the known w/c ratio (Snellings, 2016):

Wj,rescaled(n) = Wj,measured(n) · (1+w/c)   (Equation 3.1),

where Wj(n) corresponds to the content of the component j after n-days of carbonation.

3.3 Brick sampling and crushing

The brick sampling and crushing methodology was adapted from the BS 3921:1985 normative (BS 3921:1985, 1985). First, six bricks were selected from different locations in a brick palette. Next, bricks were crushed with a jaw crusher to a powder fraction of <1cm. A representative 1kg subsample was subsequently taken by coning and quartering, which was further ground with a mortar and pestle to pass a 500μm sieve. The sample could be used both for the efflorescence test (Section 7.2.2) and for the leaching test (Section 3.5.1).

3.4 Mineralogy

3.4.1 Qualitative X-ray powder diffraction

Qualitative X-ray powder diffraction (XRD) was applied for identifying salt deposits formed on bricks investigated during the field survey and on samples subjected to the efflorescence test.

Sampling

Salt deposits were gently scraped from bricks (field survey) and samples (efflorescence test). For the former this was done on higher parts of the facades (above the 1.5 m height line), to exclude cases of salt accumulation due to rising damp.

Sample preparation

The collected samples were initially gently ground and then sieved through a 63 μm sieve, to separate the salt deposit from sand grains inadvertently removed from the brick surfaces together with efflorescence. The efflorescence enriched fraction was ground further, and then sprinkled over a silicon sample holder.

Measurement & data analysis

The diffraction patterns were gathered with a Philips PW1830 diffractometer using CuKα radiation (45kV, 30mA). Table 3.1 shows the diffractometer settings: a long scan (57 min) was applied for the field survey samples, while for the efflorescence test its duration (6 min) was optimised for gypsum and calcite identification. The mineral phases were identified with the Diffrac.Suite Eva software.

Table 3.1 The diffractometer settings applied to efflorescence identification.

	Angle range [°]	Step size [°]	Time / step [s]	Scan time [min]
Field survey	5-70	0.02	1	57
Efflorescence test	10-40	0.04	0.5	6

3.4.2 Quantitative phase analysis

Quantitative phase analysis (QPA) was applied to study the mineralogical evolution of carbonating cement paste. The sample preparation and quantitative analysis strategy were partly adapted from the works of Mertens (2009) and Snellings (2016).

Sample preparation

The cement paste powder (2.7g < 500μm) was manually mixed with a ZnO internal standard (0.3g). The mixed powder was then ground in a McCrone XRD-mill during 5min. Isopropanol (5mL) was used as a grinding medium, to preserve the sample's microstructure and composition (Zhang and Scherer, 2011). After grinding, the fine powder was recuperated by flushing with isopropanol. In order to limit the risk of

carbonation during drying, the suspension was first centrifuged at 4000RPM during 20 min in a Jouan C3i centrifuge. Finally, the separated wet powder paste was dried to a constant mass at 30°C in presence of $CaCl_2$ desiccant and soda-lime CO_2-scrubber for approximately 20min. The anhydrous cement samples were prepared following the same procedure, but the ZnO was added at 20wt% and milling duration was extended to 10min.

Measurement

The dry powder sample was first disintegrated by gentle grinding and sieving through a 250μm sieve. The powder was then side-loaded into a sample holder. The diffraction patterns were collected with a Philips PW1830 diffractometer using CuKα radiation (45kV, 30mA). The standard 2θ scan range were taken to be 5–70° with a step size of 0.02° 2θ and a counting time of 2s.

Quantification strategy

The phases were first identified with the Diffrac.Suite Eva software. The Rietveld quantification was then performed with TOPAS® Academic (TA) software using the Fundamental Parameters Approach. Table 3.2 lists the mineral structures used for refinements.

Table 3.2 List of mineral structures used for refinements.

Mineral	Reference	PDF number*
α-quartz	(Le Page and Donnay, 1976)	46-1045
Alite M3	(de Noirfontaine *et al.*, 2011)	-
Anhydrite	(Cheng and Zussman, 1963)	37-1496
Aragonite	(Caspi *et al.*, 2005)	01-073-3251
Belite β	(Mumme *et al.*, 1995)	33-302
C3A orthorhombic	(Nishi and Takéuchi, 1975)	01-070-0859
Calcite	(Maslen *et al.*, 1993)	5-586
Ettringite	(Goetz-Neunhoeffer and Neubauer, 2006)	41-1451
Ferrite	(Redhammer *et al.*, 2004)	01-074-3672
Gypsum	(Boeyens and Ichharam, 2002)	33-311
Hemicarboaluminate	(Runčevski *et al.*, 2012)	41-0221
Monocarboaluminate	(François *et al.*, 1998)	01-087-0493
Monosulphate	(Allman, 1977)	01-083-1289
Portlandite (CH)	(Chaix-Pluchery *et al.*, 1987)	4-733
Zincite	-	361451
Vaterite	(Kamhi, 1963)	33-628

* Powder Diffraction File (PDF) number is a unique identification reference for a powder diffraction pattern of a mineral phase

The structural parameter variation was constrained to ±1%. The structural and peak shape parameters of anhydrous cement phases were refined for the anhydrous cement samples and kept fixed in the analysis of the cement paste. The same strategy was followed for the phases detected in the non-carbonated and fully carbonated cement paste. The refined global parameters were the specimen displacement and the background polynomial function combined with a 1/x term. The two-coefficient-Chebyshev function was applied for the anhydrous cement, while three terms were used for the hydrated and carbonated cement paste samples. The March-Dollase preferred orientation correction (Dollase, 1986) was applied to anhydrite and CH phases.

3.4.3 Thermogravimetric analysis

The cement paste powder (± 50mg, < 500μm) was further ground with mortar and pestle until all coarse grains were crushed. Thermogravimetric (TG) analyses were performed with Netzsch STA 409 PC Luxx® over the range of 25–1000°C at a heating rate of 10°C/min. The subsamples (10mg) were measured in alumina crucibles under an inert atmosphere of N_2 at a flow rate of 60 ml/min. CH content was determined by integration of its DTG (first TG derivative) peak. A DTG peak at around 100°C is a result of overlapping CSH dehydration and a loss of water from between columns in the ettringite structure

(Lothenbach *et al.*, 2016). Grounds *et al.* (1988) have demonstrated on a study of synthetic ettringite that the loss of this structural water is indicative of structure decomposition, as it goes along with a formation of ettringite decomposition products. Due to the overlapping, ettringite amount quantification was not possible, but it was nevertheless possible to estimate it qualitatively. It was realised by visual analysis of DTG curves, by their comparison with samples showing maximal (non-carbonated cement paste) and minimal (sample subjected to the longest carbonation duration) ettringite content.

3.4.4 Hydrochloric acid test

A drop of 1M hydrochloric acid (HCl) was placed on efflorescence covering the brick sample surface. In case calcite was present in efflorescence, a reaction took place:

$$CaCO_3 + 2HCl \rightarrow Ca^{2+} + 2Cl^- + H_2O + CO_2\uparrow \hspace{3cm} \text{(Equation 3.2)}$$

The released CO_2 bubbles signalled the presence of calcite.

3.5 Chemistry

3.5.1 Leaching test

A < 500μm powder sample (5g for cement paste, 50g for brick powder) was gently mixed with 100g of ultra-pure water (>18 MW/cm³) supplied from Millipore and sealed in a plastic container. After seven days the powder was gently mixed with solution and left to rest for 10min, and subsequently 3.5ml of solution was taken and filtered with the Chromafil® PET-45/25 filter (pore size: 0.45μm). The samples were acidified with 70μl of 14M HNO_3 and stored in a fridge until testing. The Ca, K, Na, Mg and S (later recalculated to SO_4) were measured by Elvira Vassilieva (KUL, Division of Geology) with a Varian 720 ES (simultaneous inductively coupled plasma–optical emission spectrometry (ICP-OES) with axially viewed plasma) supplied with double-pass glass cyclonic spray chamber, concentric glass nebulizer SeaSpray and "high solids" torch. The instrument features a Cooled Cone Interface, echelle monochromator and custom-designed Vistachip CCD detector mounted on a triple-stage Peltier device and cooled to -35°C. The instrument provides true simultaneous measurements and full wavelength coverage from 167 to 785 nm, given its ability to determination of a series of elements from one single run. Solutions were presented to the spectrometer using the Varian SPS3 Sample Preparation System. Calibration solutions were prepared from certified Plasma HIQU single element solutions CHEM-LAB (Belgium). One stock solution containing all elements to be measured was prepared and then diluted to create a series of five standards with the concentrations covering the range of the samples. A blank was also included in the calibration. All solutions were made from ultra-pure water (Millipore) and stabilized with ultra-pure grade nitric acid. The final concentration of acid was matched to the one of the sample solutions. Sensitivity, linear dynamic range and freedom from spectral interferences were taken into consideration during wavelength selection for each element.

3.5.2 Wavelength-dispersive X-ray fluorescence spectrometry

Anhydrous cement powders were subjected to the wavelength-dispersive X-ray fluorescence spectrometry (WD-XRF) analysis. The cement samples were in form of a fine powder completely passing through a sieve of < 80μm and thus did not require further grinding. The samples were measured with an automatic sequential wavelength dispersive XRF spectrometer Philips PW 2400 in a semi-quantitative way with Super-Q software. The equipment was supplied with a high frequency HT generator (60 kV, 125 mA, 3000 W max., 0.0005 % stability), super sharp end window X-ray tube (60 kV, 125 mA, 3000 W max., Rhodium anode), eight analysing crystals (LiF 200, LiF 220, PE 002, Ge 111, PX1 multilayer, PX2 multilayer, PX4 multilayer, TlAP 100 coated), scintillation counter (0° to 104° 2theta, 1000 KCPS max.), and goniometer (theta/2theta decoupled). The standard error was an estimated error and was the largest of following errors: (1) the counting statistical error, (2) the background and line overlap correction error and (3) the matrix correction error. The analyses were realised by Pieter L'hoëst at the Department of Materials Engineering at KU Leuven.

3.5.3 Scanning Electron Microscopy and Energy Dispersive X-ray analysis

A brick sample was mounted on a sample holder with a carbon glue and dried under vacuum overnight. The samples were coated with Pd-Au in an EDWARDS S150 coater. The measurement was realised with

a FEI XL30 FEG scanning electron microscope (Schottky gun) equipped with an Energy Dispersive X-ray detector (SEM-EDS) at the Department of Materials Engineering (MTM) of KU Leuven. The images were collected at accelerating voltage in a range of 10-15kV (see the SEM pictures for exact values). The EDS spectra of selected points were collected at a working distance of 10mm and accelerating voltage of 25kV and analysed with Genesis 4.61 software in a semi-quantitative manner, applying correction for atomic number, absorption, and fluorescence (ZAF correction).

3.6 Physical properties

3.6.1 Vacuum saturation
Sample preparation

Ten brick samples were cut from five bricks, randomly selected from a pallet. First, all the brick sides (approx. 5mm thick) were removed from the bricks. Next, two 1cm thick samples were cut with a wet saw from each brick. The samples were then oven-dried at 105 °C until constant mass.

Test procedure

The dried samples were first weighed (m_{dry}). The samples were then placed in a tightly closed desiccator connected to a vacuum pump, and depressurised to a level of ≤ 270 mbar. Next, the desiccator was filled with distilled water at a flow rate of 5cm/h, until water reached a level of 5cm above the samples. The desiccator was then pressurised back to the standard air pressure level. The samples were left immersed in water for another 24 hours. The samples were then removed from water and immediately weighed in air (m_{wet}) and under water (m_{under}). The vacuum water content (w_{sat}) was then calculated according to:

$$W_{sat} = \frac{m_{wet} - m_{dry}}{m_{wet} - m_{under}} \cdot \rho_{water}$$ (Equation 3.3),

where ρ_{water} is the density of water.

The experiment was realised at the Civil Engineering Department, Building Physics Section, KU Leuven, under guidance of Jelena Todorovic.

3.6.2 Free water uptake
Sample preparation

Ten brick samples were cut from five bricks, randomly selected from a pallet of bricks. First, all the brick sides (approx. 5mm thick) were removed from the bricks. Next, the bricks were cut with a wet saw into three equal samples, out of which two were selected. The samples were then oven-dried at 105 °C until constant mass.

Test procedure

The dry samples were first weighed (m_{dry}) and measured to determine the bottom surface area (A) and height (H). The test was realised by placing samples in a dish filled with water and submerging them to a depth of up to 5mm. The sample's orientation was chosen to be perpendicular to the brick's stretcher side. The lateral and top sides of the brick were sealed with a plastic film, to limit the water evaporation during the experiment. The plastic film was perforated at the top to allow air to escape from the pores upon water uptake. The water uptake was monitored by weighing the samples (m_{wet}) at regular time intervals. The water inflow G was determined from:

$$G(t) = \frac{m_{wet}(t) - m_{dry}}{A}$$ (Equation 3.4),

and plotted against square root of time, see Figure 3.1. Typically the plot consists of two well defined phases. Their intercept allows determining the capillary water content (w_{cap}), while the slope of the first stage corresponds to the capillary absorption coefficient (A_{cap}).
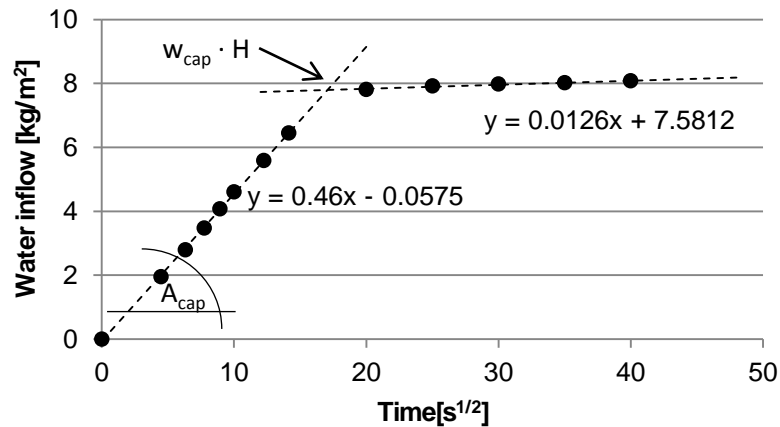
Figure 3.1 Analysis of the water inflow in function of time.

The experiment was realised at the Civil Engineering Department, Building Physics Section, KU Leuven, under guidance of Jelena Todorovic.

3.6.3 Surface tension

The interfacial tension of the solutions was measured with the pendant drop method using a CAM 200 tensiometer from KSV. Ten images per drop were captured every 30 seconds by a CCD firewire camera (512x480) with telecentric zoom optics combined with LED based background lightning. The interfacial tension was derived by analysing the shape of the drop and by fitting the shape of the drop with the Young-Laplace equation. The measurements were realised at the Department of Chemical Engineering, Soft Matter, Rheology and Technology Section, KU Leuven, under guidance of Rob Van Hooghten.

4 Field Survey on persistent efflorescence

4.1 Introduction

Persistent efflorescence – stains of slightly soluble salts that do not wash off naturally – is a growing problem in the construction industry. Besides the occurrence in the UK and the Netherlands (Bowler and Winter, 1996; Brocken and Nijland, 2004), the Belgian brick producers are receiving progressively more complaints, as building owners blame their products for the flaw. In the opinion of the Belgian brick producers, persistent efflorescence occurs more frequently, develops quicker than before, and gets more pronounced over time. However, the Belgian cases have not been yet addressed by a systematic study and hence little is known about their nature, which leaves the brick manufacturers helpless in preventing GE formation. In particular the composition of efflorescence, its visual aspect and the characteristics of masonry components in use are of interest, as these can already indicate the mechanism of efflorescence formation, its sources and also indicate the contribution of brick and mortar. These together constitute a departure point for the next steps of this research project.

In order to contribute to the knowledge on this issue a field survey was carried out, to determine the major factors associated with its occurrence. In this survey, 28 cases of Belgian buildings affected by persistent efflorescence were analysed. Some of these cases were identified from the complaints of building owners to brick producers, other cases were found during an exploration of the Leuven area in Belgium by the researcher.

4.2 General observations on persistent efflorescence

The investigated cases concern a type of permanent efflorescence, which after having developed on a masonry surface does not wash off with natural weathering. In two cases the building facades had been cleaned with high-pressure water jets, which removed the efflorescence stains temporarily, but did not restore the facades' original appearance. In both cases efflorescence has reappeared, indicating that the efflorescence source is not affected by the treatment. The observed persistent efflorescences came in different appearances, ranging from a seemingly thin whitish veil present within the porous surface of a material to a locally developed thicker crust on top of the material's surface (Figure 4.1). However, upon closer inspection the former often revealed to be composed of characteristic local accumulations as well (Table 4.1). In any case, it greatly alters the aesthetic aspect of the masonry façade. In contrast to early efflorescences of easily soluble salts, often being soft and thick, these persistent efflorescences gave the impression of being very compact and strongly adhering to the brick surface, while simultaneously generally being very thin. In most cases the efflorescence affected the bricks to a much greater extent than the mortar joints.

Figure 4.1   Efflorescence develops preferentially on (A), (B) facades and (C) edges which are exposed to an intensified action of rain and wind. The capital letters indicate orientation of the facades: S – south, W - west, E – east.

Table 4.1 The photographs of GE cases identified during the field survey. Cases are identified by their field survey codes.

FS10	FS23	FS24	FS29
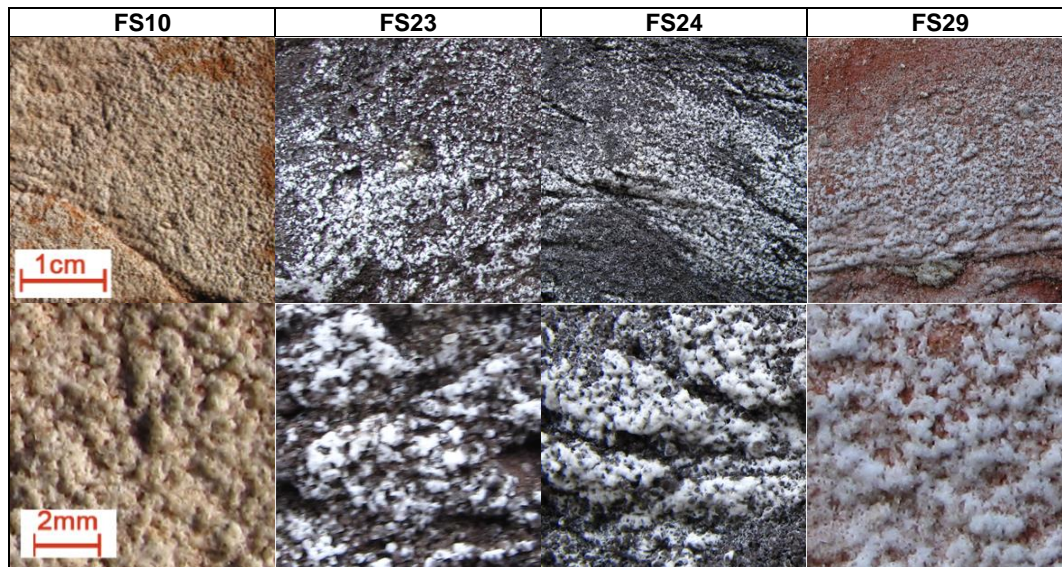
The investigated building facades were all constructed with mechanically produced 'hand' moulded clay bricks, which are most commonly used for facade masonry in Belgium. In all cases, the most affected facades of the building were those oriented West to South, with efflorescence being most pronounced on the edges and the upper parts of the facade, facade orientations and locations that typically receive relatively frequent and intensive wind-driven rain.

The year of construction was identified for 15 of the 28 cases, and ranged from 1997 to 2007. The other cases were probably constructed in a similar period, as they had an equally modern appearance. None of the 28 studied cases hence concerns older constructions, and the problem thus appears to exclusively affect buildings erected during approximately the last two decades. Based on observations by building owners, it is moreover noted that the efflorescence does not appear directly after construction but is instead perceived only several years after construction. However, as these observations of such delays are based on visual assessments, it is not clear whether persistent efflorescence indeed develops with a delay, or whether it is just a very slow process that goes unnoticed in its early stages.

4.3 Mineralogy analysis of persistent efflorescence

To determine the efflorescence composition, efflorescence samples were collected and analysed by qualitative XRD (Section 3.4.1), revealing four primary categories in the studied persistent efflorescence cases. Table 4.2 presents the results of sample analyses and case evaluations. Out of the four identified minerals – gypsum, calcite, hematite and quartz – only the former two are potential persistent efflorescence components. As sampling involved surface scraping, hematite and quartz were inadvertently collected together with the efflorescence products. In most cases where gypsum was identified in a sample, it was present in a substantial amount compared to the other identified minerals. As it is not a raw brick component, it is clear that its accumulation at the surface of masonry is due to the efflorescence formation. Unlike for gypsum, the origin of calcite is uncertain, since there are several possible sources of calcite at the brick surface. Besides being recognised as a potential efflorescence forming mineral (Dow and Glasser, 2003), calcite also naturally occurs in clays, and is moreover applied as a clay mix and brick sanding component. In most cases where calcite was identified in a sample, it was present in very low amounts, and its origin can therefore not be unambiguously determined. Hematite is a mineral which naturally occurs in clay and is also used as a brick pigment. The evaluation of XRD scans was hindered by the presence of quartz, which produces very intense and overlapping peaks.

Table 4.2 Evaluation of the scraping samples collected from the investigated constructions. For each identified mineral: G – gypsum, C – calcite, H – hematite and Q – quartz its relative content is approximated: +++ dominantly present, ++ present, + present in low amounts, ? possibly present, - not identified. Each case is categorised as gypsum (G), calcite (C), mixed (G+C) or ambiguous (A) efflorescence.

Case n°	Composition (XRD)				Case evaluation	Case n°	Composition (XRD)				Case evaluation
	G	C	H	Q			G	C	H	Q	
FS01	++	+	-	+++	G	FS23	+++	+	-	+	G
FS02	-	+	-	+++	A	FS24	+++	+	-	+	G
	-	-	-	+++		FS25	-	+	+	+++	A
FS03	+	+	-	+++	G		-	+	-	+++	
	+++	+	-	-		FS26	-	+++	-	+++	G+C
FS07	-	+	-	+++	A		+++	-	-	++	
FS08	++	+	-	+++	G	FS27	+++	+	+	++	G
FS10	+++	?	-	+ +	G	FS28	-	++	+	+++	G+C
FS11	+	++	-	+++	A		+++	+	-	+++	
FS13	-	++	-	+++	A	FS29	+++	?	-	+++	G
FS14	-	+	-	+++	A		+++	?	-	++	
FS16	+++	+++	+	+++	G+C	FS30	+++	?	-	+	G
FS17	-	+	-	+++	A	FS31	+	+	-	+++	A
FS18	+++	+	-	+++	G		-	++	+	+++	
FS19	+++	+	-	+++	G	FS32	+	++	-	+++	G+C
FS20	+++	+	-	+	G		+++	+	-	+++	
FS21	+++	?	-	+++	G	FS33	+	+	-	+++	A
FS22	+	++	-	+++	C	FS34	++	++	+	+++	G+C

Based on the sample mineral composition and visual observations, the investigated cases are divided into four efflorescence categories (Table 4.2). There are 13 cases categorised as gypsum efflorescence (G), where only gypsum was identified in substantial amounts in the collected samples. Only one case is assigned to the calcite efflorescence category (C), in which substantial amounts of calcite were accompanied by (very) low amounts of gypsum. The mixed efflorescence (G+C) category comprises five cases where both gypsum and calcite were identified in substantial amounts, and here we distinguish three further groups. The first group comprises two cases where the collected sample contains substantial amounts of both gypsum and calcite (FS16, FS34). The second group consists of two cases for which one of the collected samples was identified as gypsum efflorescence, while the sample collected from another area was identified as calcite efflorescence (FS28, FS32). In the last group we discern a single case, for which most of the building facades were affected with characteristic "lime leach" stains, accompanied by some areas covered with hazy gypsum efflorescence (FS26). For nine cases the evaluation of samples is inconclusive, and they are assigned to the ambiguous (A) category. For these cases the origin of calcite in the efflorescence is uncertain, because of its very low amount in the sample or the use of sand/lime sanding in the brick; in three cases gypsum was found, but in very low amounts. Another possibility could be that efflorescence was in an amorphous form which cannot be identified with the XRD method.

4.4 Brick properties and persistent efflorescence
In many cases the applied brick type was identified, which permits analysis of the relation between brick properties and persistent efflorescence. However, it was not possible to acquire data for the exact batches of bricks used for construction of the investigated buildings. We have thus used the available technical specifications declared by brick producers.

4.4.1 Physical properties
The brick technical specifications were available for 15 cases, yielding data about cold water absorption and initial rate of absorption (IRA). The values declared by producers were determined according to the EN 771-1 (2011) and EN 772-11 (2000) standards, respectively. They are represented in Figure 4.2, grouped along the specific efflorescence composition found for these 15 cases. This data analysis serves to check whether a correlation exists between the GE risk and the hygric properties, as reflected by IRA and

cold water absorption, respectively. The IRA and water absorption values found for gypsum efflorescence cases are not limited to a specific range, but are rather spread over average values found for this brick type.
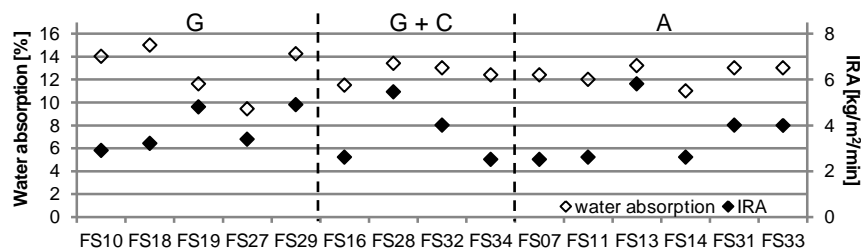

Figure 4.2   Water absorption and the initial rate of absorption (IRA) of the identified brick types. The efflorescence categories are indicated above the graph: G – gypsum efflorescence, G+C – gypsum and calcite efflorescence, A – ambiguous cases.

4.4.2 Chemical properties

Bricks may contain calcium sulphate in the form of anhydrite, which potentially can be a source of gypsum efflorescence. For some of the identified brick types data regarding the SO_4^{2-} content was available, as declared by the brick producers based on EN 772-5 (2002) (Table 4.3). Those data are used here to estimate the amount of gypsum which could be possibly derived from the water soluble sulphate (originating from anhydrite and possibly alkali sulphate(s)), assuming that all the extracted and recrystallised to gypsum.

Table 4.3 Chemical characteristics of the identified brick types.

Case n°	Group	SO_4^{2-} content [wt%]	Gypsum/brick [g]	Case n°	Group	SO_4^{2-} content [wt%]	Gypsum/brick [g]
FS10	G	0.248	7.25	FS07	A	0.014	0.43
FS11	A	0.172	5.18	FS14	A	0.014	0.43
FS13	A	0.056	1.64	FS34	G+C	0.014	0.43
FS29	G	0.044	1.27	FS28	G+C	0.006	0.17
FS18	G	0.020	0.58				

4.5 Discussion

The field study allows concluding that the persistent character of the analysed efflorescence cases can often be primarily attributed to slightly soluble gypsum. This agrees with the findings reported for the UK and the Netherlands, like most of the other outcomes of our field survey – visual appearance, recent occurrence, newly erected buildings, exposure to wind-driven rain. Of these, the grey-white visual appearance and the role of wind-driven rain render this gypsum efflorescence different from the gypsum weathering crusts often found on calcareous stones. These crusts are commonly black, frequently develop on sheltered sections, and are known to be formed via interaction with polluted air (Steiger *et al.*, 2011). These differences between the observed gypsum efflorescences and the gypsum weathering crusts corroborate that the gypsum efflorescence components are probably derived from the brick masonry itself: the grey-white appearance precludes interaction with polluted air, and the role of moisture transfer suggests sources inside the masonry.

The physico-chemical analysis provides more insight into the contribution of the bricks to the gypsum efflorescence. The cold water absorption and initial rate of absorption values obtained for the bricks in our efflorescence cases cover the range commonly found for this brick type. These physical parameters therefore do not seem to control the efflorescence. Instead, it appears that the exposure to wind-driven rain, rather than the moisture transfer properties itself, is a dominant factor. Furthermore, the field survey indicates that even small amounts of gypsum may create distinct discolorations of the brick surface. The chemical analysis tells that such small amounts of gypsum may be derived from the small amounts of anhydrite that are found in most of the studied bricks. While this does not prove the bricks are a definite

source for the efflorescing gypsum, their potential contribution cannot be ruled out based on our observations. On the other hand, some of the identified brick types seem to be very poor gypsum sources (e.g. less than 0.43g), what indicates that mortar joint could also contribute to the GE formation.

4.6 Conclusions

Persistent staining of masonry surfaces by gypsum crystallisation is on the rise in the UK, in the Netherlands and in Belgium. The field survey has resulted in a number of important observations. Gypsum efflorescence is a recent problem, which is restricted to facades constructed during the last few decades. It appears to develop in a slow or delayed way, since it is often only perceived a number of years after construction of the facade. It significantly affects the façade appearance, and when observed in closer detail it reveals compact accumulations of gypsum on the brick surface. The role of moisture in general, or wind-driven rain in particular, seems important, given that gypsum efflorescence exclusively affects facade sections with high exposure to wind-driven rain. The occurrence of gypsum efflorescence does appear to be unrelated to the physical or chemical properties of the brick. For instance, the analysis of bricks' declared technical properties did not reveal any significant dependency on the cold water absorption, initial rate of absorption or potential anhydrite contents of the bricks. As for the latter, it indicates that in some cases (high sulphate content) bricks can likely contribute to the GE formation, while in others (bricks deficient in sulphate) the mortar joint can possibly serve as its source. All these observations agree with the earlier studies by Bowler and Winter (1996) and Brocken and Nijland (2004).

5 Experimental cement paste carbonation

5.1 Introduction

Masonry mortar is a potential GE source, as calcium sulphate is deliberately added and interground with Portland cement clinker to provide control on the setting properties. However, its contribution to the GE-risk has long been neglected, as quickly after cement hydration it is mostly bound to virtually insoluble ettringite and monosulphate phases (MacGregor Miller and Melander, 2003). Synthetic ettringite and monosulphate do however decompose back to gypsum upon carbonation (Nishikawa *et al.*, 1992; Xiantuo *et al.*, 1994; Grounds *et al.*, 1988). The risk of the formation of a GE-source in (cement mortar) masonry joints may hence be high, as it is reported that 2 years of exposure is sufficient for their full carbonation (Brocken *et al.*, 2000).

Nevertheless, the carbonation of ettringite and monosulphate as cementitious materials' components is not well documented. Depletion in ettringite in the carbonated zone of concrete blocks has been reported, while experimental carbonation of similar materials yielded a considerable increase in water soluble sulphate (Brocken and Nijland, 2004). This indicates gypsum formation upon ettringite decomposition, though gypsum has not been identified as a carbonation product. This may partly be due to the fact that the amount of gypsum formed upon cement paste carbonation may be below the detection limit of conventional techniques.

Ettringite and monosulphate stability are dependent on the pH of the pore solution, which is controlled by the content and availability of CH. Its stabilising effect has been reported for synthetic ettringite (Pajares *et al.*, 2003) and mentioned in a study on masonry mortar carbonation (Brocken *et al.*, 2000), though no dedicated study has addressed the relation between CH content in cement paste and ettringite stability. Supplementary cementitious materials are commonly blended in with ordinary Portland cement. Many of them exhibit pozzolanic properties resulting in lower CH content in hydrated cement (Snellings *et al.*, 2012). While their accelerating effect on cement paste carbonation has been reported (Šavija and Luković, 2016), it is not clear whether it also affects the rate of gypsum formation.

This work therefore focuses on characterising the phase development(s) during cement paste carbonation, with a particular interest in identifying calcium sulphate formation. Investigations of cementitious materials' carbonation are mostly applied to large samples, which on one hand allow following the dimensional aspect of carbonation, but on the other hand yield samples being only partly carbonated due to formation of a carbonation front (Šavija and Luković, 2016). For this reason this study was carried out using finely crushed cement paste, which additionally allowed for more precise characterisation of cement phases due to the absence of aggregates, and furthermore accelerated the carbonation process. The mineralogical analysis was carried out with QPA and TG analyses, while the water soluble sulphate amount was determined by chemical analysis applied to the extracts from a leaching experiment. While the latter technique was suitable for monitoring sulphate release upon carbonation, its source could not be identified. On the other hand, the amount of gypsum formed upon carbonation was too low to be detectable by the QPA and TG methods. A novel approach was hence applied – a simple dissolution monitoring experiment, which allowed identifying and quantifying slight amounts of calcium sulphate based on the leaching progress of Ca^{2+} and SO_4^{2-} ions. The applied methodology allowed also studying the relation between CH and ettringite content. The analysis has been carried out on cement paste samples prepared from ordinary Portland cement and a cement blended with fly ash and blastfurnace slags. The comparison of those two demonstrated the effect of pozzolanic components on gypsum formation upon carbonation. The results of this study yield preliminary directions for limiting the GE source formation in cement paste.

The chapter starts with a brief introduction to materials and methods (Section 5.2). The results part is initiated by demonstrating gypsum formation upon cement paste carbonation in Section 5.3.1. Next, the more general discussion on phase development proceeds in Section 5.3.2, while the problem of variable RH during the experiment is addressed in Section 5.3.3. The delay in ettringite destabilisation and premises indicating its decomposition to gypsum are examined in Sections 5.3.4 and 5.3.5. The discussion

part starts in Section 5.4.1 which addresses the applicability of the obtained results to a masonry mortar joint. A broader discussion on limiting the GE risk is split into two sections. The effect of SCMs and lime are addressed in Section 5.4.2, while the potential for limiting calcium sulphate(s) additions to cement are explored in Section 5.4.3. Section 5.5 summarizes the main conclusions, and the analysis of repeatability is covered in an appendix (Section 9.1.1).

5.2 Materials and Methods

Two commercial cements were selected for this study. Ordinary Portland cement (CEM I 52.5 HES) was chosen as a reference, while a blended cement (CEM II/ B-M (S-V) 32.5N) was selected due to its common application in masonry works. The anhydrous cement powders were characterised with QPA (Section 3.4.2) and WD-XRF (Section 3.5.2) methods.

The carbonated cement pastes' preparation, sampling, storage, and results normalisation have been explained in Section 3.2. Considerable bleeding was observed for the CEM II paste samples. After curing, the surplus water was removed and weighed, thus allowing to calculate the corrected $w/c_{CEM\ II}$ = 0.39. During the carbonation phase the cement pastes were frequently sampled to monitor the evolution of CH by TG (Section 3.4.3), ettringite and monosulphate by QPA (Section 3.4.2), and water soluble sulphate content by leaching test and ICP-OES analysis (Section 3.5.1). In addition, the leaching process of the fully carbonated cement paste samples was investigated by additional sampling after 10min, 1hr, 6hr, 1d, 2d, and 3d (besides the default 7d). The TG and QPA samples were mostly analysed within a couple of days, while the samples for leaching test were analysed after 1.5 years. For QPA results a satisfactory fit quality was obtained, characterised by weighted pattern R value in range of 19-21.

The sample preparation procedure for QPA involved 5 minutes of McCrone grinding with isopropanol. During this process (partial) solvent exchange took place, replacing free water in cement with isopropanol. Isopropanol was later removed by drying. On the other hand, no such treatment was applied to the TG and 'water soluble SO_4^{2-}' samples, hence they contained also some free water. Nevertheless, all the samples were normalised to dry mass by applying correction based on the w/c ratio (Section 3.2.4). In consequence, this yielded some overestimation for the QPA results, as the normalisation to dry mass did not correct for the (partial) free water removal.

Anhydrous cements' composition

The mineralogical (QPA) and chemical (WD-XRF) composition of the two anhydrous binders was analysed and results are provided in Table 5.1 and 5.2, respectively. The blended cement contained two (amorphous) SCM components: granulated blastfurnace slag and siliceous fly ash. Their addition was at a level of 23.7wt% according to the determined amorphous phase content by QPA.

Table 5.1 Mineralogical compositions (QPA) of both anhydrous cements.

Component	CEM I [wt%]	CEM II [wt%]
Alite M3	66.7	51.8
Belite β	14.9	5.3
C3A orthorhombic	3.1	4.4
Ferrite	5.6	3.9
Calcite	4.6	5.0
Gypsum	1.1	2.0
Anhydrite	0.7	0.4
α-Quartz	0.8	3.5
Amorphous	2.5	23.7

The XRF analysis of sodium yielded non-significant results in case of CEM I and no sodium identification for CEM II, which is usually present at a level of 0.3wt% in typical Portland cement clinker (Taylor, 1997). These shortcomings can possibly be attributed to low sodium X-ray yields due to its low atomic mass, and to insufficient correction for the absorption of sodium X-rays by a polyester film covering the bottom of

the XRF powder cup. The oxides wt% and LOI sum up to 87.36wt% and 91.30wt% for CEM I and CEM II, respectively. Deficiencies of up 10% are not uncommon due to the limited capability for light element quantification by XRF. In case of CEM II this range is exceeded by 2.64%, what suggests that the oxides' contents may be slightly underestimated.

Table 5.2 Chemical compositions (WD-XRF) of both anhydrous cements, the main oxides (>0.1wt%) and Na_2O are listed, the minor oxides (<0.1wt%) content is provided as a sum. Results presented as a value ± standard error. Loss on ignition (LOI) was determined with a TG (Section 3.4.3).

Oxide	CEM I [wt%]	CEM II [wt%]
CaO	52.30 ± 0.45	46.03 ± 0.48
SiO_2	17.73 ± 0.17	23.45 ± 0.19
Al_2O_3	3.85 ± 0.08	8.30 ± 0.13
SO_3	3.81 ± 0.19	5.03 ± 0.07
Fe_2O_3	3.21 ± 0.18	2.86 ± 0.17
MgO	1.25 ± 0.05	2.11 ± 0.07
K_2O	0.43 ± 0.05	0.73 ± 0.08
TiO_2	0.37 ± 0.02	0.68 ± 0.03
ZnO	0.13 ± 0.01	<0.10
SrO	0.12 ± 0.01	0.16 ± 0.01
Cl	<0.10	0.13 ± 0.01
Na_2O	0.03 ± 0.13*	not identified
Sum of minor oxides (<0.1wt%)	0.21	0.34
LOI	3.86	4.50
Total	87.36	91.3

the result is not significant due to a high standard error

5.3 Carbonation experiments

5.3.1 Calcium sulphate formation upon cement paste carbonation

Table 5.3 summarises the leaching experiment on fresh (0d) and fully carbonated (155d) cement paste samples. Similar trends were observed for both CEM I and CEM II compositions. Both non-carbonated paste samples yielded very high amounts of leached calcium, which could be attributed to a high content of CH in a fresh cement paste. Upon carbonation, CH transformed into virtually insoluble calcium carbonate, and it resulted in a major drop in the Ca concentration. In contrast, the amount of water soluble Na^+ and K^+ cations dropped markedly. This may be likely attributed to their sorption by silica gel, which formed upon CSH phase decalcification induced by carbonation (Anstice *et al.*, 2005). However, most interesting is the increase of water soluble sulphate content, from negligible amounts found for the fresh cement pastes to considerable amounts formed upon carbonation. Nevertheless, the source of sulphate cannot be identified based on these results.

Table 5.3 Concentrations of ions leached from fresh (0d) and fully carbonated (155d) cement pastes.

	Concentration [mmol/100g anhydrous]				
	SO_4^{2-}	Ca^{2+}	K^+	Na^+	Mg^{2+}
CEM I 0d	0.1	60.2	9.5	10.7	0.00
CEM I 155d	13.9	15.3	1.1	3.8	0.02
CEM II 0d	0.1	48.6	9.1	8.5	0.00
CEM II 155d	10.0	12.1	1.0	2.9	0.05

Synthetic ettringite is reported to decompose to gypsum upon carbonation (Nishikawa *et al.*, 1992; Xiantuo *et al.*, 1994; Grounds *et al.*, 1988); however gypsum formation in carbonated cementitious material has not been yet reported. It may be related to the fact that the amounts of formed gypsum are below the detection limits of techniques commonly applied to its identification: QPA and TG. Figure 5.1 and Figure 5.2 show that indeed, no gypsum was identified in 155d carbonated cement samples neither by TG nor by QPA methods, respectively. Figure 5.1 illustrates that the DTG curves of the 155d carbonated cements did not show the characteristic gypsum dehydration peak in the range of 120-150°C (Lothenbach *et al.*, 2016), nor were the characteristic gypsum peaks found in the XRD spectra, see Figure 5.2. While depletion in ettringite upon carbonation of cementitious materials was already reported (Brocken *et al.*, 2000; Brocken and Nijland, 2004), it has not been accompanied by gypsum identification yet.
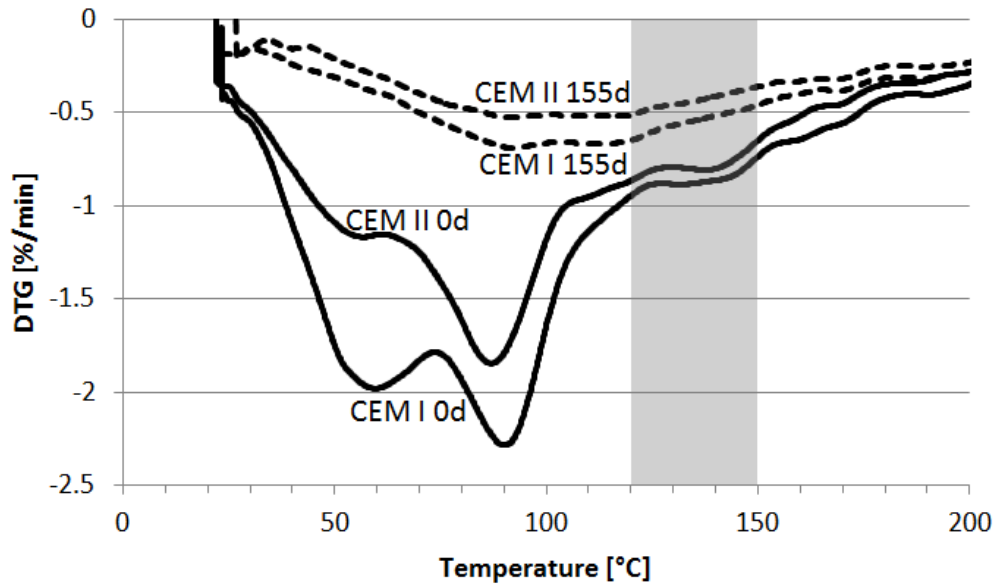

Figure 5.1   DTG curves for the non-carbonated (0d) and carbonated (155d) cement paste of CEM I and CEM II. Gypsum thermal dehydration takes place in the selected range.
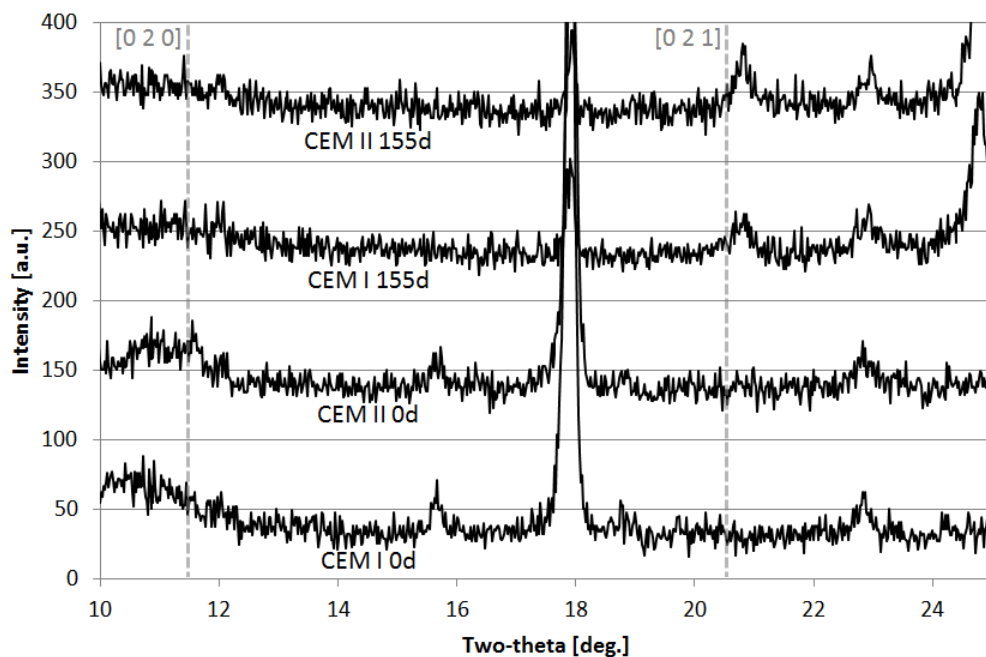

Figure 5.2   XRD spectra of for the non-carbonated (0d) and carbonated (155d) cement paste of CEM I and CEM II. The two most intensive gypsum reflection locations are indicated with the dashed line.

We have thus applied a novel approach for its identification, by monitoring the dissolution of Ca^{2+} and SO_4^{2-} ions from the fully carbonated samples. This was carried out by taking additional samples during the 7 days leaching experiment. Figure 5.3 shows the result of the dissolution monitoring experiment as the relation of 'SO_4^{2-} vs Ca^{2+}' concentrations, where the seven points for each cement type correspond to sampling at different time intervals (10min, 1hr, 6hr, 1d, 2d, 3d and 7d). The horizontal and vertical order follows the sampling time. The test revealed that the release of water soluble SO_4^{2-} and Ca^{2+} is highly correlated, as the 'SO_4^{2-} vs Ca^{2+}' trend lines show slopes ($a_{CEM\ I}=0.973$ and $a_{CEM\ II}=0.977$) and R^2 values ($R^2_{CEM\ I}=0.9998$ and $R^2_{CEM\ II}=0.9996$) close to 1. The shift from the y=x dotted line can be explained by an initial quick dissolution of some other Ca compounds. This demonstrates that the main source of the leached Ca^{2+} and SO_4^{2-} is a single compound characterized by $Ca^{2+}/SO_4^{2-} = 1$, proving calcium sulphate formation upon cement paste carbonation.
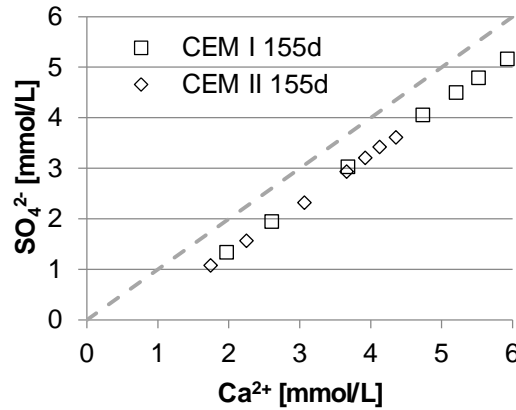

Figure 5.3   Correlation between leaching of SO_4^{2-} and Ca^{2+} ions from carbonated cement pastes. The dotted line represents a y=x equation.

5.3.2 Phase development and water soluble sulphate release

Figure 5.4 and Figure 5.5 show ettringite, CH and water soluble sulphate content evolution during carbonation of CEM I and CEM II pastes, respectively. Both plots are supported by the numerical data presented in Table 5.4 and Table 5.5. Each component exhibited phases of major change in its content. These phases are indicated in the graphs and in the tables; for the former by alternating each component's plot with solid and dashed lines, and for the latter in the 'Phases' row. The moment of their initiation and termination was estimated from the graphs. The water soluble sulphates originate from gypsum dissolution, as demonstrated in the previous section. Their levels were measured in leachates, which were characterised by varying pH depending on the progress of carbonation of the tested cement paste sample. Fresh samples could yield pH values as high as 12.45 (Taylor, 1997) due to the abundant presence of CH, while for the carbonated samples it could drop down to a level of 7-8 (Anstice *et al.*, 2005; Šavija and Luković, 2016). However, CH presence has only a slight decreasing effect on gypsum solubility (Taylor, 1997). Small amounts of monosulphate were detected by QPA in CEM I (AFm in Table 5.4), but not in CEM II (Table 5.5). Monosulphate is often poorly crystalline (Taylor, 1997) and lack of its identification by QPA does not preclude its presence in CEM II as well, but in a less crystalline form. On the other hand, calcite was added at similar level to both anhydrous CEM I and CEM II cements (Table 5.21) and its presence may prevent monosulphate formation during cement paste hydration (Kuzel and Pöllmann, 1991).

Figure 5.4 and Figure 5.5 confirm that both CEM I and CEM II pastes exhibited similar trends upon carbonation: the CH content decrease due to its carbonation to calcium carbonate, ettringite decomposition and water soluble sulphate release. The initial high level of RH hampered CH carbonation during the first days, as will be addressed in more detail in the following section. CH did not carbonate completely, but it equilibrated at a residual content of 0.5-1g/100g anhydrous. The ettringite decomposition appeared to be delayed and took place in two steps: a first one leading to a major drop in its content in a relatively short time, followed by a much slower decomposition of ettringite residues. The water soluble sulphate release also occurred in two stages: first a major release took place, which appeared

delayed in respect to ettringite decomposition, followed by a stagnant phase and a late final release. Their major release (SO_4^{2-}[1] phase) was initiated sooner for CEM II (18 days) than for CEM I (35d), but nevertheless for both cements it was completed within 84 days. The second release phase (SO_4^{2-}[2]) continued until the experiment termination, hence it cannot be excluded that further sulphate release was feasible. Small amounts of monosulphate were identified in CEM I paste, which similarly to ettringite decomposed upon carbonation. However, for the graphs' clarity, monosulphate evolution was not plotted, but included in Table 5.4.
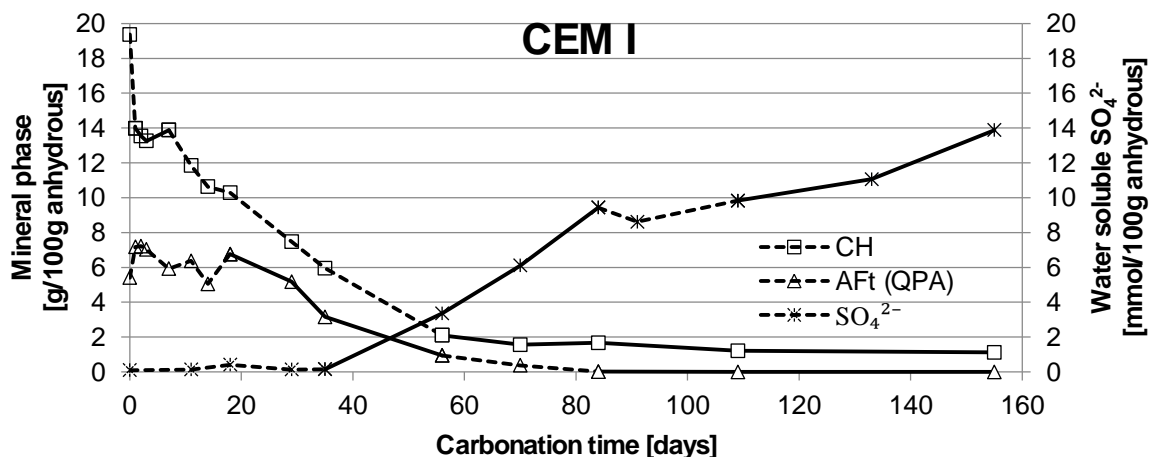

Figure 5.4   Ettringite (AFt(QPA)), CH and water soluble SO_4^{2-} content evolution upon CEM I paste carbonation. Each component's plot is alternated with solid and dashed lines; each segment corresponds to a phase distinguished in Table 5.4.
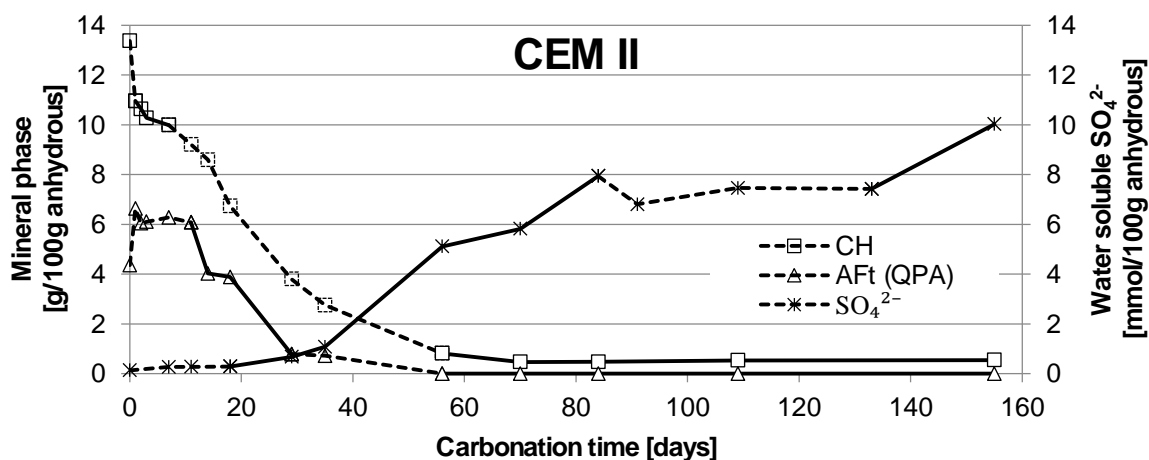

Figure 5.5   Composition evolution of CEM II paste, the graph outline is explained in the caption of Figure 5.4.

Table 5.4 Evolution of CEM I cement paste composition during the accelerated carbonation. For convenience, the monosulphate and ettringite names are shortened to their respective mineral group names: AFm and AFt. Minerals' content is expressed in g/100g anhydrous, while the extracted water soluble SO_4^{2-} in mmol/100g anhydrous. The ettringite content measured by TG is expressed qualitatively by: +++ initial content, ++ and + - moderate and low content relative to the initial one, respectively, ? possibly present, and - not identified. The periods of distinct content change are separately distinguished in the Phases row, and consecutively numbered for each component (e.g. CH[1]). These periods are also marked in the values rows by greyed cells. Next to the phase name a relative change expressed in percentage of the total change is provided. NA stands for not analysed.

CEM I							
Phases				Age [days]	AFt		SO_4^{2-} (ICP-OES)	CH (TG)	AFm (QPA)
					QPA	TG			
AFt QPA [1] (86%)	AFt TG	SO$_4^{2-}$ [1] (68%)	CH [1] (29%)	0	5.4	+++	0.1	19.4	0.7
				1	7.2	+++	NA	14.0	0.0
				2	7.2	+++	NA	13.5	0.3
				3	7.0	+++	NA	13.3	0.1
			CH [2] (65%)	7	5.9	+++	NA	13.9	0.5
				11	6.4	+++	0.1	11.8	0.4
				14	5.1	++	NA	10.6	0.3
				18	6.8	++/+++	0.4	10.3	0.3
				29	5.2	+	0.1	7.5	0.2
				35	3.2	+	0.2	6.0	0.0
AFt QPA [2] (14%)				56	0.9	?	3.4	2.1	0.0
				70	0.4	-	6.1	1.6	0.0
		SO$_4^{2-}$ [2] (30%)		84	0.0	-	9.4	1.7	0.0
				91	NA	NA	8.6	NA	NA
				109	0.0	-	9.8	1.2	0.0
				133	NA	NA	11.1	NA	NA
				155	0.0	-	13.9	1.1	0.0

Table 5.5 Evolution of CEM II cement paste composition during the accelerated carbonation. The table outline is explained in the Table 5.4 caption.

CEM II						
Phases				Age [days]	AFt		SO$_4^{2-}$ (ICP-OES)	CH (TG)
					QPA	TG		
AFt QPA [1] (87%)	AFT TG	SO$_4^{2-}$ [1] (79%)	CH [1] (19%)	0	4.4	+++	0.1	13.4
				1	6.6	+++	NA	11.0
			CH [2] (72%)	2	6.0	+++	NA	10.6
				3	6.1	+++	NA	10.3
				7	6.3	+++	0.3	10.0
				11	6.1	+++	0.3	9.2
				14	4.0	++	NA	8.6
AFt QPA [2] (13%)				18	3.9	++	0.3	6.7
				29	0.8	+	0.7	3.8
				35	0.7	+	1.1	2.8
				56	0.0	-	5.1	0.8
				70	0.0	-	5.8	0.5
				84	0.0	-	7.9	0.5
				91	NA	NA	6.8	NA
				109	0.0	-	7.5	0.5
		SO$_4^{2-}$ [2] (27%)		133	NA	NA	7.4	NA
				155	0.0	-	10.0	0.5

5.3.3 RH during carbonation

Figure 5.6 shows that the RH in the cabinet was not stable during the cement paste carbonation. The frequent and quick RH drops are related to disturbances by opening the cabinet for cement paste sampling. At these moments the RH meter was measuring the typically winter-low relative humidity (25-40% RH) of the laboratory room. Another disturbance can be observed in the period of 100d-113d. Humidity in the cabinet was controlled by a NaBr salt solution, while in this period water has completely evaporated from the salt dish. It was then immediately replenished, what restored a stable humidity level in the cabinet.

The initial high RH level was induced by placing the fresh and wet cement pastes into the carbonation cabinet. Upon their drying, the humidity was absorbed by the NaBr salt solution and the RH level progressively dropped to the level of approximately 53% RH. This initial high RH level has nevertheless influenced the CH carbonation rate. The composition evolution graphs (Figure 5.4 and Figure 5.5) and tables (Table 5.4 and Table 5.5) show that considerable amounts of CH carbonated over the first day (CH[1] phase), that could be attributed to the carbonation of the surface layers of cement paste grains. However, further carbonation was hampered until day seven. The optimal RH range for carbonation falls within 50-70% (Hewlett, 2004), while any higher RH may lead to water condensation in pores and their blockage, in consequence majorly hindering the carbonation process. Indeed, it took 7 days until RH level dropped below 70% (Figure 5.6), what explains the observed slower rate of CH carbonation.
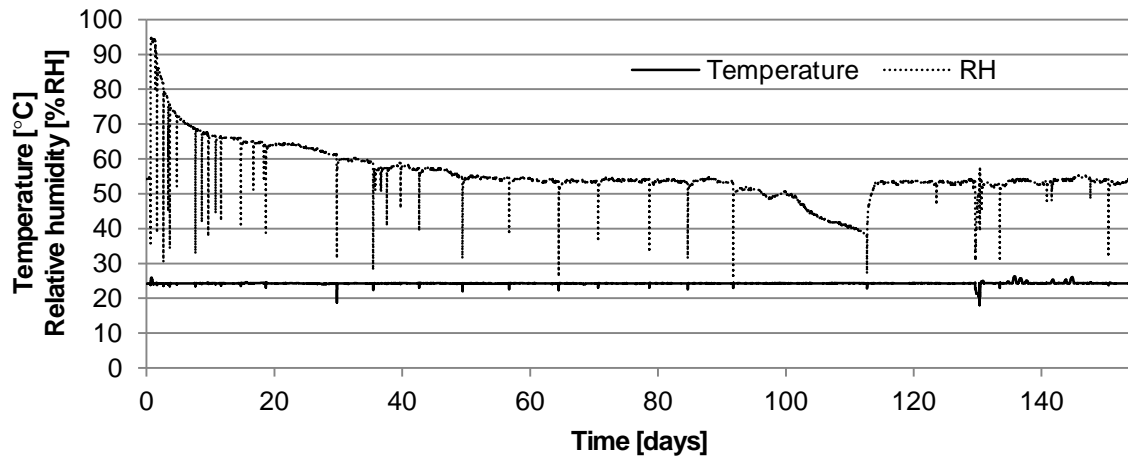
Figure 5.6 RH and temperature variation over the carbonation experiment duration.

5.3.4 CH delays ettringite decomposition

CH is a major product of OPC hydration, as reflected in its high content (19.4g/100g anhydrous) in the cured, non-carbonated CEM I paste. CEM II yielded much less CH (13.4g/100g anhydrous) due to the addition of fly ash and ground blastfurnace slag. Their effect is twofold: they simply dilute OPC whose hydration produces CH, and both components show pozzolanic activity leading to CH consumption during cement hydration (Snellings *et al.*, 2012). Ettringite decomposition is initiated at a pH below 10.7 (Myneni *et al.*, 1998), while CH contributes to its stabilisation by causing a higher pH. The ettringite decomposition was reflected by a drop in its content, as determined both by QPA and TG results (Figure 5.4 and Figure 5.5). Table 5.4 and Table 5.5 show that its initiation appears to be related to the CH content, as ettringite decomposition in both cements was initiated when CH reached similar threshold levels of 10.3 and 9.2g/100g anhydrous for CEM I and CEM II, respectively. This is consistent with the reported stabilising effect of CH on synthetic ettringite (Pajares *et al.*, 2003) and as a component of mortar (Brocken *et al.*, 2000). Ettringite decomposition was delayed by an induction period lasting approximately 18 days for CEM I and 11 days for CEM II (based on QPA results). The difference may be explained by a higher initial CH content in CEM I paste, that required more time for carbonation to reach the CH threshold level.

Table 5.4 and Table 5.5 show that the main ettringite decomposition phase AFt QPA[1] was considerably longer for CEM I (38 days) than for CEM II (18 days). Both cement pastes showed initially a similar CH content, therefore the observed difference cannot be attributed to this. However, the average rate of CH carbonation during the AFt QPA[1] phase for CEM II (0.30g/day) was higher by 36% than for CEM I (0.22g/day) and this can be attributed to the fly ash and granulated blast-furnace slag that CEM II contains and that have been reported to induce faster carbonation (Šavija and Luković, 2016).

5.3.5 Ettringite decomposition to gypsum

The leaching experiment showed that water soluble sulphate was released upon cement paste carbonation, while the leaching monitoring experiment identified its source as calcium sulphate. Table 5.4 and Table 5.5 demonstrate that the ettringite content (QPA) decreased during carbonation because of its structural decomposition (TG). Studies on carbonation of pure ettringite established that its TG peak decrease is indicative of decomposition of ettringite's structure and gypsum formation (Grounds *et al.*, 1988). However, Figure 5.4 and Figure 5.5 show that the sulphate release appears delayed with respect to the ettringite decomposition and took place in two steps.

Table 5.6 compares the amounts of sulphate released during carbonation with the amount which can possibly originate from the ettringite (AFt) and monosulphate (AFm) decomposition. The estimated amount of sulphates released from the ettringite (and monosulphate) decomposition is given as a range, because the content of ettringite quantified by QPA was varying during the initial induction period. This variation can be likely attributed to a particularly high sensitivity of both minerals to the sample preparation conditions. Both phases are reported to (partly) decompose upon drying, grinding and storage (Snellings, 2016). The measured total amount of water soluble sulphate released upon carbonation from

CEM I agrees with the possible amount formed upon decomposition, while for CEM II is stays only slightly lower. This corroborates the hypothesis that the main source of gypsum formed during cement paste carbonation is the decomposition of ettringite and monosulphate. The content of both phases in cement paste determines thus the abundance of potential GE source. On the other hand, the observed delay and sulphate release in two steps reflect the complex nature of the mechanism of hydrated cement carbonation and is at odds with the direct process observed for the pure ettringite (Grounds *et al.*, 1988). It may be hypothesised that ettringite decomposition in cementitious materials might go through some intermediate decomposition steps until gypsum is formed, but more evidence is required to elucidate the nature of this reaction. This could be possibly addressed with synchrotron X-ray powder diffraction, a method providing higher resolution and accuracy than the XRD method used here.

Table 5.6 Comparison of the SO_4^{2-} containing phases in cement paste: ettringite (AFt) and monosulphate (AFm) with the amount of water soluble sulphate released during the first sulphate release phase (SO_4^{2-} [1]) and the total amount (Total SO_4^{2-}) after 155d carbonation. The content of AFt and AFm is recalculated to the amount of sulphate which would be released upon their complete decomposition based on their chemical formula. The AFt amount is given as a content range during the induction period, while for AFm its initial value is used. The SO_4^{2-} (WD-XRF) is the amount of sulphate in anhydrous cement, recalculated from the WD-XRF data on SO_3 in Table 5.2.

CEM I	g/100g anhydrous	mmol SO_4^{2-}/100g anhydrous
AFt	5.1 - 7.2	12.1 - 17.3
AFm max	0.7	1.1
AFt + AFm	-	**13.1 - 18.3**
SO_4^{2-} [1] (ICP-OES)	-	9.4
Total SO_4^{2-} (ICP-OES)	-	**13.9**
SO_4^{2-} (WD-XRF)	4.6	**47.6**

CEM II	g/100g anhydrous	mmol SO_4^{2-}/100g anhydrous
AFt	4.4 - 6.6	**10.4 - 15.9**
SO_4^{2-} [1] (ICP-OES)	-	7.9
Total SO_4^{2-} (ICP-OES)	-	**10.0**
SO_4^{2-} (WD-XRF)	6.0	**62.9**

CEM I paste yielded more sulphate release upon carbonation than CEM II (Total SO_4^{2-}), although anhydrous CEM I contained less sulphur than CEM II (SO_4^{2-}(WD-XRF)). The latter was also reflected by a lower content of calcium sulphate(s) in the cement composition (see anhydrite and gypsum in Table 5.1). Moreover, only a small fraction of sulphur (CEM I - 29%, CEM II -16%) from anhydrous cement was released as water soluble SO_4^{2-} upon ettringite and monosulphate breakdown. It indicates that a major amount of sulphate might be persistently bound in other hydrated cement phases, which did not release upon carbonation. CSH phase is the main product (60-70wt%) of cement hydration (Spence, 1992). Fu et al. (1994) reported that it can indeed accommodate considerable amount of sulphate ions (even 5wt% of gypsum as compared to the mass of C3S used for CSH preparation). However, it needs to be noted that this high capacity was questioned in other studies (Škapa, 2009). While the results of this study suggest that sulphates were absorbed by a CSH phase, it would be worth confirming it by SEM-EDS or microprobe analysis of the CSH phase to determine its sulphur content. However, this is out of the scope of the present project and should be addressed in future studies.

The major ettringite (AFt QPA [1] phase) and monosulphate decomposition was accomplished by the end of the major CH carbonation phase (CH(2) phase), see Table 5.4 and Table 5.5. Therefore, substantial CH carbonation can be used as an indicator of ettringite and monosulphate decomposition in cementitious systems, and it can be conveniently measured with TG and QPA methods. However, it may be not applicable to all cases, as ettringite was identified in cement mortar joints, where CH was completely carbonated to calcite (Brocken *et al.*, 2000). Gypsum formation is delayed compared to ettringite decomposition and considerable amounts may still be immobilised in the intermediate ettringite's decomposition products, even when CH carbonation is virtually completed.

5.4 Discussion

5.4.1 Carbonated mortar as a GE source

The reported concrete carbonation rates are rather slow, between 0.06 and 1.20 mm per year (Pade and Guimaraes, 2007), appearing to contradict the hypothesis of GE source formation in masonry joint. However, masonry (cement) mortar may completely carbonate within two years (Brocken *et al.*, 2000), while there are also known cases where one year was sufficient[1]. This is attributed to the fact that a thin (10-12mm) mortar joint is surrounded by a porous brick, which provides a high contact surface with CO_2 from air compared to the joint's volume. Moreover, mortar joints (Derluyn *et al.*, 2011) are typically more porous than concrete (Kumar and Bhattacharjee, 2003). In literature, the statement of full carbonation is mostly related to the observation of complete portlandite carbonation, while this study establishes that gypsum formation is delayed and may be only partly released at this stage. Nevertheless, GE is reported to develop after a couple of years only hence it is feasible that a major sulphate release could have occurred by that time. It corroborates then that gypsum formation in a mortar joint is likely to happen in masonry, providing a GE source. Moreover, the time required for the carbonation of a mortar joint may also explain the observed delay in GE formation.

5.4.2 Effect of SCMs and lime on GE source formation

The formation of GE source upon cement paste carbonation is dependent on the CH content which controls the pH of the pore fluid and hence the ettringite and monosulphate stability. While pozzolanic SCMs accelerate carbonation, lime addition may delay, or even virtually arrest it.

SCMs' impact on cement carbonation and gypsum formation

Limestone is used in commercial cements as filler, and its addition affects cement paste carbonation. Typically calcium carbonate precipitates on the CH crystals, creating a protective layer which hampers the carbonation process. However, in presence of limestone addition, its fine particles become the preferential locations for calcite precipitation, hence inducing a faster and more extensive CH carbonation (Šavija and Luković, 2016). Moreover, the results of this study confirmed reported accelerated cement paste carbonation for cement composition containing pozzolanic SCMs (Šavija and Luković, 2016). It was reflected by faster steps of a chain reaction leading to gypsum formation. First, addition of SCMs induced both lower initial CH content, and its faster carbonation than in OPC. In turn ettringite decomposed both sooner and faster. In consequence, the last reaction – delayed gypsum formation was initiated earlier than in pure OPC and the present study has revealed that the major sulphate release has been accomplished at the same time.

While both limestone and pozzolanic additions accelerate CH and ettringite carbonation in cement paste, they do not necessarily induce a faster gypsum formation. This effect has not been observed for the investigated cement containing additions of fly ash and blast furnace slag, while for cement formulations with limestone no such data is available yet.

Lime addition stabilises ettringite

It has been demonstrated that CH stabilises ettringite in cement paste, however upon its carbonation CH transforms to calcite and may lead to ettringite decomposition back into gypsum. This process can possibly be hindered by substituting part of anhydrous cement with CH. Lime mortars have been used in masonry over centuries, however they were superseded by Portland cement for commercial applications. Nowadays, lime and cement-lime mortar are still in use, but mainly for conservation purposes.

The effect of lime addition on carbonation of masonry joints was investigated by Brocken *et al.* (2000). Lime addition to OPC resulted in formation of a narrow and dense carbonation zone in the masonry joint, which mainly hindered further CO_2 diffusion. The carbonation zone was followed by a CH enriched zone. It was reported that for a 2 year old masonry mortar the joint was depleted in ettringite only in a 0.5mm carbonation zone, while it was still present in the internal CH-rich zone. No such effect was observed for an OPC mortar without lime addition, in which CH carbonated completely throughout the

---

[1] Jan Elsen, personal communication

mortar joint. Cement-lime mortars may thus hinder ettringite and monosulphate decomposition, preventing hence from gypsum formation in masonry mortar.

5.4.3 Limiting calcium sulphate(s) addition

The amount of calcium sulphate formation upon cement paste carbonation can be limited by reducing its addition to the anhydrous cement. This could be possibly achieved in two ways: by limiting the ratio of calcium sulphate(s) addition in the clinker, or by diluting the OPC with SCMs.

Optimum sulphate content of cement

Taylor (1997) reviewed the literature on sulphate optimisation in Portland cements. Optimisation of the setting properties requires typically at least 2% SO_3, which originates from the cement components and calcium sulphate(s) addition. Adding more has little effect on setting, as long as it does not lead to a 'false set', gypsum precipitation from solution supersaturated by hemihydrate. Moreover, too high addition may lead to damaging expansion in water as reflected by SO_3 content constrained by national normatives to levels of around 2.5-4.5%. Because of the complex nature of sulphate optimisation, the calcium sulphate(s) addition is usually derived empirically based on strength tests. A recent study on four cement types (Tsamatsoulis and Nikolakakos, 2013) has demonstrated that cements with no addition of calcium sulphate(s) yielded 85-90% of their optimised strength, at SO_3 levels of 0.75-1.47wt% only (SO_3 originating from cement components). It demonstrates hence that major reduction in sulphate content does not significantly compromise the strength performance. Such low levels might possibly be insufficient for providing desirable setting properties, but it nevertheless reveals potential for a sulphate content decrease and hence the GE-risk reduction.

Diluting effect of SCMs

There are numerous cement compositions available commercially which contain SCMs. As their addition dilutes the OPC, these cements contain less of the reactive aluminate phases. In consequence, it potentially limits the necessary calcium sulphate(s) addition. It is indeed reported that the optimum calcium sulphate(s) addition decreases with the degree of clinker replacement by blast furnace slag and limestone (Ghosh, 2003) as well as for natural pozzolana and fly ash as confirmed by the recent study of Tsamatsoulis and Nikolakakos (2013).

Final Remarks

The sulphate content of cement can be possibly lowered by both decreasing calcium sulphate(s) content and addition of SCMs. Nevertheless, the cement producers prefer to shift the sulphate content to the higher boundary allowed by normatives to effectively counteract shrinkage, as well as to reduce the price of Portland cement due to lower price of gypsum (Škapa, 2009). Therefore, reduction of sulphate content in commercial cements appears feasible, and should not result in significant alteration of their performance.

5.5 Conclusions

An experiment for monitoring phase development upon cement paste carbonation was successfully designed and implemented. Application of a novel experimental approach yielded identification of calcium sulphate in carbonated cement paste. This corroborates that both ettringite and monosulphate present in cement paste decompose to calcium sulphate, as previously reported for synthetic phases only. Both brick and carbonated mortar joint can thus serve as GE sources in masonry. While the content of CH showed an effect on carbonation rate and delay of ettringite decomposition, it did not affect the rate of gypsum formation significantly. However, this interpretation is restricted to the investigated two cement types, as deliberate addition of lime to cement may substantially hinder the carbonation process and thus the amount of formed gypsum. This can be achieved also by limiting the calcium sulphate(s) addition to cement, as it appears that its reduction to some level should not compromise significantly its performance. Both ways may hence possibly limit a risk of GE by minimising the amount of gypsum formed upon mortar joint carbonation, but they require further research.

6 Accelerated gypsum efflorescence

6.1 Introduction

In the past thirty years, we have seen a dramatic increase of GE cases for ceramic brick masonry. Its characteristic features indicate that the GE source is the masonry itself, while the formation process involves source dissolution, moisture transport and efflorescence formation. Moreover, GE has most likely been triggered by some recent changes in the properties of masonry constituents.

However, up to now, neither a method for its assessment nor a solution to the problem is available. Even though there are numerous well-established experimental methods dedicated to investigating the impact of crystallisation of well-soluble salts on porous building materials (Espinosa-Marzal and Scherer, 2010; Lubelli et al., 2014), these have rarely been applied to gypsum. The reason lies on the one hand in the fact that gypsum is mostly discussed in relation to the formation of black gypsum crusts via interaction with air pollution (Charola et al., 2006). Simulation of these requires specific tests. On the other hand, GE is a relatively recent problem and exclusively affects masonry. The only experimental study addressing GE was carried out by Bowler and Winter (1997), but their test procedure reveals many drawbacks. The main disadvantage is the at-least-one-year duration, which is far too long for applied research or quality control applications. The available knowledge on GE indicates that an optimal test method should be capable of separately assessing the contributions of: (i) the brick's GE-source; (ii) the mortar's GE-source; (iii) the impact of mortar admixtures; and (iv) the brick moisture properties towards the GE-risk. The Bowler and Winter (1997) procedures do not fulfil these requirements; instead they simultaneously address a combination of these factors. Moreover, the actual GE formation mechanism remains unclear. While common salts like NaCl simply form efflorescence upon drying (Rodriguez-Navarro and Doehne, 1999), gypsum demonstrates the apparent tendency to accumulate just beneath the brick's surface under wick test conditions (Franke and Grabau, 1994, 1998). This clearly contrasts with the widespread GE occurrence in the field. On the other hand, the investigations by Bowler et al. (1997, 1998) suggest that surface precipitation of gypsum can be triggered in presence of mortar admixtures.

This results in a situation where the producers of construction materials are helpless in preventing GE, as there is no experimental test method allowing for a fast and reliable GE-risk assessment. Since GE is getting progressively more common and pronounced every year, an urgent and effective solution is necessary. The first and required step is hence providing a test method capable of identifying the factors responsible for the recent outbreak of this persistent surface blemish. Our main aim is therefore to develop an accelerated test method (ATM) which reliably reproduces GE formation. The developed test method should be versatile, by being adjustable for separate testing of the contributions of brick and mortar GE-sources, brick moisture properties and mortar admixtures towards the GE-risk. Next to this, the results of the optimized test applied to gypsum solution should shed light on the controversies regarding gypsum's subflorescence tendency, which contrasts with the widespread GE occurrence in practice.

The chapter starts with the Section 6.2, introducing the ATM and providing its detailed description. The discussion of results is distributed over two sections. The ATM methodology deviates from the common efflorescence tests, hence its validation is addressed in Section 6.3. Particular attention is given also to the issue of the gypsum's subflorescing behaviour, which is controversial compared to the commonly observed GE. The ATM development required applying numerous improvements, and these are illustrated with dedicated experiments in Section 6.4. The chapter is summarised in Section 6.5, while accessory data are gathered in appendices in Sections 9.1.2 and 9.1.3.

6.2 Accelerated test method

The optimized ATM setup is a final version of a setup gradually developed from the basic wick test design (Figure 2.1). While the latter already brought several improvements in comparison to Bowler and Winter's set-up (Bowler and Winter, 1997), a first series of tests revealed that it still suffered from numerous flaws. Several attempts were hence undertaken to improve it, resulting in numerous modifications applied to the

basic wick test setup and protocol. They are first introduced in the sections below, and then addressed in more detail in the following ones.

6.2.1 Experimental protocol

In order to control well the climate conditions and assure their even level for multiple setups tested simultaneously, it was decided to carry out the experiments in a climate cabinet (Weiss SB22 1000, Figure 6.1 C), which was capable of accommodating 108 setups distributed over two levels. Every test variation was realised with four setups (=1set) distributed evenly in the cabinet, which allowed for testing a maximum of 27 sets at one time.

Calcium sulphate occurs in the mineral forms of anhydrite ($CaSO_4$), hemihydrate ($CaSO_4{\cdot}0.5H_2O$) and gypsum ($CaSO_4{\cdot}2H_2O$), but only the latter species was found in the GE cases from the field survey. The experimental conditions were thus carefully adjusted to accelerate the physical processes behind efflorescence formation without however inducing the formation of the other calcium sulphate species. Gypsum dehydration to hemihydrate may occur already above 40°C (Charola and Centeno, 2002), hence the experimental temperature was chosen at 35 ± 2°C. Humidity was set at 21% ± 4% RH, which was the limit for the climate cabinet in use. These conditions differ much from the average Belgian climate: the average monthly temperatures in Brussels vary between 3.3°C (average for January) and 18.4°C (average for July), while the average monthly relative humidity varies between 72.5% (average for April) and 88.8% RH (average for December)[1]. The test conditions were hence preliminarily validated by running a simple gypsum crystallisation test. Gypsum solution (2.2 g/L) was placed on a glass dish in the climate cabinet and left to evaporate. After one day the deposit from the glass dish was collected and identified as gypsum by XRD. These optimised and validated conditions are referred later as 'accelerated conditions'. In a few instances the efflorescence tests were realised under laboratory conditions (24 ± 2°C, 53 ± 7% RH).
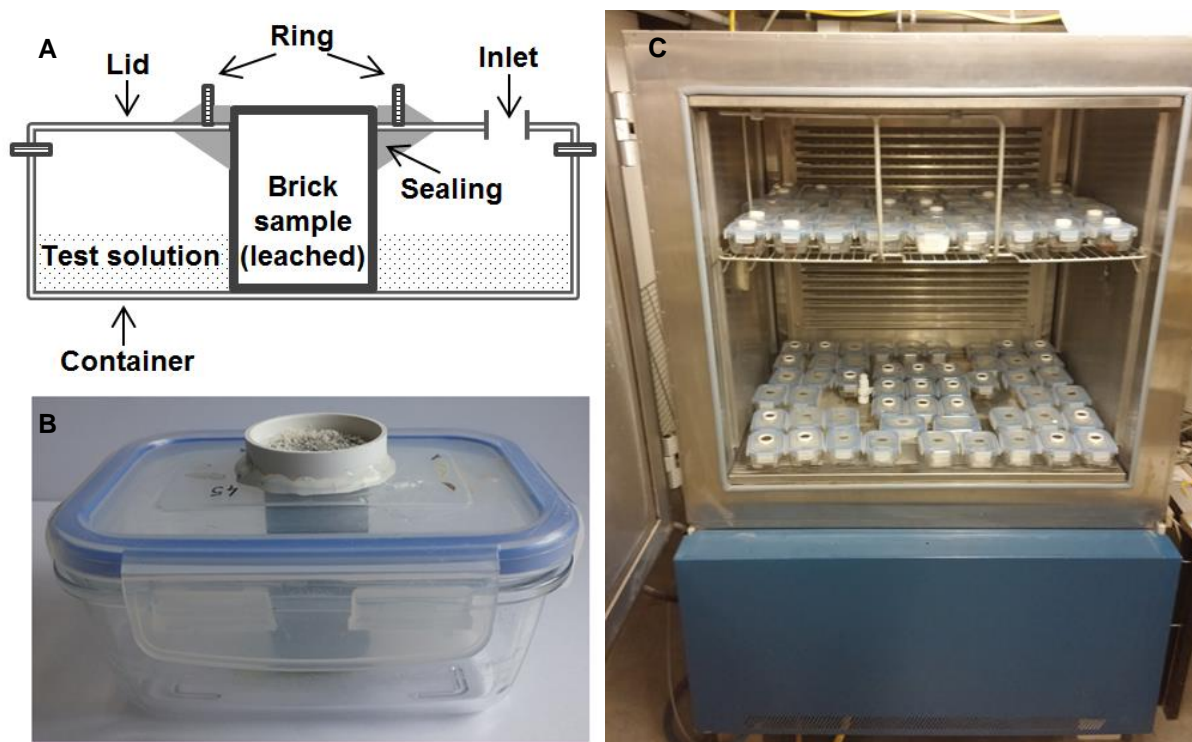

Figure 6.1   Scheme (A) and a photograph (B) of the optimized ATM setup, and a climate cabinet filled with the ATM setups (C)

---

[1] https://www.meteo.be/meteo/view/fr/360955-Normales+mensuelles.html [Accessed 9 May 2017]

The experimental protocol was based on a basic wick test (Figure 2.1 and Figure 6.1 A and B), where a porous sample (transport medium) stays in continuous contact with a test solution. Upon their contact the test solution is absorbed by a porous medium due to capillary action and transported to the surface, where drying takes place. The extent of the latter depends on temperature, relative humidity and air speed. The basic wick test protocol was modified by introducing frequent wetting phases, i.e. applying 3ml distilled water (measured with an automatic pipette Transferpette) to the sample surface. This procedure served the purpose of mimicking the process of frequent wetting of masonry surface by wind-driven rain. The presence of the wetting ring (Figure 6.1 A and B) assured repeatable and complete wetting of the bricks samples' surfaces. Afterwards, the setups were covered with a plastic foil to limit evaporation, and stored under laboratory conditions for the duration of the wetting phase.

The experimental schedule is shown in Figure 6.2. Before the test, photographs of the raw dry samples were taken. The test started with a wick phase, which was then alternated with wetting phases over five days. Each wetting and wick phase took approximately 8 and 16 hours respectively, except for the first wick phase lasting for 24 hours. Before and after each wick phase the whole setups were weighed. The procedure was repeated until Friday evening, when the lids containing the brick samples were detached from the setups and dried in the climate cabinet over a weekend under the test conditions. On Monday morning the dry samples were photographed, the lids with brick samples were then mounted back to their respective setups and the WW cycling was restarted. When needed the test solution could be replenished via the perforated inlet. After four weeks the test was terminated and the efflorescence was sampled and analysed by XRD and HCl test methods.
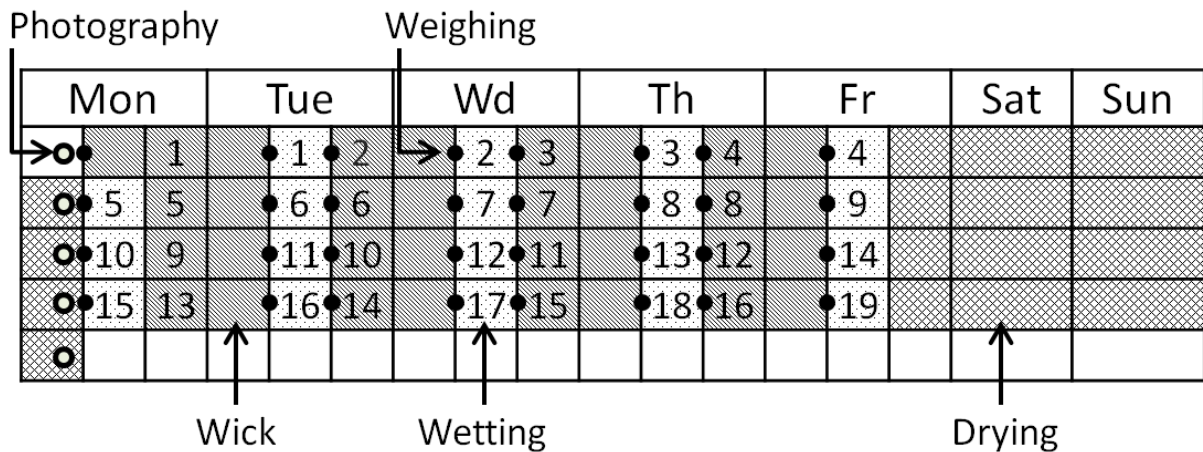

Figure 6.2   The default experimental schedule for the optimized ATM. The wick and wetting phases are consecutively, but separately numbered.

6.2.2 Optimised setup

The leached brick sample, the lid and the plastic ring (Figure 6.1 A and B) were all sealed together with a hot melt adhesive. The plastic ring (⌀ = 37mm, height = 10mm) was positioned so it surrounded the exposed sample surface. The lid contained an inlet (⌀ = 5mm) covered with a perforated scotch tape.

Brick sample

The GE extent appreciation depends on the type and colour of a brick surface, therefore one brick type was consistently used in this study as an efflorescence medium. The choice of the brick type was made among bricks identified during the Field Survey (see FS19 case in Chapter 4), with a preference for a dark coloured brick that would contrast well with the whitish efflorescence.

Cylindrical samples (⌀ = 30mm, height = 62mm) were drilled out of a set of bricks randomly selected from a brick pallet (density 1826 kg/m^3, capillary absorption coefficient 0.68 kg/(m^2·s$^{0.5}$), capillary and saturated moisture content 210 and 325 kg/m^3 respectively). Three samples per brick were cut perpendicular to the brick's stretcher (the exposed brick side in a masonry wall), which then served as the exposed brick core side during the test. This way the test simulated efflorescence formation on the same

side as under field conditions. After drilling, samples were subjected to a leaching procedure by placing them in a tank with demineralised water maintained at a temperature of 40°C. Each 24 hours the leachate's conductivity was measured, after which the samples were again submerged in fresh demineralised water. This procedure was repeated until the measured leachate conductivity reached a constant background value. Once this was achieved, samples were oven-dried at 105°C.

Test solutions

Depending on the research question, the test solution could be pure water, a salt solution, or water mixed with masonry components being evaluated as a GE source, i.e. powdered brick or carbonated cement paste. On the other hand, the setup could be also easily adjusted for testing solely the effect of admixtures on the GE-risk, by adding admixtures to the gypsum solution. Furthermore, the brick cores could be prepared from different types of brick to assess the effect of their moisture properties.

The salt solutions were prepared from pro analysis quality salts: calcium sulphate dihydrate (gypsum, $CaSO_4 \cdot 2H_2O$) (Section 6.3.2) or sodium chloride (halite, $NaCl$) (Section 6.3.1). Both salt solutions were prepared at the same concentration of 2.2 g/L, equivalent of 85% gypsum saturation at 20°C (Charola *et al.*, 2006). This limits the effect of the higher $NaCl$ solubility on the formation rate and extent of efflorescence. For convenience, we refer to the experimental setups containing brick samples impregnated with different salts or pure water, by simply gypsum, $NaCl$ or water setups.

6.2.3 Summary of setup and protocol

The modifications applied to the setup are illustrated in Figure 6.1 A and B, and relate to:
- selecting an inert adhesive type applied for sealing,
- mounting a plastic ring surrounding the sample surface,
- providing a perforated inlet in the lid,
- and leaching the brick sample prior to the test.

Furthermore, a test protocol was developed to:
- run multiple tests simultaneously by using a climate cabinet providing constant and even climate conditions,
- accelerate the efflorescence formation by optimizing the climate conditions,
- simulate rain episodes under field conditions by applying frequent surface wetting,
- monitor the setups' drying rate by collecting and processing their weight over the duration of the experiment,
- obtain high quality photographs of the brick surface and efflorescence by optimizing the photography procedure,
- quantify the efflorescence extent by applying digital image analysis to the collected photographs,
- and identify efflorescence species with the aid of the XRD and HCl analysis.

6.2.4 Data collection and processing

Drying rate

The aim of the frequent weighing (Mettler Toledo PB3002-L balance with ±10mg precision) was to monitor the drying rate (DR) evolution. The drying rate expresses the rate of water evaporation normalised to the drying surface area. The drying process takes place at the sample surface, hence salt crystallisation at or below the sample surface might alter the setup's wick behaviour, which can be diagnosed by means of the DR graphs. The setup's mass varied during the experiment, due to frequent wetting application followed by wick periods, as illustrated in Figure 6.3. The whole setups were weighed: before the wetting phase (m_1): between the wetting and wick phase (m_2); and, after the wick phase (m_3), and the corresponding times t_1, t_2 and t_3 were recorded.

The wetting phase started with a wetting of the sample's surface (3ml of water), which is then mostly absorbed by a brick, and partly lost due to evaporation. The setup's mass after the wetting phase equals hence to:

$$m_2 = m_1 + \Delta m_{abs} \tag{Equation 6.1},$$

where Δm_{abs} is the mass of water absorbed by a brick sample. During the wick phase water evaporated at the brick surface, first the absorbed wetting water (Δm_{abs}), followed by the test solution water (Δm_{TS}). The setup's mass after the wick phase can be hence expressed as:

$$m_3 = m_2 - \Delta m_{abs} - \Delta m_{TS} = m_1 + \Delta m_{abs} - \Delta m_{abs} - \Delta m_{TS} = m_1 - \Delta m_{TS} \tag{Equation 6.2}.$$
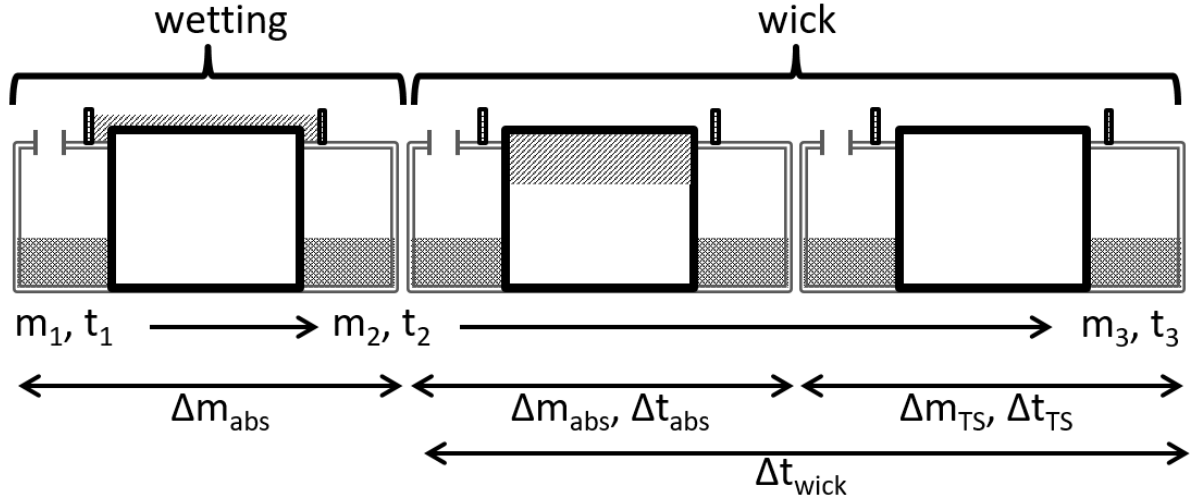

Figure 6.3 Mass changes during the wetting and wick phases.

The DR for the n-th wick phase can then be expressed as:

$$DR_n = \frac{\Delta m_{TS,n}}{A \cdot \Delta t_{TS,n}} \ [\text{kg/(m}^2\text{·day)}] \tag{Equation 6.3},$$

where: DR_n is the drying rate during the n-th wick phase, $\Delta m_{TS,n}$ is the mass loss due to water evaporation from a test solution during the n-th wick phase, A is the surface area of the exposed brick surface, and $\Delta t_{TS,n}$ is the duration of the test solution evaporation during the n-th wick phase.

The Δm_{TS} can be derived directly from the Equation 6.2: $\Delta m_{TS} = m_1 - m_3$, while the duration of the test solution wick equals to:

$$\Delta t_{TS} = \Delta t_{wick} - \Delta t_{abs} = t_3 - t_2 - \Delta t_{abs} \tag{Equation 6.4},$$

where Δt_{wick} is the duration of the total wick phase, and Δt_{abs} is the duration of the wetting water wick.

The Δt_{abs} is unknown and was estimated from the average wick rate of the ATM setups tested with water under accelerated conditions: $\Delta t_{abs} = 0.01$ days (see the W setup in Table 6.13). The DR_n can be hence calculated using the following equation:

$$DR_n = \frac{m_{1,n} - m_{3,n}}{A \cdot (t_{3,n} - t_{2,n} - 0.01)} \ [\text{kg/(m}^2\text{·day)}] \tag{Equation 6.5}.$$

Figure 6.4 shows three typical drying behaviours found in this study: high drying rate (High DR) maintained over the course of the experiment for the setups tested with water (W set), a rapid drying rate drop (DR drop) occurring for the setups tested with gypsum solution (G set), and a moderate drying rate drop (Moderate DR drop) for a modified setup tested with gypsum solution (G-S2 set).
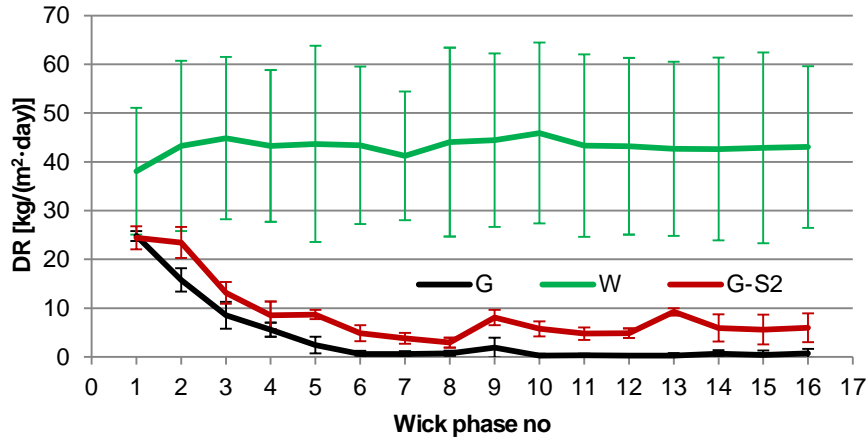
Figure 6.4 Examples of different drying rate behaviours.

The total mass of water evaporated from the test solution after n wick phases (CE_n, cumulative evaporation) was determined according to the following equation:

$$CE_n = \frac{\sum_{i=1}^{n} m_{1,i} - m_{3,i}}{A} \ [\mathrm{kg/m^2}]$$

(Equation 6.6).

Digital image analysis

The formed efflorescence was frequently photographed (Figure 6.2) to monitor its changes. Efflorescence is less apparent on a wet sample surface, hence the brick samples were dried before photographing (see Section 6.4.1 for details). A photography stand was placed in a room with no daylight ingress, and the working area was illuminated by room lighting and two side lamps, to create stable and repeatable light conditions (Figure 6.5). The JPG photographs were taken with a Canon G10 mounted on a tripod, using the following fixed settings: white balance calibrated with a grey card, resolution 4416 x 3312, F-stop f/8, exposure 1/5 sec., ISO 80, small AF frame, centre-weighted average metering mode, macro mode, and 2 sec. shutter delay.

Figure 6.5 Photography stand.

The collected photographs (Figure 6.6 A) were treated with ImageJ software to determine the efflorescence coverage (%E) on the entire top brick surface. They were first transformed to an 8-bit grey scale and subsequently to black and white by applying a threshold of 130-255 (Figure 6.6 B), yielding an image where white pixels corresponded to efflorescence and black ones to the unaffected brick surface. The threshold range was chosen based on multiple trials (by visual assessment), aiming at maximizing the overlap of actual efflorescence coverage on original photographs with white pixel coverage resulting from image analysis. Calculation of the non-normalized efflorescence coverage (IA) required (i) activating the 'Area fraction' setting, (ii) selecting the brick surface only, (iii) and applying the measure tool.
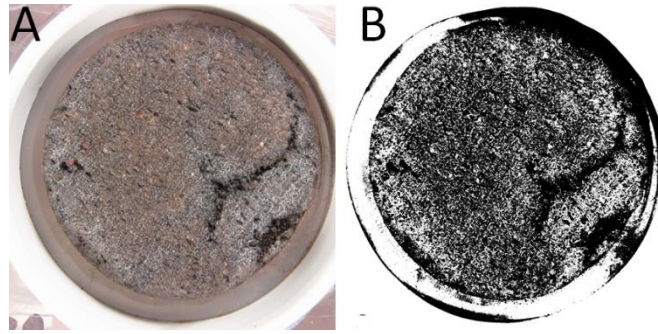
Figure 6.6 The original photograph (A) and after transforming to grey scale and applying a B&W threshold (B).

The efflorescence coverage after n wick phases (IA_n) was normalised against the raw sample surface appearance (IA_{raw}) yielding the normalised efflorescence coverage after n wick phases ($\%E_n$):

$$\%E_n = \frac{IA_n - IA_{raw}}{100 - IA_{raw}}$$
(Equation 6.7).

Deposit identification

Two samples per set were analysed for efflorescence composition: one by XRD and the second with an HCl test. Selected samples were also examined with SEM and analysed with an Energy Dispersive X-Ray setup. A detailed description of procedures can be found in Sections 3.4.1, 3.4.4, and 3.5.3.

6.3 ATM validation

The ATM was typically carried out under accelerated climate conditions (of $35 \pm 2°C$ and $21 \pm 4\%$ RH), which raises the question of its dependability. Therefore, an ATM validation was executed by investigating whether this procedure reproduced the expected crystallisation behaviour of halite and gypsum.

6.3.1 Halite efflorescence

Gypsum is reported to preferentially accumulate within the porous material, what is sometimes explained by its low solubility and thus mobility (Charola et al., 2006; Steiger and Heritage, 2012). In contrast, NaCl is reported to show high propensity towards abundant efflorescence formation (Rodriguez-Navarro and Doehne, 1999). It crystallises under the same mineral form of halite under both laboratory and accelerated climate conditions, it thus constitutes a good proxy for validating the efflorescence test and additionally evaluating gypsum crystallisation behaviour. To partly account for the effect of low gypsum solubility, the NaCl solution was prepared at the same concentration as the gypsum solution (2.2 g/L, solubility of NaCl - 357g/L). The sodium chloride setups performance was compared under laboratory and accelerated conditions, see Table 6.1 for the details on the setups' design and test protocol.

The test protocol applied to NaCl setups did not include WW cycling, as NaCl is highly soluble and each wetting phase would have likely completely dissolved the precipitated salt. In consequence, the default experimental schedule was not followed; instead the setups were subjected to a continuous wick regime. This yielded considerable differences in the total wick phase duration for both 'Accelerated wick' and 'Laboratory wick' schedules. In addition, the duration of the 'Laboratory wick' schedule was extended to 154 days due to a very slow formation of NaCl efflorescence.

Table 6.1   Overview of the ATM experiment variations and their settings. The setups' names are coded according to the following scheme: Y-Z, where Y stands for the test solution, while Z describes a deviation from the optimal ATM procedure. The test solution is distilled water (W) or a salt – halite (NaCl) or gypsum (G) dissolved in distilled water.

The Z can stand for:
- using a silicone adhesive of type 1 or 2 (-S1 or -S2) instead of the hot melt adhesive;
- using brick samples with cut surface (-CS) instead of ones with original surface;
- using non-leached brick samples (-NL) instead of leached ones;
- carrying out the test under laboratory climate conditions (-lab, $24 \pm 2°C$, $53 \pm 7\%$ RH) instead of the accelerated ones ($35 \pm 2°C$, $21 \pm 4\%$ RH);
- or carrying out the test under continuous wick conditions (-wick), instead of applying the WW cycling.
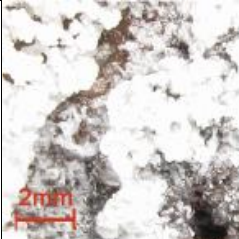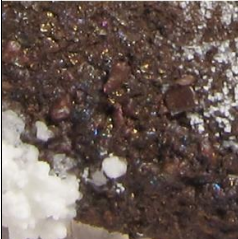
In many cases the deviations from the default settings induced modifications to the default experimental schedule, hence also the characteristic 'test duration' and 'test solution wick duration' are provided. The darker cells correspond to settings which deviate from the default settings.

Code	Default settings	NaCl-wick	NaCl-lab wick
Test solution	*Any*	*NaCl*	*NaCl*
Adhesive	Hot melt	Hot melt	Hot melt
Surface	Original	Original	Original
Leaching	Leaching	Leaching	Leaching
Climate	Accelerated	Accelerated	Laboratory
Wick / WW	WW	Wick	Wick
Schedule	Default (Figure 6.2)	Accelerated wick	Laboratory wick
Test duration	28 days	20 days	154 days
Test solution wick duration *	8 days	20 days	154 days
# of setups	4	4	4

* The 'test solution wick duration' does not account either for the wetting phase duration, or for the wetting water evaporation during the wick phase. For instance, the optimized ATM took 28 days in total, while the wick phases lasted for ten days, out of which eight days were spent on the test solution wick.

Table 6.2 shows that both NaCl test variations yielded abundant NaCl efflorescence, therefore the wick test under accelerated conditions reproduces correctly the expected effloresing propensity of NaCl (Rodriguez-Navarro and Doehne, 1999).

Table 6.2 Summary of the ATM experiment on NaCl setups. The efflorescence coverage for the sample shown in the picture is followed by the average value ± standard deviation (SD) for a set of four samples. The relative mineral content estimated by XRD is approximated: + + + dominantly present, + + present, + present in low amounts, ? possibly present, – no efflorescence mineral phase identified. The amount of efflorescence which is dissolved by HCl is expressed as: + + + complete dissolution, + + major dissolution, + partial dissolution, – no reaction. The efflorescence composition is evaluated based on the XRD and HCl test results, the ? mark stands for an unknown efflorescence species. In addition, descriptive drying behaviour categorisation is provided together with an overview and magnified sample's photography in the end of the test. A more detailed summary of the initial and final DR, and the final efflorescence extent can be found in Section 9.1.2.

Setup's code	NaCl-wick	NaCl-lab wick
Efflorescence coverage	91 (90 ± 4) %	22 (25 ± 9) %
XRD	+ + + Halite	+ + + Halite
HCl test	− HCl	− HCl
Efflorescence composition	Halite	Halite
Drying rate	High DR	High DR
Overview photography		
Magnified photography		

6.3.2 Gypsum efflorescence

Gypsum shows somewhat particular crystallisation behaviour. It is generally assumed that the location of salt crystallisation in porous media coincides with the location of the drying front, i.e. a drying front at the surface yields salts crystallisation at the surface (efflorescence), while crystallisation below the surface (subflorescence) is induced when the drying front shifts to below the surface. This does not seem to hold for gypsum, as it is reported to yield subsurface crystallisation even under experimental conditions designed to promote efflorescence formation. Franke and Grabau (1994, 1998) subjected samples of historical bricks to a wick test using gypsum solution. No efflorescence developed on the surface even after a few weeks, an interval during which a major DR drop was observed. After the experiment samples were cut into 2 mm slices, which were then analysed for the content of soluble sulphates, revealing their accumulation only in the first 2 mm layer. This experiment was coupled with an SEM-EDS analysis of a sample cross-section, which revealed Ca enrichment along a similar depth, confirming the gypsum accumulation in this subsurface layer. Similar conclusions can be drawn from a study of Cardell et al. (2008). They applied a wick test with gypsum solution to a limestone sample. No efflorescence was observed after the test, but the optical microscopy pictures of sample' cross-sections showed gypsum accumulation just below the sample's drying surface. This subflorescing propensity of gypsum is also reported for non-calcareous stones like sandstones (Snethlage and Wendler, 1997) and granites (Charola et al., 2006). Gypsum subsurface accumulation was also demonstrated for yet another material type - gypsum plaster (Seck et al., 2015). A plaster sample was exposed to cycles of imbibition and drying, which yielded no substantial gypsum crystallisation at the surface, but again a major drop in evaporation rate was observed. The sample's pore structure was analysed with X-ray microtomography, what clearly revealed formation of a 1 mm deep subsurface zone of a higher density, caused by gypsum crystallising in the subsurface porosity. It needs to be underlined that the above discussed experiments provide optimal conditions for efflorescence formation i.e. the drying front location is promoted at the sample surface while efficient drying conditions enhance efflorescence growth. Nevertheless, gypsum exhibits an

apparent tendency for crystallisation just under and within the surface, even under these efflorescence-favourable conditions. Moreover, as this phenomenon was reported for a wide range of materials, these studies suggest that the subsurface accumulation is not induced by a specific host material property, but it is rather a gypsum's intrinsic property.

The wick and WW procedures were applied to gypsum solution under both accelerated and laboratory climate conditions (Table 6.3). The default experimental schedule (Figure 6.2) was followed only for the G setups, while continuous wick regimes (Section 6.3.1) were applied to the G-wick and G-lab wick test variations. In addition, the timing of the 'Laboratory WW' schedule (Figure 6.7) differed majorly from the default experimental schedule, as the wick phase duration had to be extended to three days to allow for complete wetting water evaporation under 'slower' laboratory drying conditions. Consequently, the $\Delta t_{abs} = 2$ days was separately estimated from the DR data of the water setups tested under laboratory conditions (see W-lab in Table 6.13) and applied to calculate the DR (Equation 6.4).

Table 6.3 Overview of the ATM experiment variations and their settings, see Table 6.1 for the explanation of the setups' codes and the layout.

| Code	G	G-wick	G-lab	G-lab wick
Test solution	$CaSO_4 \cdot 2H_2O$	$CaSO_4 \cdot 2H_2O$	$CaSO_4 \cdot 2H_2O$	$CaSO_4 \cdot 2H_2O$
Adhesive	Hot melt	Hot melt	Hot melt	Hot melt
Surface	Original	Original	Original	Original
Leaching	Leaching	Leaching	Leaching	Leaching
Climate	Accelerated	Accelerated	Laboratory	Laboratory
Wick / WW	WW	Wick	WW	Wick
Schedule	Default	Accelerated wick	Laboratory WW (Figure 6.7)	Laboratory wick
Test duration	28 days	20 days	28 days	154 days
Test solution wick duration	8 days	20 days	10 days	154 days
# of setups	9	4	4	4
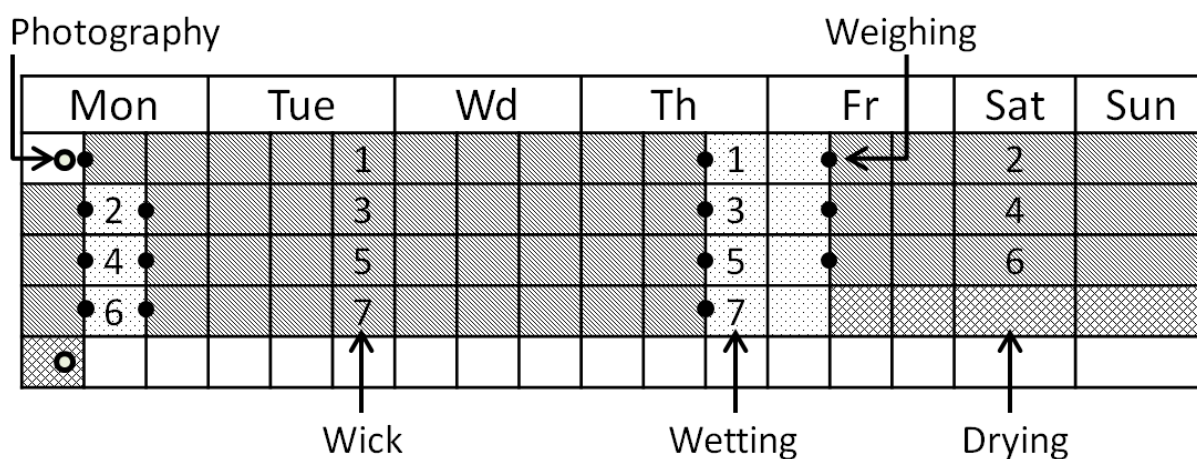
Figure 6.7 The 'Laboratory WW' experimental schedule for the WW test realised under laboratory climate conditions. It majorly deviates from the default experimental schedule in Figure 6.2 (see the text for explanation).

Only gypsum was identified in the ATM samples, including the G-wick and G-lab wick setups, which did not visually show any efflorescence (Table 6.4), but where the sampling procedure might have picked up traces of a very fine, non-distinguishable GE or of a subsurface gypsum deposit. Gypsum accumulation was consistently accompanied by a major DR drop in all cases but for the G-lab setups where the difference can be attributed to insufficient test duration; this problem is further discussed in Section 6.4.3. The NaCl setups tested under the same conditions and at the same concentration showed High DR and yielded considerable efflorescence (Table 6.2), the low solubility of gypsum cannot hence solely account for the generally rare occurrence of its surface accumulations on building materials. This specific gypsum

behaviour was observed under both laboratory and accelerated conditions, the DR drop was hence neither related to a specific drying regime.

Table 6.4 Summary of the ATM experiments on gypsum setups, the table layout is explained in Table 6.2.

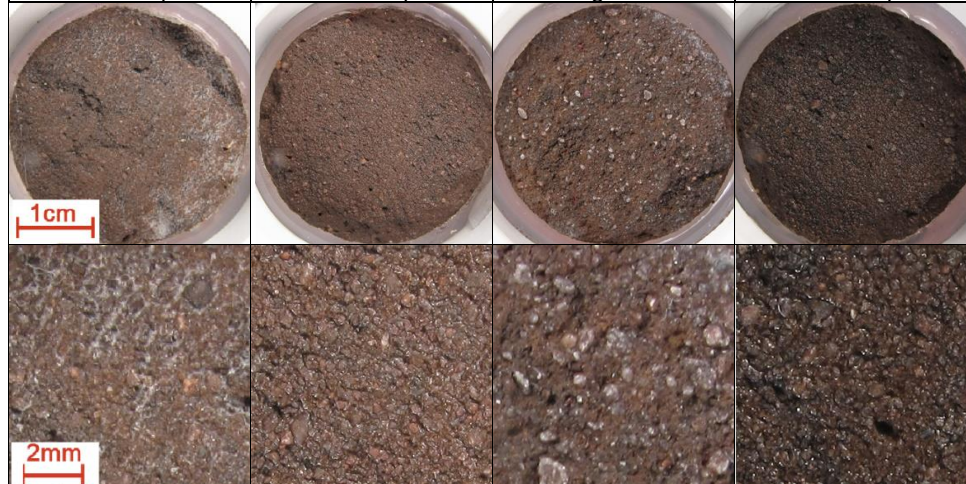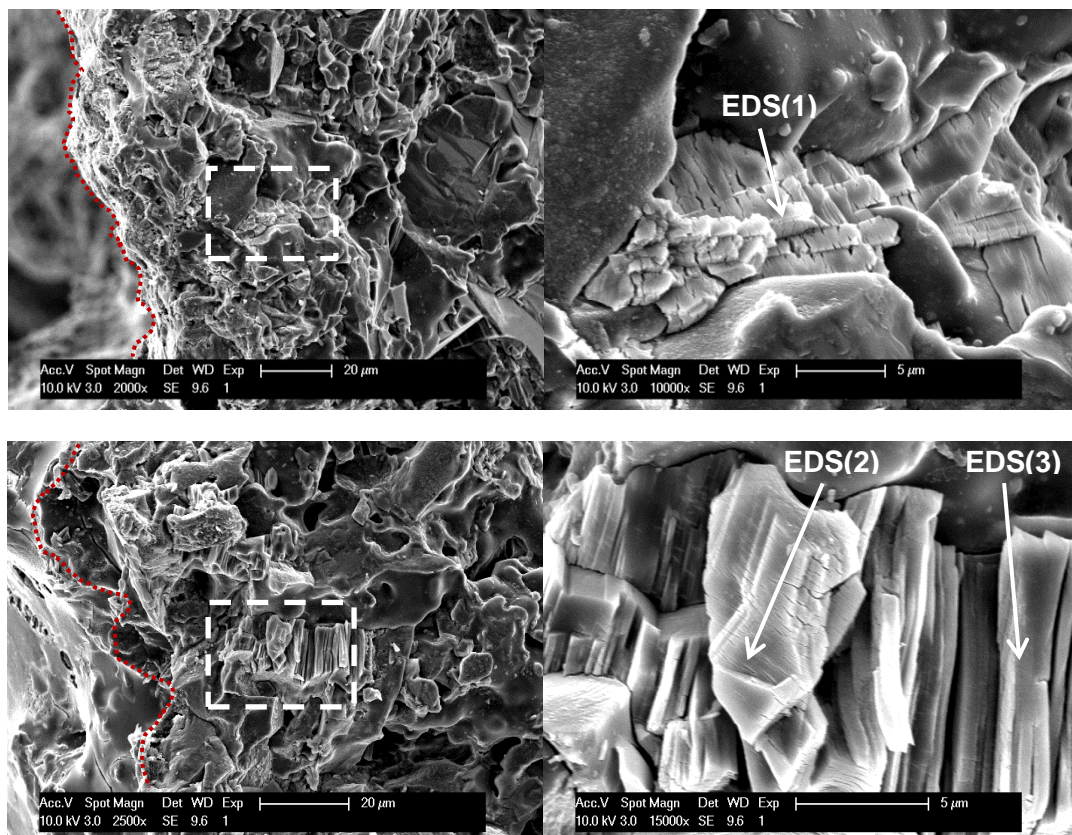| G	G-wick	G-lab	G-lab wick
11 (13 ± 4) %	2 (3 ± 1) %	4 (2 ± 1) %	0.5 (0.4 ± 0.3) %
+ + + Gypsum	+ Gypsum	+ Gypsum	+ Gypsum
− HCl	− HCl	− HCl	− HCl
Gypsum	Gypsum	Gypsum	Gypsum
DR drop	DR drop	High DR	DR drop

Figure 6.8   Left: SEM images of a cross-section sample taken from a gypsum (G) setup, the red dotted line marks the brick core's outer surface. Right: magnification of the dashed region of the corresponding image on the left. The arrows indicate three points probed with EDS: EDS(1), EDS(2), and EDS(3).

47

Multiple cross-section samples were taken from the gypsum (G) setups and analysed with SEM, see two examples in Figure 6.8. A consistent pattern was observed in all of them: the pores close to the surface were heavily filled with densely packed stacks of gypsum crystal plates, as identified by the EDS analysis (EDS(1): CaO 47 mol%, SO_3: 49 mol%; EDS(2): CaO 49 mol%, SO_3: 48 mol%; EDS(3): CaO 50 mol%, SO_3: 48 mol%).
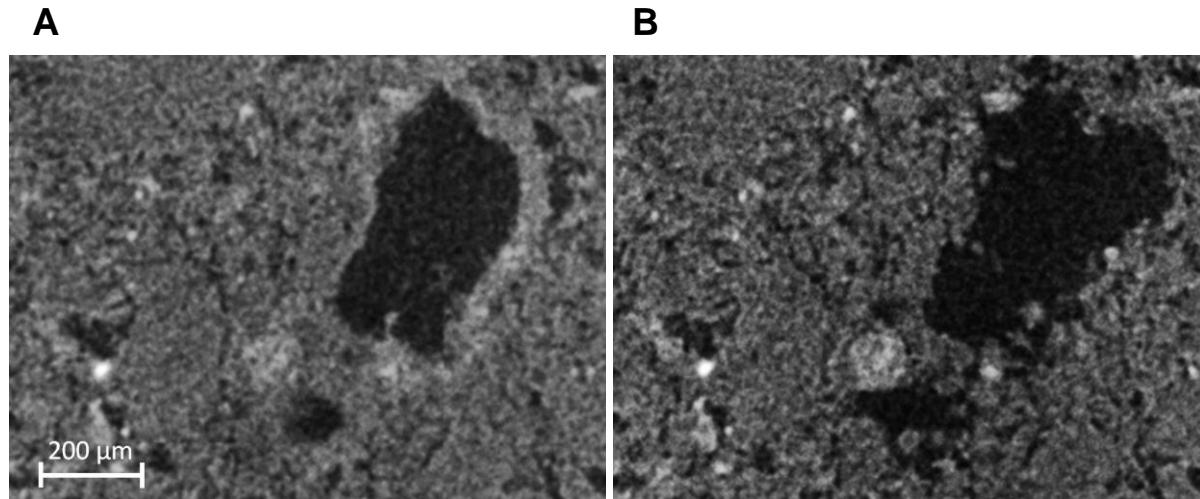
A **B**

Figure 6.9 Computer tomography images taken on a brick sample from a gypsum (G) setup. Both images show (the same) part of the sample's cross-section situated 350μm below the sample's surface. The image A is taken on the original sample, while the image B is taken after subjecting the sample to a leaching procedure (Section 6.2.2) in order to remove the accumulated gypsum. The images were collected with GE Nanotom set at 80kV and 160 microA using a 0.5 mm Al filter (courtesy of Steven Claes, Building Physics Section, KU Leuven).

A more in-depth investigation of gypsum pore-clogging and its effect on transport properties, combining the experimental approach with numerical modelling is addressed in a separate coupled project carried out at the Building Physics Section of the Civil Engineering Department, KU Leuven by Jelena Todorovic and Hans Janssen (2014, 2015). In the framework of this project, a brick sample from the gypsum (G) setup was analysed by computer tomography (Figure 6.9). The dark colours correspond to areas of low density (e.g. pores) while the bright areas to dense sample's components (e.g. sand, fired clay, gypsum). Image A shows a cross-section from the original wicking sample, while image B presents the same cross-section collected after subjecting the sample to a leaching procedure (Section 6.2.2) to remove the accumulated gypsum. Comparison of both images shows that gypsum accumulated on the walls of the large pore, but was removed by the leaching procedure. Similar observations can be made for the fine pores surrounding the macropore – in the original image (A) these fine pores are difficult to distinguish within the brick's volume due to gypsum presence, while after leaching (B) a system of interconnected pores can be discerned. This confirms gypsum's propensity towards subsurface accumulation, which is hence likely responsible for constraining the wicking process and for resultantly inducing the observed major DR drop. While both SEM and X-ray tomography allow visualising this phenomenon, it can be conveniently identified with a combination of the drying rate and mineral composition analyses. The latter approach is used in this thesis to identify cases of gypsum pore clogging for the tested ATM setups.

A salt's propensity for efflorescence or subflorescence formation may be also related to whether the salt crystallisation is initiated at the liquid-air (e.g. wet brick surface) or the solid-liquid (e.g. brick pore surface) interface. In the former case efflorescence formation is more probable, while the latter may induce subsurface accumulation and possibly explains the observed gypsum subflorescing tendency. Crystallisation experiments in glass capillaries simulate the drying and crystallisation process in porous materials and allow observing the interface on which the crystallisation is initiated. NaCl and Na_2SO_4 were investigated in this way (Rodriguez-Navarro and Doehne, 1999; Shahidzadeh-Bonn et al., 2008), however, gypsum has not been yet addressed and should be the subject of future research.

The accelerated test yielded gypsum accumulation below the sample surface, hence correctly reproducing its reported crystallisation behaviour, but remaining at odds with the commonly observed GE phenomenon, though. These controversies are further addressed in the following sections.

Gypsum: experimental subflorescence vs field efflorescence

The accelerated test on gypsum solution provided an unlimited GE source and optimal conditions for fast GE formation. Nevertheless, Table 6.4 shows that the test yielded slight GE only, as compared to the characteristic abundant deposits found in the field, illustrated by photographs in Table 4.1. Though being controversial, this discrepancy is in line with the British brick industry experiences. Many thousands of millions of bricks with considerably high levels of anhydrite were used in the UK for over a century, and only very few efflorescence problems were reported (Bowler and Fisher, 1989). These cases hence stay in agreement with the ATM test applied to gypsum solution. The lack of efflorescence on these old buildings might be explained by gypsum subsurface accumulation; however this hypothesis has not been experimentally proven on the masonry samples. On the other hand, extensive gypsum subsurface enrichment is well documented for numerous historical German masonry constructions affected by black gypsum crusts formation (Franke and Schumann, 1998). While the crust formed from a reaction between masonry surface and air pollution, the considerable gypsum subsurface accumulation was likely formed upon gypsum recrystallisation and confirms its tendency for subsurface precipitation. If this hypothesis is true, then it implies that while a sufficient GE-source presence is necessary, it is by itself not sufficient to yield abundant GE. As the GE problem has started to occur in the UK only in the 80's (Bowler and Winter, 1996), it might have been triggered by introduction of some extra factor(s). Indeed, Bowler *et al.* (1997, 1998) have already demonstrated that gypsum crystallisation at the surface of masonry can be triggered by surfactant based masonry mortar admixtures. Calcium sulphate is a ubiquitous component of various building materials, but gypsum deposits are only rarely reported to accumulate on their surface upon drying (Seck *et al.*, 2015). This rare occurrence might therefore be a consequence of both its tendency to crystallise below the surface and its limited solubility.

The factors determining crystallisation location

The crystallisation location depends on the complex interplay between many factors, like the properties of the supersaturated solution, the drying conditions, the properties of the transport medium's surface, and the crystal growth pattern (Rodriguez-Navarro and Doehne, 1999). The first parameter is of importance for highly soluble salts of which supersaturated solutions may show significantly altered viscosity and surface tension. Nevertheless, this should not be significant for the scarcely soluble gypsum. We have moreover demonstrated that, on the one hand, gypsum's tendency for subflorescence formation is not directly related to the drying rate. On the other hand, formation of sodium chloride efflorescence shows that the brick porous matrix is not a barrier itself for crystallisation at the surface. It appears hence that the propensity for efflorescence formation may be mineral-specific, as shown on the example of efflorescing halite and subflorescing gypsum. It is not clear though, whether the origin of this behaviour is a specific crystal growth or other mineral related parameter. In addition, the salt's crystallisation behaviour may be affected by even small amounts of accessory substances, as demonstrated by the mortar admixtures effect (Bowler and Winter, 1997; Bowler and Sharp, 1998), which is further addressed in the next chapter.

6.4 ATM development

The optimised setup and protocol as presented in Section 6.2 did not come about as a one-step evolution from the basic wick test. Instead, preliminary experiments realised with the basic wick test revealed many flaws in its design and yielded unreliable results. The test was progressively improved, and numerous modifications were applied until a robust test was obtained. The improvements are discussed in the following sections.

6.4.1 Efflorescence quantification

The main aim of the designed test was to evaluate and compare the efflorescence extent on different ATM setups. It was realised both by means of a visual assessment and digital image analysis. However, efflorescence evaluation proved to be difficult, as its appearance is sensitive to many factors. First, its appearance depends on the brick colour and texture. It can be easily noticed in the field, where efflorescence on dark buildings is much more striking than on light coloured masonry. Nevertheless, this

problem was resolved by using consistently the same dark-coloured brick type as a transport medium over the whole research project duration. Secondly, its appearance depends highly on the dryness of the surface, as even field efflorescence cases which appear severe during dry summer days, turn much less pronounced during rainy autumn periods. The same was observed for the ATM setups during the test and after brick sample drying. Thirdly, light conditions highly influence efflorescence appreciation, bright light making it more contrasting with the brick background. Finally, while the image analysis provides a convenient numerical expression of the discoloration extent, it does not account for the specific appearance of abundant GE which is indicative of a high GE-risk.

Efflorescence dryness

During the optimised ATM test a brick sample and its surface stayed saturated with a test solution or the wetting water, which altered the efflorescence's visibility. The brick sample photographs were hence collected only after drying the samples over a weekend. The effect of drying is demonstrated on additionally collected photographs before and after the weekend drying phase (Table 6.5). When dry, white efflorescence was well visible, strongly contrasting with the dark brick sample surface. The white appearance was due to translucency, the ability for light scattering of a dry and finely crystalline deposit. However, surface wetness changed the efflorescence's optical properties from translucent to transparent, thus allowing light to pass through it without scattering. As a result, the deposit became barely discernible from the brick's surface, regardless of its considerable presence at the surface. Drying the samples before efflorescence evaluation is hence necessary to yield a reliable efflorescence extent assessment.

Table 6.5   Comparison of the overview and magnified samples' photographs; from left to right: before the test (Raw), after the 4th wetting phase (Wet), after the weekend drying phase (Dried) and after the 5th wetting phase (Wet). The values provided in brackets next to the setup's code are the sample's %E.
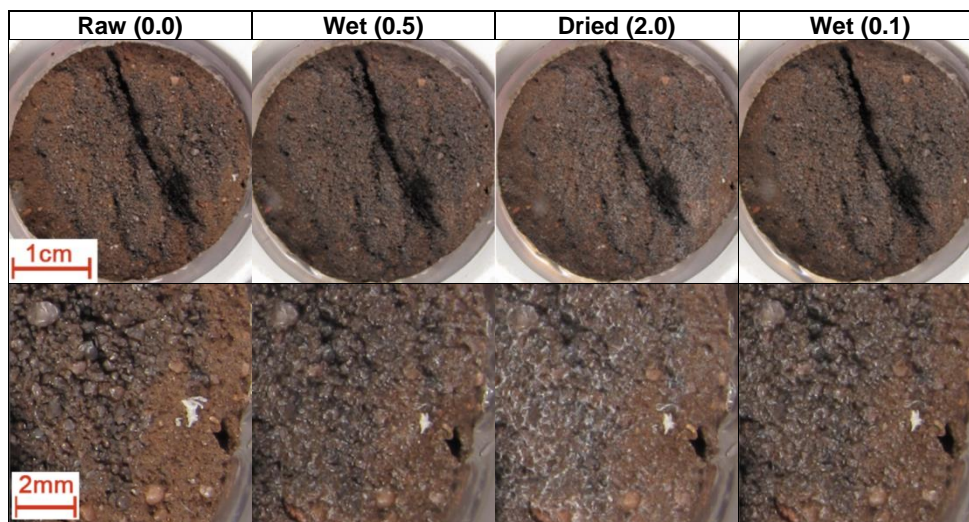
Repeatability

The setups' photographs were taken over many months at different times of the day, while the efflorescence appearance depends strongly on the light conditions. The photography stand and camera settings were thus adjusted to create stable light conditions and produce repeatable photographs with well visible efflorescence. The repeatability was assessed by taking triplicate photographs of the same gypsum setup every day over five days. This yielded low variation in the efflorescence coverage of about 10.3 ($\pm$ 1.0%) (Figure 6.10), which is negligible compared to the data scatter reported for the investigated setups (see an overview of the %E results in Section 9.1.2).
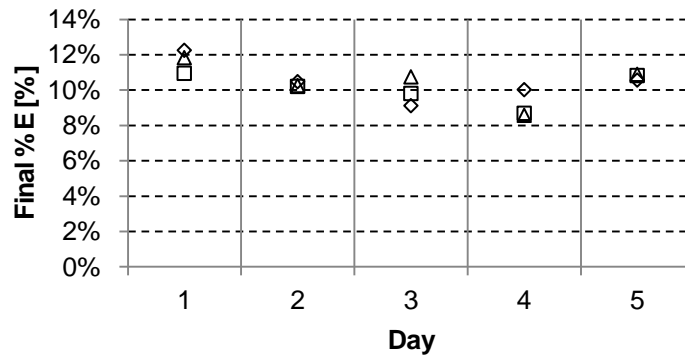
Figure 6.10 Repeatability of the efflorescence coverage quantification.

Abundant efflorescence quantification

The %E quantifies the spatial efflorescence coverage, but does not distinguish between intergrain and abundant efflorescence cases. The latter is a characteristic feature of GE observed for the FS cases (Table 4.1), and is hence indicative of a high GE-risk. However, the digital image analysis may lead to misleading results when applied to evaluating efflorescence abundance, which can be illustrated comparing the NaCl-lab wick and W-S2 sets (Table 6.6).
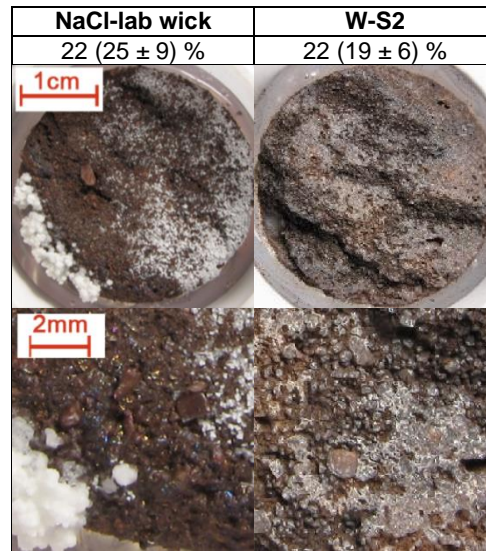
Table 6.6 Overview of the ATM experiment variations and their settings, see Table 6.1 for the explanation of the setups' codes and the layout.

Code	NaCl-lab wick	W-S2
Test solution	*NaCl*	*Water*
Adhesive	Hot melt	Silicone 2
Surface	Original	Original
Leaching	Leaching	Leaching
Climate	Laboratory	Accelerated
Wick / WW	Wick	WW
Schedule	Laboratory wick	Default
Test duration	154 days	28 days
Test solution wick duration	154 days	8 days
# of setups	4	4

Table 6.7 shows that the NaCl-lab wick setup yielded locally abundant efflorescence, but its average %E was at a similar level as for the W-S2 setup, which yielded only insignificant drape-like efflorescence. In order to evaluate GE-risk it is therefore necessary to additionally distinguish abundant GE cases visually, and this was applied in the GE source and factors evaluation studies addressed in the following Chapter 7. The %E value was hence used secondary to the visual assessment.

Table 6.7 Summary of ATM experiments, the table layout is explained in Table 6.2.

NaCl-lab wick	W-S2
22 (25 ± 9) %	22 (19 ± 6) %

6.4.2 Inert adhesive

The brick samples were initially sealed into the plastic lids using a silicone adhesive. However, upon inadvertently changing the brand of silicone product it was observed that this had a major impact on the GE extent. The effect of adhesive was assessed on water (W, W-S1 and W-S2) and gypsum (G, G-S1 and G-S2) setups sealed with two popular silicone products (S1 and S2) and with a hot melt adhesive (G and W sets), see Table 6.8.

Table 6.8 Overview of the ATM experiment variations and their settings, see Table 6.1 for the explanation of the setups' codes and the layout.

Code	G	G-S1	G-S2
Test solution	$CaSO_4 \cdot 2H_2O$	$CaSO_4 \cdot 2H_2O$	$CaSO_4 \cdot 2H_2O$
Adhesive	Hot melt	Silicone 1	Silicone 2
Surface	Original	Original	Original
Leaching	Leaching	Leaching	Leaching
Climate	Accelerated	Accelerated	Accelerated
Wick / WW	WW	WW	WW
Schedule	Default	Default	Default
Test duration	28 days	28 days	28 days
Test solution wick duration	8 days	8 days	8 days
# of setups	9	4	4
Code	**W**	**W-S1**	**W-S2**
Test solution	*Water*	*Water*	*Water*
Adhesive	Hot melt	Silicone 1	Silicone 2
Surface	Original	Original	Original
Leaching	Leaching	Leaching	Leaching
Climate	Accelerated	Accelerated	Accelerated
Wick / WW	WW	WW	WW
Schedule	Default	Default	Default
Test duration	28 days	28 days	28 days
Test solution wick duration	8 days	8 days	8 days
# of setups	7	4	4

While the average DRs for the water setups varied considerably (Figure 6.11 A), they showed high SDs and hence it cannot be concluded that the adhesive quality affected the wick performance. The overlap of results can be clearly noticed on the scatter graphs comparing the initial and final DRs (Figure 9.1 A and B). This high variation in DR is likely related to uneven drying conditions in the volume of the climate cabinet. This problem is also addressed in this study, but restricted to investigating the effect of location on the extent of formed GE (Section 6.4.8) by using setups with gypsum solution. While in some cases this high variation may not allow to compare the average magnitude of DR, it still allows to assess the trend of DR, and detecting a DR drop is the main reason for applying this procedure. Nevertheless, this particular problem should be addressed in the future. The effect of location on the drying rate can be investigated in a similar way as in Section 6.4.8, by using water ATM setups instead of the gypsum ones. Improvement of the air circulation installation in the climate cabinet may possibly reduce this undesirable effect.
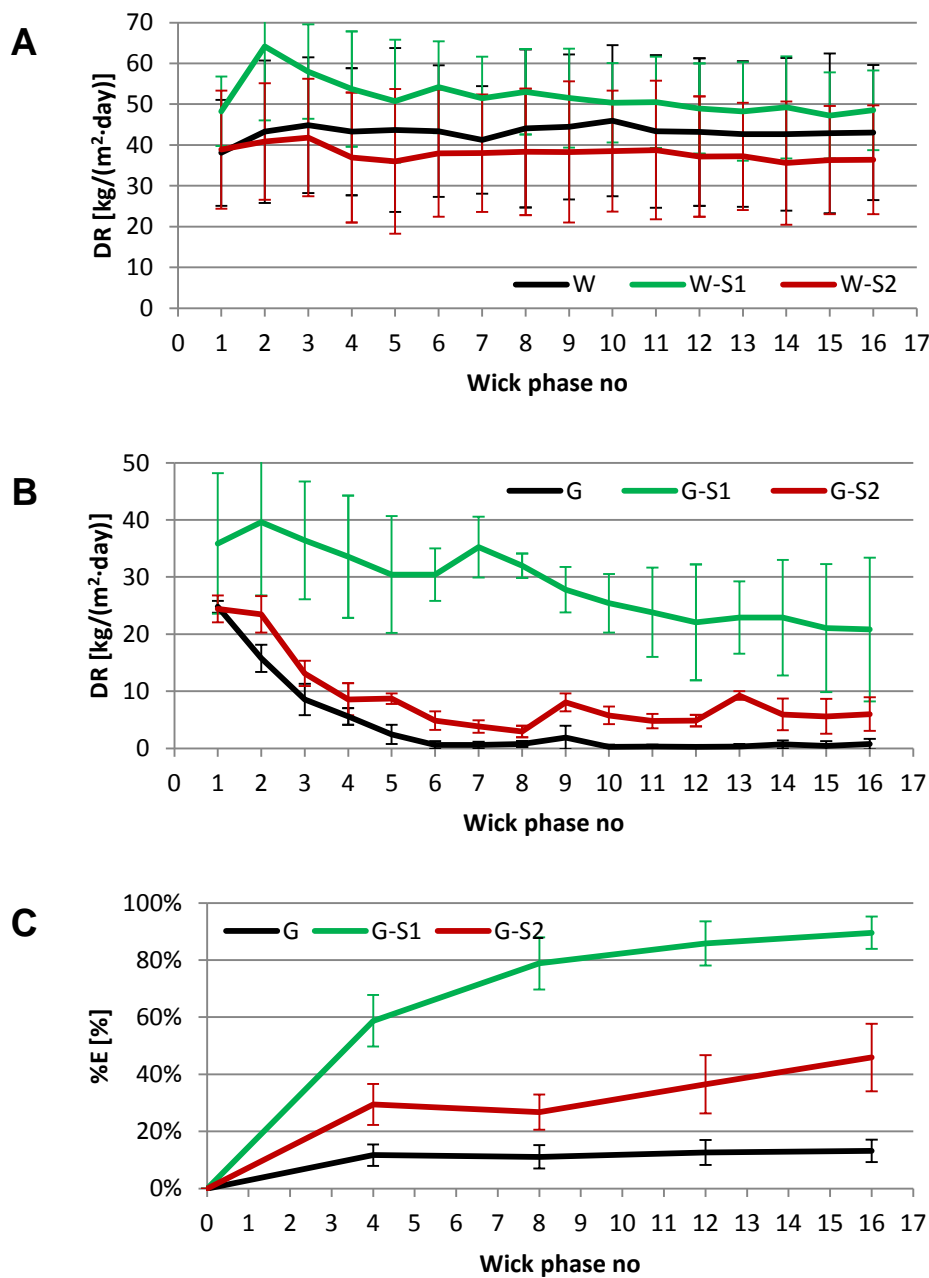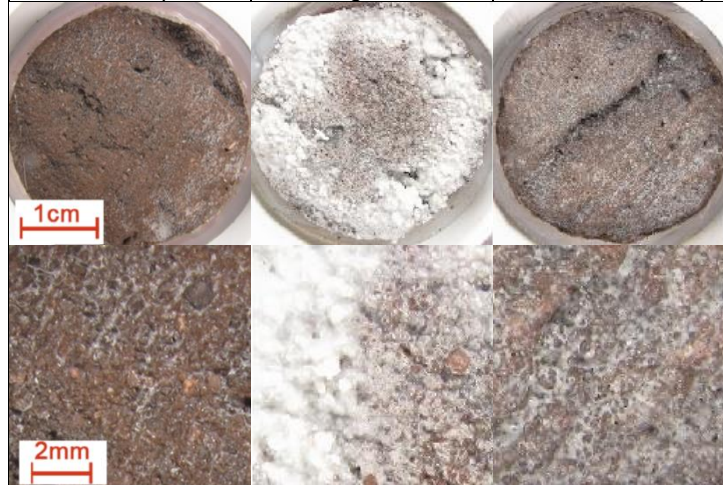

Figure 6.11 Drying rate evolution of the WW water and gypsum setups (A and B) and efflorescence coverage progression for the gypsum setups (C). Data shown as average ± SD.

In contrast, the gypsum setups' performance was greatly affected by the adhesive quality, as illustrated by photographs showing massive GE formation on the silicone S1 setups, contrary to slight GE on the hot melt (G) and moderate GE on silicone S2 setups (Table 6.9). The DR (Figure 6.11 B) and %E (Figure 6.11 C) evolution graphs show that the GE growth was directly linked to the DR behaviour. The major DR drop observed for the hot melt setups (G) inhibited any further GE growth. In contrast, the high DR for the G-S1 setups sustained gypsum solution transport to the surface and continuous GE accumulation. The silicone G-S2 setups showed intermediate behaviour, a major DR drop was also observed but a considerable DR was maintained after it and allowed hence for a slow but steady GE growth.

Table 6.9   Summary of the ATM experiments on the effect of adhesive, the table layout is explained in Table 6.2.

G	G-S1	G-S2
11 (13 ± 4) %	92 (90 ± 6) %	52 (46 ± 12) %
+ + + Gypsum	+ + + Gypsum	+ + + Gypsum
− HCl	− HCl	− HCl
Gypsum	Gypsum	Gypsum
DR drop	High DR	Moderate DR drop

The gypsum subflorescing propensity as observed for the hot melt adhesive setups is in agreement with the previous experimental results on wick and drying tests applied to gypsum solution (Franke and Grabau, 1994; Franke and Grabau, 1998; Seck *et al.*, 2015). In contrast, the application of silicone adhesives yielded moderate to massively abundant GE. No major effect on the water setups' performance tells that the adhesives did not directly affect the wick performance. On the other hand, the close-up efflorescence photographs demonstrate that GE exhibited different morphologies depending on the adhesive quality: from compact intergrain filling for hot melt (G), through compact surface layer (G-S2) to abundant crust (G-S1) for silicone adhesives. It is hence likely that some components of silicone altered the gypsum crystallisation behaviour, in turn enhancing its surface accumulation. The complete composition of both commercial silicone products was not provided by producers, but some information was available from the safety data sheets regarding content of potentially dangerous substances in (Table 6.10). While their composition was clearly very different, the effect of those specific components on gypsum crystallisation behaviour is difficult to assess. Addressing this problem requires first determining which silicone components are water soluble and hence can possibly migrate during the wick experiment from the sealant towards the brick surface. In the next step these water soluble components could be separately tested for their effect on gypsum crystallisation behaviour using e.g. the ATM setup with solution composed of the identified component mixed with gypsum solution. This is however outside of the scope of this project.

Table 6.10 Partial composition of S1 and S2 silicones derived from their safety data sheets.

S1	S2
<5% vinyltrimethoxysilane (cross-linking agent)	<10% non-specified petroleum distillates
	0.1-<1% Methyltris(methylethylketoxime)silane
	0.1-<1% Vinyltris(methylethylketoxime)silane
	0.1-<1% 2-Butanone oxime
	0.1-<5% Methyltris(methylisobutylketoxime)silane

The minerals' crystallisation behaviour is sensitive to the presence of other substances, e.g. surfactants (Canselier, 1993). Numerous substances like copolymers (Montagnino *et al.*, 2011), polycarboxylic acids (Badens *et al.*, 1999), citric and tartaric acid, and setting retarders (Middendorf and Budelmann, 1995) have been reported to majorly modify gypsum growth morphology and habit. It is hence plausible that some components present in commercial silicones migrated to the brick sample and may have altered the gypsum crystallisation behaviour. In contrast, the hot melt adhesives do not contain additional components, and their sealing mechanism is based on a purely physical reaction of melting and solidification.

The choice of an adhesive for a crystallisation test is critical, and care should be taken to select an inert and solvent-free sealant. As demonstrated, a seemingly simple and robust crystallisation test could yield completely unreliable results when common silicone adhesives are used. Moreover, the tests have also demonstrated that while gypsum shows an intrinsic propensity towards subsurface accumulation, this property is very sensitive to the presence of even minor amounts of accessory substances.

6.4.3 Climate conditions

Gypsum efflorescence takes a couple of years to develop under field conditions, while its reproduction under laboratory conditions was accomplished only after at least one year (Bowler and Winter, 1997; Bowler and Sharp, 1998). In the present study accelerated climate conditions (35 ± 2°C and 21 ± 4% RH) were applied to accelerate its reproduction, and were compared with the laboratory ones (24 ± 2°C, 53 ± 7% RH). The effect of climate conditions on the rate of efflorescence formation was assessed on water, gypsum, and sodium chloride setups.

Table 6.11 shows that the difference in the drying conditions between the laboratory (W-lab wick) and accelerated conditions (W-wick) translated to a 17 times higher average DR for the latter. The vapour pressure difference between surface and environment calculated according to the Arden Buck equation (Buck, 1981), under the 'accelerated' and 'laboratory' conditions are 4.5 kPa and 1.4 kPa, respectively, thus they did only partly contribute to such a high difference in the DR. It is hence the higher air flow in the climate chamber which mainly enhanced this effect.

The effect of accelerated drying conditions on the efflorescence formation was evident for the NaCl setups, resulting in a rapid formation of an extensive deposit (see NaCl-wick photographs in Table 6.2). It was also reflected in a 14 times higher average DR than under laboratory conditions (Table 6.11). Under accelerated conditions efflorescence was initiated very early, after only two days, while it took more than 122 days under laboratory conditions. This long delay might be explained by a high supersaturation necessary for triggering NaCl crystallisation, which was achieved much slower under laboratory conditions. The slower evaporation rate might also facilitate the diffusion process to counteract advection, further delaying supersaturation and NaCl precipitation.

Table 6.11 Average drying rates of the water and sodium chloride setups.

Setup	Average DR [kg/(m^2·day)]
W-wick	34 ± 6
W-lab wick	2.1 ± 0.2
NaCl-wick	23 ± 4
NaCl-lab wick	1.61 ± 0.04

Figures 6.12 A and B present the DR evolution of wick setups under accelerated and laboratory conditions, respectively. The W-wick set (Figure 6.12 A) exhibits two characteristic minima in DR at 10 and 16.5 days. These were caused by a complete evaporation of the test solution from some W-wick

55

setups. The wick process and evaporation were hence terminated, what resulted in reducing the average DR. The setups were refilled with water after noticing the problem. The W-lab wick and Na-Cl wick setups (Figure 6.12 B) show substantial DR fluctuations after 80 days. Both setups were tested under laboratory conditions and these fluctuations were caused by a malfunction of the air-conditioning system.
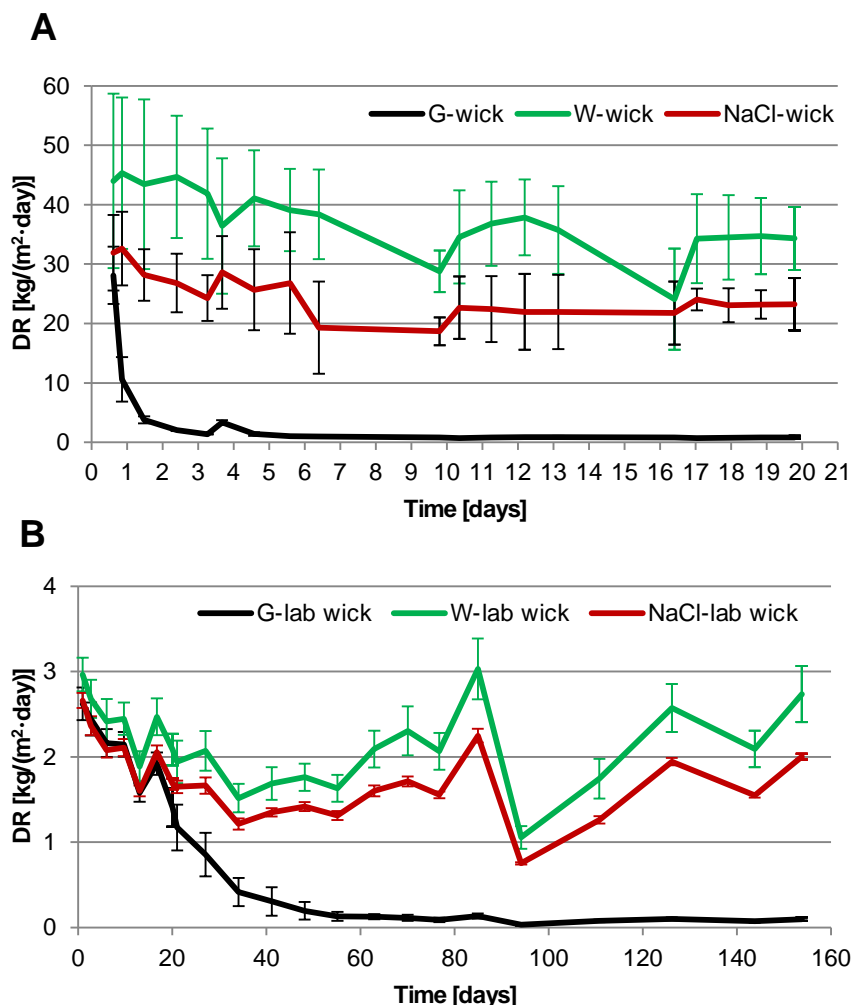

Figure 6.12 Drying rate evolution of the wick setups under accelerated (A) and laboratory conditions (B). Data shown as average ± SD.

The NaCl test solution transport to the surface was not majorly constrained by pore clogging, as NaCl efflorescence resulted only in a slight DR reduction as compared to the water setups (Figure 6.12 A and B). This allowed for uninterrupted NaCl efflorescence accumulation over time. On the contrary, the effect of the fast drying conditions for gypsum setups was abruptly quenched by the pore clogging effect of gypsum, majorly hindering the DR. It could be observed for both wick (G-wick set in Figure 6.12 A) and WW (G set in Figure 6.13 A) gypsum setups under accelerated conditions. The major DR drop was also observed for the wick gypsum setup under laboratory conditions (G-lab wick, Figure 6.12 B), but not for the WW one (G-lab, Figure 6.13 B). The latter followed strictly the DR of the appropriate water setups (W-lab). Under laboratory conditions the DR drop for gypsum wick setups (G-lab wick, Figure 6.12 B) progressed slowly and was mostly accomplished only after some 50 days. The duration of the test solution wick for the G-lab setups of 10 days (Figure 6.13 B) was hence insufficient to suppress DR what explains the lack of a DR drop. Both W-lab and G-lab sets exhibited similar fluctuations in DR, which were caused by a malfunction of the air-conditioning system.

A DR drop translates into a major restraint on the gypsum solution transport to the surface, which must also affect GE formation. Figure 6.11 C shows that indeed GE growth has been completely inhibited already after 4 wick phases for the gypsum WW set (G).
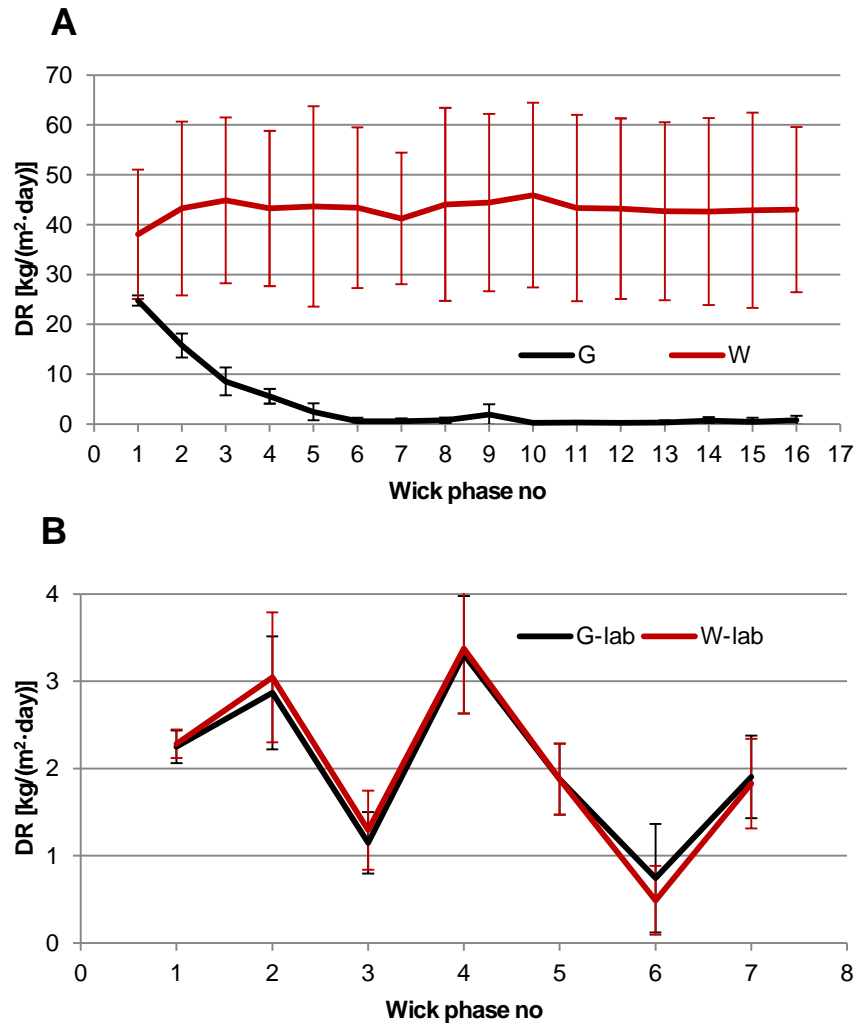
A

B

Figure 6.13   Drying rate evolution of the WW setups under accelerated (A) and laboratory conditions (B). For the latter no significant difference was observed between gypsum (G-lab) and water (W-lab) setups, see the text for explanation. Data shown as average ± SD.

Table 6.12 summarizes characteristic data derived from the gypsum DR plots, comparing the DR before (Initial DR) and after the transition to the low DR phase (Transition DR), and the time and amount of gypsum solution needed to accomplish this transition.

Table 6.12   Comparison of characteristic data derived from DR plots for wick and WW gypsum setups under both climate conditions. There is no data available for the G-lab setups, as the wick phase duration was too short to induce a DR drop. Data shown as average ± SD. The amount of gypsum solution [kg/m²] was calculated from the cumulative evaporation (Equation 6.6).

Setup	Initial DR [kg/(m²·day)]	DR drop duration [days]	Transition DR [kg/(m²·day)]	Gypsum solution [kg/m²]
G-wick	28 ± 5	3.3	1.4 ± 0.1	22 ± 9
G	25 ± 1	3.4 (6 wick phases)	0.6 ± 0.7	37 ± 4
G-lab wick	2.6 ± 0.2	55	0.13 ± 0.05	53 ± 8
G-lab	2.3 ± 0.2	Total = 10 days	–	–

Similarly as for the water and sodium chloride setups, the initial DR for gypsum was majorly higher under the accelerated conditions compared to the laboratory ones. Nevertheless, the beneficial effect of the fast drying was abruptly suppressed, as the DR dropped by a factor of 40 after about six wick phases for the G setup and by a factor of 20 after three days for the G-wick setups. The same effect was observed under

laboratory conditions, though it was taking place less rapidly and less extensively. For the 'G-lab wick' setup, the transition was accomplished after about 55 days, yielding a DR decrease by a factor of 20. This was also associated with a two times higher amount of gypsum solution evaporated during the slow transition, than under the accelerated conditions. A higher amount of gypsum could be hence accumulated during a slow process, before the DR drop was accomplished. This indicates that the amount of accumulated gypsum is not directly related to the DR drop. Instead, its distribution in the pore structure is likely to have a more profound effect in decreasing the permeability.

The acceleration of efflorescence formation by applying a more severe drying regime can be theoretically achieved for the less soluble gypsum, but is constrained by its subflorescing propensity. Abundant NaCl efflorescence could be formed after a couple of days of a wick test under accelerated conditions, compared to 122 days under laboratory ones. In contrast, gypsum would not form abundant surface deposits regardless of climate conditions and test duration. However, gypsum surface accumulation could be triggered in presence of accessory substances, as demonstrated on the example of the G-S1 setup (Table 6.9), which was discussed in Section 6.4.2. Under such conditions gypsum behaved similarly to sodium chloride, yielding abundant GE already within a few days, taking advantage of the 'fast' drying conditions. This demonstrates that the accelerated climate conditions could remarkably shorten the GE test duration, given the presence of GE-triggering factors.

6.4.4 Sample leaching

Preliminary experiments on raw brick samples fed with demineralised water yielded a quick formation of considerable efflorescence, the source of which was evidently the brick sample itself. In case of evaluating a GE source introduced into the test solution, the sample-derived efflorescence component would interfere the GE-source evaluation. This undesirable effect was limited by subjecting the brick cores to a leaching procedure. The raw brick samples (W-wick NL set) and the leached ones were ATM-tested with pure water to assess the effectiveness of the leaching procedure (Table 6.13).

Table 6.13 An overview of the ATM experiment variations and their settings, see Table 6.1 for the explanation of the setups' codes and the layout.
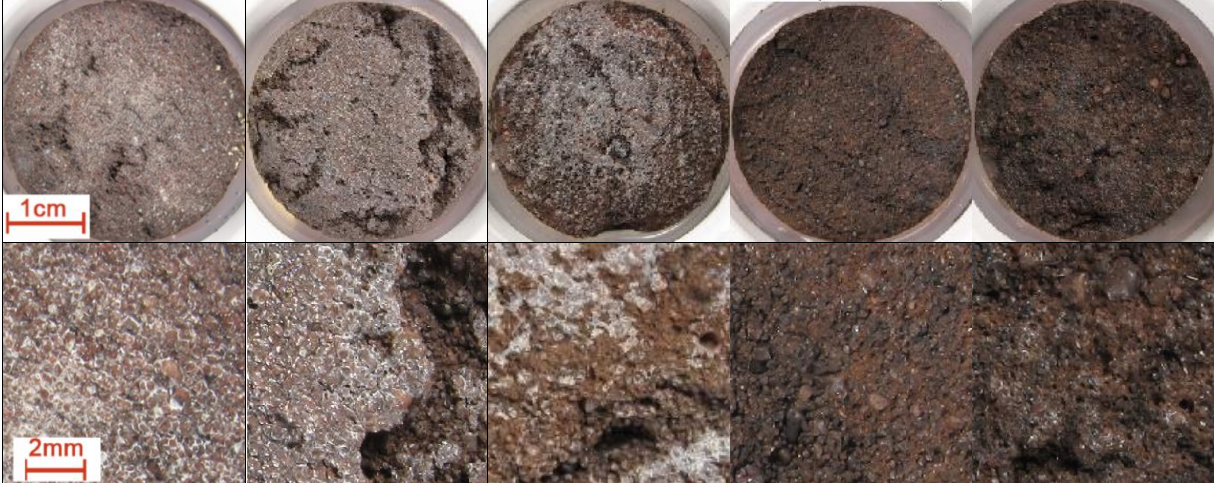
Code	W-wick NL	W-wick	W	W-lab	W-lab wick
Test solution	*Water*	*Water*	*Water*	*Water*	*Water*
Adhesive	Hot melt	Hot melt	Hot melt	Hot melt	Hot melt
Surface	Original	Original	Original	Original	Original
Leaching	None	Leaching	Leaching	Leaching	Leaching
Climate	Accelerated	Accelerated	Accelerated	Laboratory	Laboratory
Wick / WW	Wick	Wick	WW	WW	Wick
Schedule	Accelerated wick	Accelerated wick	Default	Laboratory WW	Laboratory wick
Test duration	20 days	20 days	28 days	28 days	154 days
Test solution wick duration	20 days	20 days	8 days	10 days	154 days
# of setups	4	4	7	4	4

Table 6.14 shows that the former yielded gypsum and calcite efflorescence, while XRD analysis of the rest did not reveal presence of efflorescence minerals in the sample. On the other hand, the HCl test resulted in different degrees of reaction with the sample surface, often leaving behind efflorescence of HCl insoluble species. Therefore the water setups' efflorescence was classified mostly as calcite ($CaCO_3$) or/and unknown species. It is likely that either both components were amorphous, or in insufficient amount to be identified by XRD.

Table 6.14   Summary of the ATM experiments on the effectiveness of sample leaching, the table layout is explained in Table 6.2.

W-wick NL	W-wick	W	W-lab	W-lab wick
36 (42 ± 12) %	27 (26 ± 6) %	16 (15 ± 5) %	0.4 (0.6 ± 0.2) %	0.2 (0.3 ± 0.2) %
+ + Gypsum	–	–	–	–
+ + HCl	+ + HCl	+ + HCl	− HCl	+ + + HCl
Gypsum & Calcite	Calcite & ?	Calcite & ?	?	Calcite
Moderate DR drop	High DR	High DR	High DR	High DR

The leaching procedure was hence partially effective, removing the GE source, but the calcite and unknown species efflorescence sources were preserved. This also finds confirmation in their DR behaviour (Figure 6.14): gypsum identified in the non-leached samples led to a moderate DR drop, while the leached samples maintained high DR over the test duration.
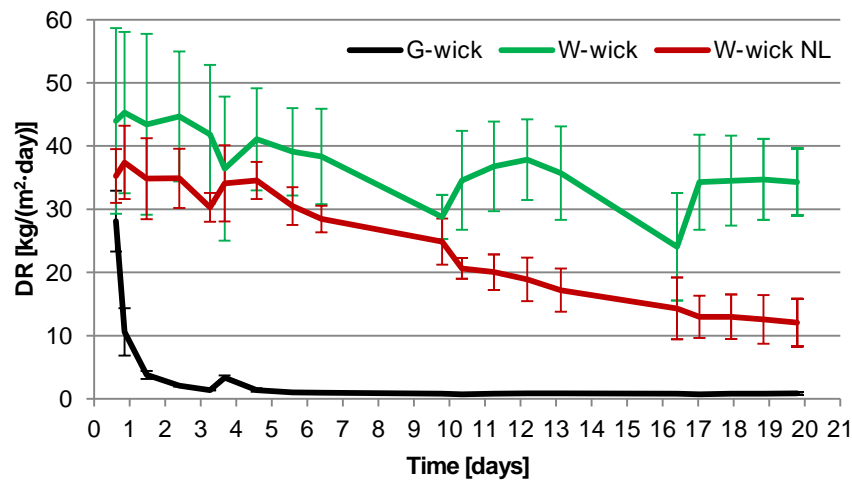
Figure 6.14 Drying rate evolution of the wick setups under accelerated conditions. Data shown as average ± SD.

The leached sample subjected to WW procedure (W) similarly yielded efflorescence composed of calcite and unknown species accompanied by a high and stable DR (Table 6.14). Its surface analysis with a stereomicroscope revealed some local inter-grain deposit formation (Figure 6.15 A). A thin drape of a few micrometres thickness could be observed on a cross-section imaged with SEM (Figure 6.15 B). SEM-EDS analysis has shown presence of 49mol% CaO, 28mol% of SiO_2 and a few other oxides. This is consistent with calcite formation on a brick matrix rich in SiO_2, what was also confirmed by the HCl test.
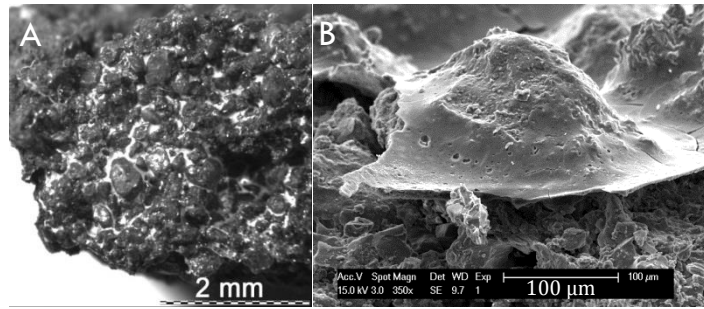
Figure 6.15 Surface (A) and cross-section (B) images of the W sample tested under the accelerated conditions, pictures taken with a stereomicroscope (A) and SEM (B).

However, no or scarce sample-derived efflorescence was observed for the water setups under the laboratory conditions (W-lab and W-lab wick in Table 6.14). It appears therefore that this effect took place exclusively under the accelerated conditions, or was significantly delayed under the laboratory ones. Indeed, the difference in the drying conditions can be translated into a 17 times higher initial DR for the water samples under the accelerated conditions (Table 6.11 and a paragraph above it).

Most importantly, the applied leaching procedure was effective against the GE source leaching, even though the calcite and unknown efflorescence species sources were preserved. The efflorescence derived from a sample might hence contribute to efflorescence formation during source evaluation and lead to %E overestimation. On the other hand, the sample-derived efflorescence does not exhibit the specific GE aspect found under field conditions, i.e. local abundant accumulations, therefore it has a limited effect on the GE-risk evaluation. Moreover, apparently the sample derived species did not interfere with GE formation on the gypsum setups, which consistently yielded pure GE only (Table 6.4). It was likely caused by fast gypsum pore-clogging which hindered any further efflorescence formation, including accumulation of the efflorescence species derived from the brick sample.
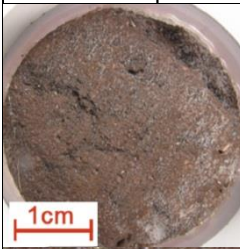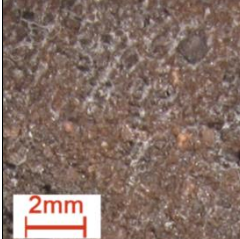
6.4.5 Brick surface quality

Ceramic bricks are typically surface-covered with sand, to give them a more desirable appearance. This is achieved in the production process, where sanded clots of clay are thrown into sanded moulds and then fired. The efflorescence formation is a surface phenomenon, hence it takes place mostly on the thin layer of brick sanding covering the majority of the brick surface, even though fired clay mix is virtually the only brick component. Fired bricks are often characterised by very fine pores of < 10 μm, but these may not be representative for the local and considerably coarser porosity of the brick sanding layer. It has been reported that the morphology of sodium chloride efflorescence depends on the porosity of a homogenous drying medium (Nachshon *et al.*, 2011; Eloukabi *et al.*, 2013), and this brings up the question on the effect of brick's heterogeneous porosity on GE formation.

Table 6.15 Overview of the ATM experiment variations and their settings, see Table 6.1 for the explanation of the setups' codes and the layout.

Code	G	G-CS	W	W-CS
Test solution	$CaSO_4 \cdot 2H_2O$	$CaSO_4 \cdot 2H_2O$	*Water*	*Water*
Adhesive	Hot melt	Hot melt	Hot melt	Hot melt
Surface	Original	Cut surface	Original	Cut surface
Leaching	Leaching	Leaching	Leaching	Leaching
Climate	Accelerated	Accelerated	Accelerated	Accelerated
Wick / WW	WW	WW	WW	WW
Schedule	Default	Default	Default	Default
Test duration	28 days	28 days	28 days	28 days
Test solution wick duration	8 days	8 days	8 days	8 days
# of setups	9	4	7	4

It was addressed by comparing brick samples with the original sanded stretcher surface (G and W) with ones having this surface cut off (G-CS and W-CS), exposing the bulk brick material (Table 6.15). However, no significant differences were found between the setups, neither in terms of efflorescence appearance and extent (Table 6.16), nor in wick behaviour (Figure 6.16). It was therefore decided to carry out the tests using brick samples with original brick surfaces, to keep the test representative of field conditions.

Table 6.16   Summary of the ATM experiments on the effect of brick surface quality, the table layout is explained in Table 6.2.

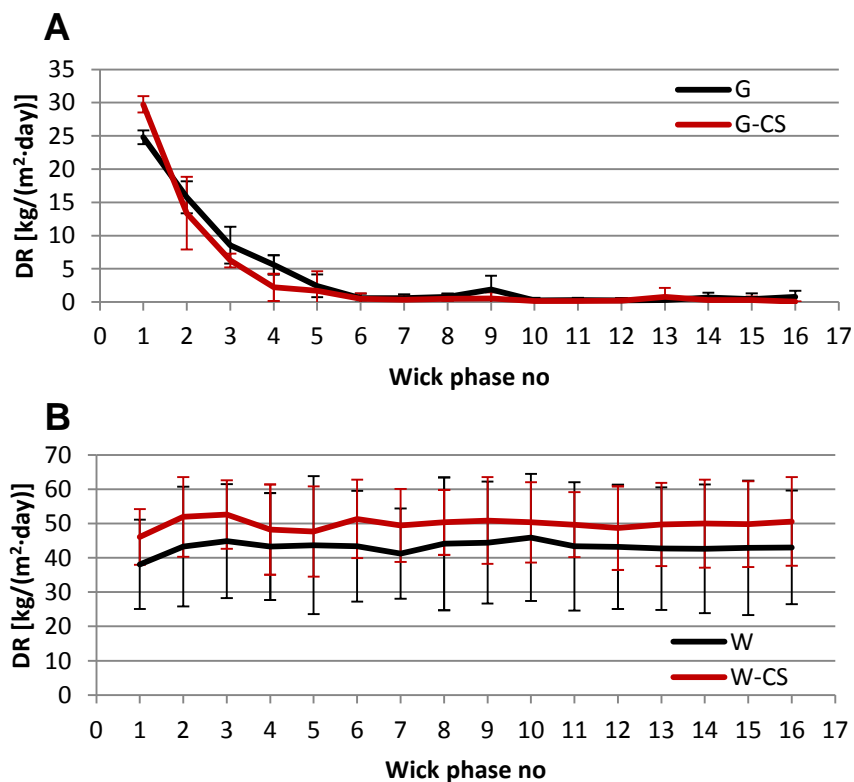| G	G-CS	W	W-CS
11 (13 ± 4) %	9 (8 ± 4) %	16 (15 ± 5) %	7 (14 ± 10) %
+ + + Gypsum	+ + + Gypsum	–	–
– HCl	– HCl	+ + HCl	+ HCl
Gypsum	Gypsum	Calcite & ?	Calcite & ?
DR drop	DR drop	High DR	High DR

Figure 6.16 Drying rate evolution of the WW gypsum and water setups (A and B). Data shown as average ± SD.
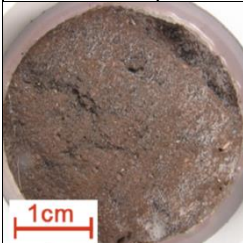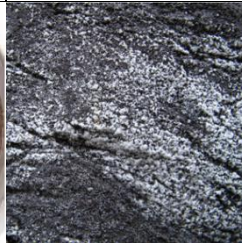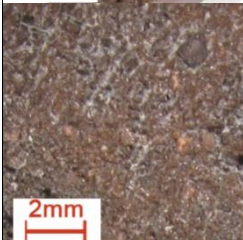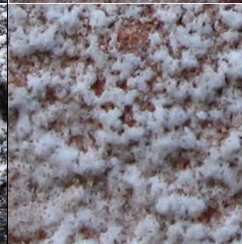
6.4.6 Wick-wetting protocol

The basic wick test simulated solely the process of continuous wick of the test solution. By contrast, under field conditions the drying of masonry is frequently interrupted by wind-driven rain hitting the drying surface, being absorbed and then evaporated. The test was hence adapted to simulate the actual masonry conditions by alternating wick phases with wetting ones. The effect of the WW procedure was compared to the pure wicking on gypsum setups, see Table 6.17.

Both gypsum WW (G) and wick (G-wick) setups under accelerated conditions quickly yielded a major DR drop, see Figure 6.16 A and Figure 6.12 A, respectively. It entails no GE formation at all for the former, while the application of frequent wetting yielded slight, intergrain GE (Table 6.18). However, the GE growth for the WW setup was inhibited already after four wick phases (Figure 6.11 C).

Table 6.17   Overview of the ATM experiment variations and their settings, see Table 6.1 for the explanation of the setups' codes and the layout.

Code	G	G-wick
Test solution	$CaSO_4 \cdot 2H_2O$	$CaSO_4 \cdot 2H_2O$
Adhesive	Hot melt	Hot melt
Surface	Original	Original
Leaching	Leaching	Leaching
Climate	Accelerated	Accelerated
Wick / WW	WW	Wick
Schedule	Default	Accelerated wick
Test duration	28 days	20 days
Test solution wick duration	8 days	20 days
# of setups	9	4

Table 6.18   Summary of the ATM experiments on the effect of the WW procedure, the table layout is explained in Table 6.2. The two last columns provide images and data on the field survey cases of GE.

G	G-wick	FS24	FS29
11 (13 ± 4) %	2 (3 ± 1) %	NA	NA
+ + + Gypsum	+ Gypsum	+ + + Gypsum, + Calcite	+ + + Gypsum, ? Calcite
− HCl	− HCl	NA	NA
Gypsum	Gypsum	Gypsum & calcite	Gypsum & possibly calcite
DR drop	DR drop	FS24	FS29

The DR calculation for every WW setup was corrected for the wetting water evaporation. The very low level of DR after the DR drop is hence related to the test (gypsum) solution wick only, and infers that the wetting water had completely evaporated from the setup during each wick phase. The DR drop was thus cyclically induced upon the test (gypsum) solution wick. Based on the available data we formulate the following hypothesis explaining this controversial behaviour.

Table 6.12 shows that the DR drop is mostly completed after 3.4 days (equivalent to six wick phases), during which water from about 26g of gypsum solution evaporated via the top sample surface leaving gypsum behind. For the wetting procedure 3ml of water was used, which was then able to dissolve only a small fraction of the accumulated gypsum. Nonetheless, it effectively restored the sample's permeability and allowed for wetting water evaporation, even though much gypsum was still present in the sample pores. It is plausible then that during the ATM test most of the accumulated gypsum narrowed the pores, without completely closing them, allowing for a test solution wick. The DR drop was then caused by an increasing number of pores becoming completely blocked by gypsum-plugs. Once a pore gets clogged, the evaporation is arrested and no further gypsum accumulation can take place, suggesting that the pore plugs are relatively fine and susceptible to dissolution even with a low amount of wetting water.

The WW gypsum tests showed that although a low amount of gypsum may initially crystallise at the surface, its further growth was quickly inhibited by pore clogging. However, these short episodes of surface accumulation may be repeated by wetting cycles, reopening the pores and progressively leading to slight efflorescence formation. Even though frequent wetting appears to contribute to GE formation, photographs in Table 6.18 show that it did not result in reproducing abundant GE as found in the field survey cases.

The wetting ring served an additional role by reducing variation of the evaporation flux over the sample surface and hence assuring even efflorescence growth. Localised crystallisation at the sample's peripheries was reported for non-shielded setups, and the beneficial effect of applying a barrier surrounding the sample surface was reported by Veran-Tissoires *et al.* (2012). Indeed, all the setups but the NaCl ones under laboratory conditions (Table 6.2) yielded an evenly distributed efflorescence, what facilitated GE-risk evaluation.

6.4.7 Test solution spills

The wick test setups were frequently moved from the climate chamber (35°C and 20% RH) to laboratory conditions (20°C and 50% RH) for weighing, solution replenishing and/or taking surface photographs. It was observed that when the setups were returned to the climate chamber, solution droplets were forming on and spilling over the bricks samples' surfaces. Moving the cooled setups from the laboratory back to the climate chamber's was likely generating an excess air pressure in the vessels, which in turn was responsible for releasing the test solution at the sample surface. These spills could possibly explain some unexpected behaviour observed during experimental trials. This problem was overcome by drilling an inlet in the cell's lid, allowing for pressure levelling. The inlet was additionally covered with a perforated scotch tape to limit the evaporation of the test solution from the cell. However, no dedicated tests were carried out to illustrate this improvement.

6.4.8 Location effect

The climate cabinet could accommodate 108 setups at the same time, spread over two levels. On the one hand this brought the advantage of testing multiple ATM variations at once, on the other hand it raised the question whether the test results are independent of the setups' locations.

It was investigated by analysing the relation between the final efflorescence extent and the setup's location in the climate cabinet. The test was carried out using 10 sets consisting of 36 gypsum setups (Figure 6.17 A) evenly distributed in the climate cabinet over two levels (Z=1 or 2) according to Figure 6.17 B. Triplicate setups were placed in each location, besides the G3 set which was made up of nine setups. The experiment yielded similar results in terms of efflorescence and DR behaviour (Figure 6.17 C) as other gypsum setups tested under similar conditions (compare with G setup in Table 6.4).

A

Code	G1-10
Test solution	$CaSO_4 \cdot 2H_2O$
Adhesive	Hot melt
Surface	Original
Leaching	Leaching
Climate	Accelerated
Wick / WW	WW
Schedule	Default (shortened to 21 days)
Test duration	21 days
Test solution wick duration	6 days
# of setups	3, G3 – 9

C

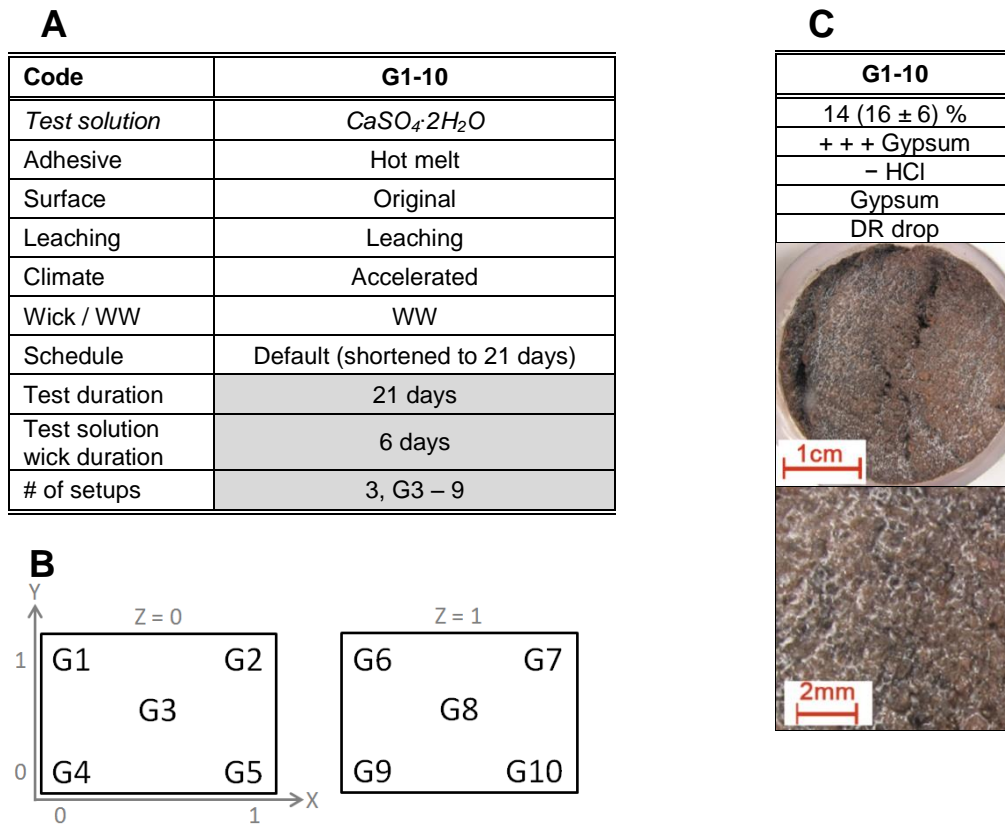| G1-10 |
|---|
| 14 (16 ± 6) % |
| + + + Gypsum |
| − HCl |
| Gypsum |
| DR drop |

B

Figure 6.17   A - overview of the ATM experiment variations and their settings, see Table 6.1 for the explanation of the setups' codes and the layout. B - the ATM setups' distribution in the climate cabinet during the location effect study. C - Summary of the ATM experiments on the location effect, the table layout is explained in Table 6.2.

The analysis of the location effect was made with the SAS JMP software. Six location effects were considered: three main effects of X, Y and Z, and three interaction effects of X*Y, X*Z, and Y*Z. From the all possible models generated with a combination of these six factors, up to five of the best models from each n-factor combination were selected, yielding in total 17 models (Table 6.19). A weak heredity criterion was applied for generating the final models. In the next step the four best models were selected based on the lowest value of the corrected Akaike information criterion (AICc). Validity of each model was assessed with the Analysis of Variance (ANOVA) method. However, there was no significant effect of the location on the efflorescence extent at the $p<.05$ level for the four selected models: $[F(1, 34) = 2.15, p = 0.15]$, $[F(1, 34) = 0.54, p = 0.47]$, $[F(2, 33) = 1.42, p = 0.26]$, $[F(3, 32) = 1.78, p = 0.17]$, respectively. The test can be hence run on multiple setups in parallel, yielding reliable results regardless of the setup's location in the climate cabinet. Detailed drying rate and efflorescence extent data are provided in the appendix in Section 9.1.2.

Table 6.19   Seventeen best models generated based on the effect of location study data, ordered by the lowest AICc value.

Model	AICc	Model	AICc	Model	AICc
Z	-93.4	X, Y, Z, X*Z	-89.5	X, Y, Z, X*Y	-87.1
Y	-91.8	X, Y	-89.3	X, Y, Z, X*Z, Y*Z	-86.4
Y, Z	-91.6	X, Y, Z	-89.0	X, Y, Z, Y*Z	-86.1
X, Z, X*Z	-91.5	Y, Z, Y*Z	-88.9	X, Y, Z, X*Y, X*Z, Y*Z	-84.2
X	-91.2	X, Y, X*Y	-87.5	X, Y, Z, X*Y, Y*Z	-84.0
X, Z	-90.9	X, Y, Z, X*Y, X*Z	-87.5		

6.5 Conclusions

The present study was designed to develop an accelerated test method for assessing GE-risk. Such a method should fulfil three main demands: (i) reliably reproduce gypsum crystallisation; (ii) majorly accelerate this process to yield results within reasonable time; and (iii) to be versatile by being adjustable to individual testing of different parameters. All these aims have been accomplished. The ATM yields gypsum subsurface accumulation in agreement with reports on gypsum crystallisation behaviour, which required selecting an inert sealant product and minimizing the interfering effect of sample derived salts by the leaching procedure. Its reliability is further enhanced by interrupting the wick process by wetting phases, which mimic the frequent episodes of rainfall under filed conditions. The test duration is remarkably shortened: from more than a year to four weeks, what was made possible (i) by setting up the ATM test on a wick test design which promotes continuous efflorescence growth and (ii) by optimizing the climate conditions. The former makes the test highly versatile, as owing to the separation of a transport medium (brick core) from the test solution (efflorescence source) it can be conveniently adjusted for separate assessment of masonry components as a GE source, the influence of admixtures or the effect of brick moisture properties. The test efficiency, and hence its applicability for industrial quality control, depends not only on its duration, but also on a possibility of carrying out multiple tests simultaneously and assuring their repeatability. This is provided by running parallel tests under conditions controlled by a climate cabinet, and their repeatability was confirmed with a dedicated test demonstrating no effect of location. The value of the test depends on the amount and quality of data which can be derived from it, hence a procedure was developed to comprehensively characterise the formed efflorescence: its discoloration extent (high quality photographs and visual and digital image analysis) and mineral composition (XRD and HCl tests), and its effect on the wick performance (DR analysis). The experiments addressed in these chapter not only illustrated the applied improvements and their benefits, but also shed some light on the GE genesis: the gypsum's intrinsic propensity towards subsurface accumulation may explain a lack of GE on old anhydrite-rich masonry, while the recent GE-occurrence might have been triggered by the introduction of some GE-triggering substances to masonry. These aspects are however addressed in more detail in the next chapter.

7 Gypsum efflorescence factors

7.1 Introduction

The field survey on Belgian GE cases revealed that the source of efflorescence originates from the masonry components themselves. Similar issues have been identified and investigated in the UK by Bowler and Winter (1997), and the published reports primarily targeted the recent introduction of mortar admixtures. The main aim of this chapter is therefore to evaluate (i) the effect of brick moisture properties, (ii) brick and cement as GE sources and (iii) mortar admixtures as potential factors triggering abundant GE formation. Addressing these research questions requires an efficient and versatile test method. For this reason we have developed and validated an accelerated test method (see Chapter 6), which is applied in this chapter to shed light on the genesis of Belgian GE cases and which can possibly be used in the future for quality control of masonry components.

The field survey study revealed that the GE outbreak is related to recent changes in the characteristics of the masonry components. However, in relation to the brick moisture properties, the field survey did not show any apparent link with the GE risk for common hand-moulded bricks. In this chapter, this potential effect was further ATM-tested via two brick types, characterised respectively by a low and a high capillary absorption coefficient. Moreover, an extruded brick was ATM-tested as well, to investigate the effect of its specific anisotropic porosity. Next, the ATM was applied to the GE source evaluation: two brick types and four commercial cement types were tested to examine whether these basic masonry components alone could yield GE formation. Multiple approaches were applied to assess the GE risk: the efflorescence extent and its composition were analysed together with the DR evolution and the GE source abundance in brick and carbonated cement paste. The evaluation of GE sources was followed by a separate set of tests addressing the effect of admixtures. Common commercial products were benchmarked to reveal whether they can overcome the typical subflorescing propensity of gypsum. In addition, a concrete superplasticizer was also ATM-tested, as a potential inert admixture enhancing mortar workability. Based on the results of this exploratory experiment, two products were selected for examination under more realistic conditions, in combination with a brick powder and as a component of a carbonated cement paste. Complementarily, a commercial premixed formulation was ATM-tested.

This chapter starts with an introduction of the tested materials and explains how the ATM test is adapted to answer the addressed research questions. In particular much attention is given to the calculation of a representative amount of the tested sample. The results and discussion are combined in three separate sections. Section 7.3 focuses on the effect of brick moisture properties, cement and brick as GE sources are examined in Section 7.4, while the effect of admixtures is addressed in section 7.5. The main conclusions are finally summarized in Section 7.6.

7.2 Materials and methods

The same optimized ATM setup (Section 6.2.2) and ATM protocol (Section 6.2.1) were applied in all tests. The GE risk was assessed by visual analysis of efflorescence photographs. In addition, in case of evaluating a brick or carbonated cement paste as GE source, its abundance was determined with a leaching test (Section 3.5.1).

7.2.1 Brick moisture properties

Three brick types: BR1, BR2, and BR1extr were selected to investigate the effect of the brick moisture properties. BR1 and BR2 are hand-moulded clay bricks with sanded surfaces. Both BR1 and BR2 were identified among the GE cases in the field survey, and they were chosen as their IRA's reflect relatively high (FS19, 4.8 kg·m^{-2}·min^{-1}) and low (FS16, 2.6 kg·m^{-2}·min^{-1}) values respectively, with respect to the spectrum for commercial clay moulded brick types (Figure 4.2). The BR1extr is an extruded brick type prepared specifically for this project, from a clay mix identical to the one used for the BR1 brick production. Extruded bricks are typically prepared from more plastic clay types though, our choice of the

clay type was motivated by primarily focusing on the effect of the extrusion process. Due to the process of extrusion the brick exhibits specific properties: its porosity gets preferentially oriented parallel to the stretcher (extrusion direction) and the surface is not sanded. Both factors may then alter the moisture properties and gypsum crystallisation. It should however be noted that extruded bricks are rarely used as facing bricks in residential buildings.

The ATM test was applied to brick cores extracted perpendicular to the stretcher surface, and subsequently leached according to the procedure explained in Section 6.2.2. Their moisture properties (vacuum water content w_{sat}, capillary absorption coefficient A_{cap}, and capillary water content w_{cap}) were determined with vacuum saturation and free water uptake tests (Sections 3.6.1 and 3.6.2). The effect of each brick type on the wick performance and GE risk was assessed with ATM setups filled with distilled water and gypsum solution, respectively.

7.2.2 Cement and brick as GE sources

Carbonated cement paste preparation

Initially, four cements were selected, because of the substantial differences in their compositions:
- B1: ordinary Portland cement (CEM I SPEED 52.5 HES), as the reference (95-100% clinker),
- B2: blended cement (CEM II/ B-M (S-V) 32.5N), as a cement commonly used for masonry construction (65-79% clinker),
- B3: sulphate resistant cement (CEM I 42.5 SR0), due to its particularly low content of aluminate phases (95-100% clinker),
- B4: pozzolanic cement (CEM IV / B-P 32.5), due to its particularly high replacement of cement clinker by natural pozzolana (45-64% clinker).

B1 and B2 are the same cement types as used in the cement carbonation chapter (Section 5.2). The carbonated cement paste was prepared similarly as in the cement paste carbonation study (Section 3.2). The carbonation procedure was slightly modified though: cement pastes were crushed to a finer fraction of 0.5-2mm (vs 2-4mm) to accelerate carbonation, while the carbonation duration was shortened to 70 days (vs 155 days). The latter was adjusted to yield only the major water soluble sulphate release - SO_4^{2-}[1] phase (Section 5.3.2). The carbonation progress of the ATM samples was assessed by comparing the amount of water soluble sulphate' release on the B1 and B2 samples, see Table 7.1. The SO_4^{2-} levels were reasonably similar to the ones from the cement carbonation study, validating the modified carbonation methodology.

Table 7.1 Comparison of water soluble sulphate released upon cement paste carbonation from the ATM (70d carbonation) and cement carbonation study (84d carbonation, SO_4^{2-} [1] phase) samples.

Binder	SO_4^{2-} [mmol/100g anhydrous]	
	ATM	Cement carbonation study
B1	8.8	9.4
B2	10.3	7.9

Representative amount of cement paste sample

Masonry is composed of a volume of bricks and mortar joints, while GE is a surface phenomenon, developing mostly on the brick's outer surface. The GE risk is then dependent on the ratio of the masonry surface to the GE source availability in the volume of masonry components. In the ATM test the efflorescence developed on the small surface of a brick core, while the GE source (brick or cement paste powder) was introduced separately in the form of a test solution. The amount of the tested GE source or mortar admixtures hence always needed to be adjusted to reflect the situation of actual masonry constructed with components of standard dimensions, to provide a reliable measure of a GE risk.

In case of testing cement paste, its amount needed to be both adjusted (i) to the surface area of a brick core and (ii) to reflect the use of cement paste instead of mortar. This was realised by first determining the amount of anhydrous binder used per brick in masonry, then rescaling it to the ATM sample, and finally calculating the amount of cement paste to be tested given its w/c ratio. The brick to mortar ratio in

masonry was determined assuming the use of a standard facing brick of WF (Waalformat) format (L21 x W10 x H5 [cm]) surrounded at the lateral, upper and lower sides by a 10mm mortar joint complying to the C 300 masonry mortar designation (CSTC, 2009), see Table 7.2. The C 300 mortar density and anhydrous cement content were calculated from a commercial recommendation for dosage of masonry mortar components (Holcim Belgique S.A., 2010), see Table 7.3.

Table 7.4 shows the intermediate calculation steps required to determine a representative amount of cement paste to be tested in an ATM setup with a brick core (d=3cm). First, the mortar joint volume per brick was calculated from the known dimensions of a WF brick and a mortar joint. Next, its mass was determined from the determined mortar density, while the amount of anhydrous cement required for its preparation was estimated from the calculated anhydrous cement content (Table 7.3). These values were then rescaled to a single ATM core according to the ratio of the surface area of the WF brick's stretcher and the ATM core's (d=3cm) top surface. Finally, the amount of cement paste was calculated from the anhydrous cement mass per ATM core and w/c ratio used for the paste preparation. The w/c ratio of the tested cement pastes was variable due to bleeding, and consequently the amount of the tested cement paste as well.

Table 7.2 Specification of the C 300 mortar designation according to a CSTC technical note (CSTC, 2009).

Mortar designation	C 300
Former Belgian designation	M2
Binder [kg] per 1m^3 sand	300
Cement / sand ratio [vol]	1:4

Table 7.3 Dosage recommendation for C 300 mortar preparation according to Holcim guideline for masonry works (Holcim Belgique S.A., 2010) and the calculated properties of mortar after mixing with water.

The dosage recommendation for C 300 mortar preparation	
Anhydrous cement mass [kg]	25
Sand [L]	90
Water [L]	20
Volume of the prepared mortar [L]	85
The calculated C 300 properties after mixing with water	
Mortar density [kg/m^3] *	2.1
Anhydrous cement per 1L mortar [kg/L]	0.29

The mortar density was calculated assuming sand density of 1500kg/m^3

Table 7.4 Amounts of mortar, anhydrous cement and cement paste calculated per single WF brick and rescaled to an ATM brick core sample.

Parameter		WF brick	ATM core
Stretcher surface area [cm^2]		105	7.07
Mortar volume [cm^3]		270	-
Mortar mass [g]		572	-
Anhydrous cement [g]		79.4	5.3
Binder type	w/c	Cement paste / ATM [g]	
B1	0.50	8.0	
B2	0.44	7.7*	
B3	0.50	8.0	
B4	0.50	8.0	

Considerable bleeding was observed for the B2 paste, the surplus water was weighed and discarded and w/c ratio was recalculated to $w/c_{B2} = 0.44$, what resulted in a lower sample mass.

Representative amount of brick sample

The evaluation of brick as GE source was realised on BR1 and BR2 bricks of the same type as in the brick moisture properties study. Similar to the cement paste sample, the amount of brick powder was calculated to be proportional to the brick core's surface area, see Table 7.5. First, the volume of brick sample per ATM core was calculated from the known WF brick volume. Next, the amount of brick powder sample for each brick type was calculated from their densities.

Table 7.5 Amount of brick samples rescaled to an ATM brick core samples calculated from the known WF brick volume, the exposed surface areas ratio and bricks' densities.

Parameter	WF brick	ATM core
Stretcher surface area [cm^2]	105	7.07
Brick volume [cm^3]	1050	70.7
Brick type	**Gross dry density [kg/m^3]**	**Brick powder / ATM [g]**
BR1	1690	119
BR2	1630	115

ATM setup preparation

The carbonated cement paste was first ground to a powder of <500μm and then the calculated amount of paste was placed in the ATM setup and topped up with 50ml distilled water.

The brick sample powders (<500μm) were prepared according to the procedure describe in Section 3.3. The calculated amount of brick powder sample was placed into a single ATM setup and topped up with 100ml of distilled water. Similarly to the cement paste carbonation study (Section 5.3.1), a dissolution monitoring experiment was applied to identify the source of water soluble sulphate.

7.2.3 Mortar admixtures

Mortar admixtures are available in form of a solution (added to a mortar mix), or as solids dispersed in a dry mortar mix. In both cases they are water soluble, hence in a wet mortar mix they are present in the liquid phase, which in turn makes them mobile during bricklaying. Bricks are porous and upon contact with a fresh mortar they absorb part of the solution from the fresh mortar mix, and this way the admixtures can get distributed over both mortar joints and bricks in masonry. For this reason the effect of admixtures was assessed in three steps. First, (i) the common products were benchmarked with a simplified experiment using a gypsum solution serving as a direct and non-limited GE source. In the next step two products were selected to assess separately their effect on the GE formation from (ii) carbonated cement paste and (iii) brick powder.

Admixtures benchmarking

Three commercial mortar admixture products A2-A4 (representing admixture types commonly applied in masonry mortars) were selected based on a survey of building material distributors in the area of Leuven (Belgium), see Table 7.6. The A2-4 admixtures are surfactant based "plasticizer and air entrainer" products, which enhance both the workability of a fresh mortar mix and promote formation of air microbubbles, the latter having a beneficial effect on the freeze-thaw performance of cement mortars. In addition to commercial mortar admixtures a common detergent A1 was also tested, because these are reportedly sometimes used instead of air-entrainers. Similar surfactant-based products were indicated as possible triggers of the recent GE cases (Bowler and Winter, 1997). Superplasticizers bring also the benefit of increasing the workability of a mortar mix, but potentially without inducing gypsum efflorescence formation. While they are widely applied in concrete, they do not find application in masonry mortars yet. A single commercial sulphonate-type superplasticizer A5 was included in the tests, as this type is usually not surface active (Pagé, 2003). However, as a consequence, these products do not induce air entrainment (Mosquet, 2003).

Table 7.6 List of admixtures used for benchmarking. The chemical composition is declared by producers.

Code	Admixture type	Chemical composition
A1	Common washing up liquid	15-30% anionic surfactant, 5-15% non-anionic surfactant
A2	Mortar plasticizer & air entrainer	Not available
A3	Mortar plasticizer & air entrainer	Not available
A4	Mortar plasticizer & air entrainer	8% detergent
A5	Concrete superplasticizer	Sulphonated melamine formaldehyde condensate

The ATM test applied to a pure gypsum solution only yielded gypsum accumulation below the brick surface, regardless of the unlimited gypsum solution supply. This simple test, after modification, can hence also serve for evaluating admixtures by determining whether these products can overcome gypsum's subflorescing propensity and trigger GE formation. This was realised simply by saturating brick cores in a gypsum (2.2g/L) and admixture solution for 5 minutes prior to mounting them in the ATM setup filled with a pure gypsum solution. The admixture dosage (Table 7.7) was calculated to reflect its concentration in a fresh C300 mortar, based on the known C300 mortar composition (Table 7.3) and the recommended admixture dosage. To our knowledge, it is common practice to overdose the admixtures though, hence as an initial attempt a three times higher dosage was applied instead. In addition, the effect of admixtures on the surface tension of gypsum solution was measured according to the '3.6.3 Surface tension' procedure.

Table 7.7   Dosage of admixtures to gypsum solution calculated based on the recommendation given by the admixture producer and C300 mortar formulation.

Code	Admixture dosage		Benchmarking admixture dosage (3x surplus)	
	Recommended by producer	Average	g/L	ml/L
A1	3-6g/L water*	4.5g/L water	13.5	-
A2	50-100ml/50kg cement	75mL/50kg cement	-	5.6
A3	50ml/50kg cement	50ml/50kg cement	-	3.8
A4	40ml/50kg cement	40ml/50kg cement	-	3.0
A5	0.2-3.4% by cement weight	1.8% by cement weight	67.5	-

No official dosage recommendation available, dosage suggested by a mason

Based on the benchmarking results, two admixtures were selected for further evaluation. An additional experiment was carried out to resolve whether the selected admixtures altered the wick process. It was realised by following the above explained procedure, but using distilled water instead of gypsum solution both for preparation of the admixture solution and as a test solution.

Carbonated cement & admixture paste

The mortars used for domestic constructions in Belgium are mostly prepared on-site (from separately purchased components) or are prepared from dry premixed commercial formulations. The two selected admixtures were tested in combination with the B1 and B2 cements, see Table 7.8. The admixtures were added to the cement powder together with water during the paste preparation. Here as well it was chosen to use a threefold surplus as compared to the recommended dosage (Table 7.7). Initially a single commercial premixed mortar (B5), containing unknown solid admixtures, was selected for testing. This mortar formulation is a common product according to building material distributors in the area of Leuven (Belgium). The 'cement & admixture' pastes were prepared, carbonated and ATM-tested according to the same procedure as for pure cement pastes.

Table 7.8 List of cement paste & admixture formulations. The admixtures dosage is calculated based on the producers' recommendation provided in Table 7.7. Some pastes showed bleeding after 28 days curing, hence their w/c ratio and ATM sample masses were corrected accordingly.

Cement paste composition	w/c	Admixture dosage (3x surplus)		Cement paste / ATM [g]
		[g/kg cement]	[ml/kg cement]	
B1+A3	0.50	-	3	8.0
B2+A3	0.50	-	3	8.0
B1+A5	0.39	54	-	7.4
B2+A5	0.35	54	-	7.2
B5	0.50	-	-	8.0

Brick & admixture

The selected admixtures were also tested in combination with the BR1 brick powder. The test solution was composed of distilled water mixed with brick powder and admixture, to allow for the interaction between the GE source (brick powder) and the used admixture. The dosage of the latter was calculated to reflect the amount of admixtures used per surface of a single ATM brick core. The recommended dosage of A3 and A5 admixtures is relative to the used amount of anhydrous cement (Table 7.7), which equals to

5.3g for an ATM core (Table 7.4). The dosage was hence calculated proportionally to the latter and increased to a threefold surplus, as for the other admixture ATM setups (Table 7.9). The setups were prepared and tested according to the same procedure as for pure brick powders.

Table 7.9   List of brick & admixture compositions. The admixtures dosage was calculated based on the producers' recommendation provided in Table 7.7.

Brick & admixture composition	Admixture dosage (3x surplus)		Brick powder / ATM [g]
	[g/ATM setup]	[ml/ATM setup]	
BR1+A3	-	0.016	119
BR1+A5	0.286	-	119

Brick and carbonated cement & admixture paste

A single additional test was applied to a test solution combining both masonry components: BR1 brick (119g) and B2+A3 cement paste (8g) powders mixed with distilled water (100ml). The former performed similar to the pure B2 cement paste (when tested alone), hence this test was addressed in the '7.4 Cement and brick as GE sources' section, instead of the '7.5 Mortar admixtures' section.

7.3 Brick moisture properties

The field survey findings indicated that GE develops on bricks characterised by a wide range of moisture properties, hence the latter do not seem to have a significant effect on the GE risk. Nevertheless, this assumption has not been verified experimentally yet, and was thus addressed with the ATM methodology in the following preliminary study. Brick cores extruded from three brick types were tested in gypsum solution and water to assess the effect of brick moisture properties on (i) the GE risk and (ii) the wick performance (Table 7.10). The three selected brick types exhibited fairly similar w_{cap}, some variation in w_{sat}, while the A_{cap} for the BR1 was considerably higher than for the BR2 and BR1extr (reflecting the difference in IRA), see Table 7.11.

Table 7.10   Overview of the ATM experiment variations and their settings. The setups' names are coded according to the following scheme: X/Y, where X stands for a brick type used as a transport medium, while Y describes the test solution. By default all tests were realised with a BR1 brick type and in such case the code is shortened to the Y symbol only. The exception are the setups listed below, where BR2 and BR1extr brick core types are used. The test solution Y can stand for:
- 2.2g/L gypsum ($CaSO_4 \cdot 2H_2O$) solution (G),
- distilled water (W),
- carbonated cement paste mixed with distilled water (B1 - B4),
- brick powder mixed with distilled water (BR1 and BR2),
- saturating a brick core with gypsum & admixture solution and then placing it in a setup with gypsum solution (G+A1 - G+A5),
- saturating a brick core with admixture (water) solution and then placing it in a setup with distilled water (W+A3, W+A5),
- carbonated cement & admixture paste mixed with distilled water (B1+A3/A5, B2+A3/A5, and B5),
- brick powder mixed with admixture and distilled water (BR1+A3 and BR1+A5),
- or carbonated cement & admixture paste mixed with brick powder and distilled water (B2+A3 & BR1).

Code	(BR1/)G	BR2/G	BR1extr/G	(BR1/)W	BR2/W	BR1extr/W
Brick core	BR1	BR2	BR1extr	BR1	BR2	BR1extr
Test solution	$CaSO_4 \cdot 2H_2O$	$CaSO_4 \cdot 2H_2O$	$CaSO_4 \cdot 2H_2O$	Water	Water	Water

Table 7.11 Moisture properties of the three investigate brick types. NA stands for not analysed.

Brick type	BR1	BR2	BR1extr
Initial rate of absorption IRA [$kg \cdot m^{-2} \cdot min^{-1}$]*	4.8	2.6	NA
Capillary absorption coefficient A_{cap}[$kg \cdot m^{-2} \cdot s^{-0.5}$]	0.80 ± 0.06	0.45 ± 0.06	0.48 ± 0.02
Capillary water content w_{cap} [kg/m^3]	214 ± 5	229 ± 3	200 ± 8
Vacuum water content w_{sat} [kg/m^3]	325 ± 7	368 ± 6	261 ± 4

The IRA values were declared by producers

7.3.1 Influence on the GE risk

The tests with gypsum solution quickly yielded a major DR drop for all the three brick types, see Figure 7.1 A. The analysis of samples scraped from their surfaces showed that it was attributed to gypsum pore clogging, see Table 7.12. While the BR1 and BR2 brick types yielded similar slight GE located within the coarse brick surface, on the BR1extr GE formed as a specific thin and shiny film, which majorly altered the surface appearance. This specific GE morphology might have been induced by the non-sanded and very smooth surface of the extruded brick. Efflorescence formation is a surface process and the surface properties may alter efflorescence morphology, what is in line with findings reported for NaCl (Eloukabi *et al.*, 2013). Nevertheless, the tested brick core types did not yield formation of any characteristic abundant GE form as found in the field survey, owing to the quick gypsum pore clogging, which constrains the moisture transport and thus the gypsum accumulation.
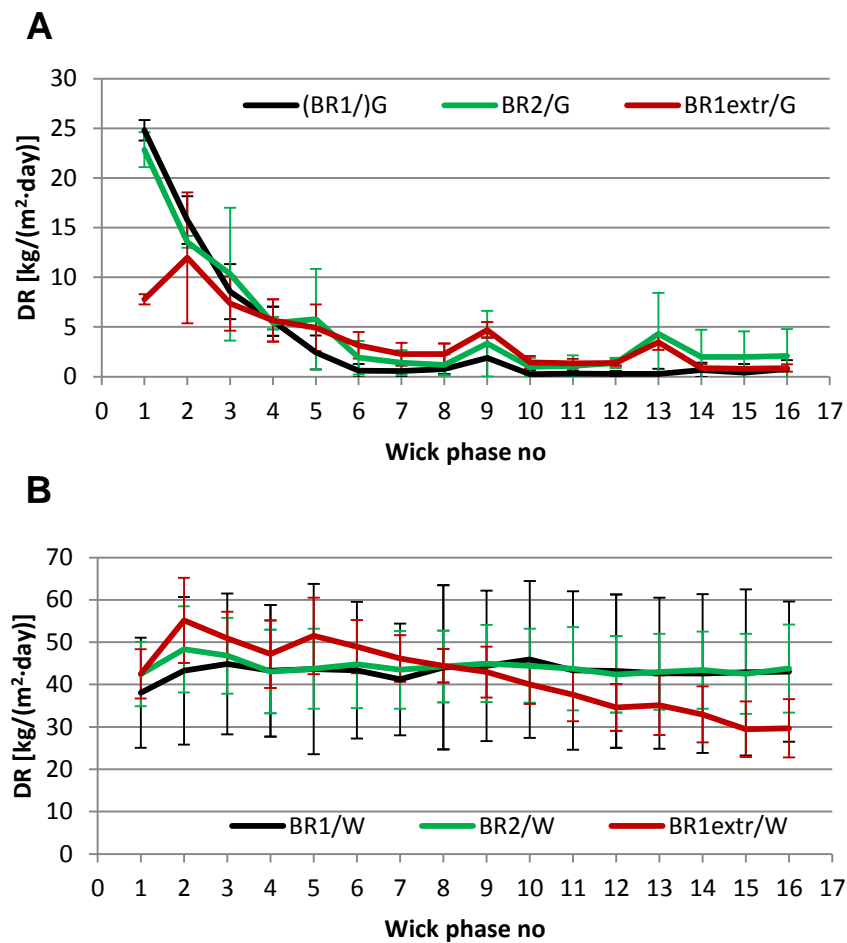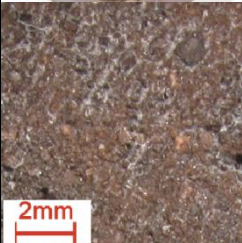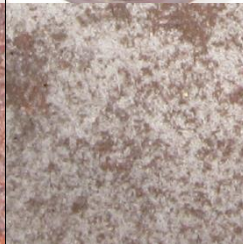
Figure 7.1 Drying rate evolution of setups tested with different brick core types: A – gypsum setups, B – water setups.

Table 7.12 Summary of ATM experiments, the table layout is explained in Table 6.2.

Setup's code	(BR1/)G	BR2/G	BR1extr/G
Efflorescence coverage	11 (13 ± 4) %	23 (24 ± 5) %	80 (75 ± 12) %
XRD	+ + + Gypsum	+ + + Gypsum	+ + + Gypsum
HCl test	− HCl	− HCl	− HCl
Efflorescence composition	Gypsum	Gypsum	Gypsum
Drying rate	DR drop	DR drop	DR drop
Overview photography			
Magnified photography			

7.3.2 Influence on the wick performance

A similar experiment, but with distilled water instead of gypsum solution, revealed that both BR1 and BR2 (hand moulded) bricks cores performed similarly in terms of the wicking process (Figure 7.1 B). The same could be observed for the BR1extr (extruded brick core) over the first eight wick phases, subsequently followed by a slight DR drop. No gypsum was identified in scrapings from the sample surfaces, but possibly even a little amount below the detection limit could have induced this slight DR drop. It shows that neither the lack of sanding, nor the specific pore orientation did affect considerably the DR.

The brick cores showed similar DR performance regardless of differences in A_{cap} (Table 7.11), hence the latter does not appear to have an important effect on the wick performance for the tested A_{cap} range. However, it does not preclude its considerable effect under field conditions. The ATM test is designed to accelerate efflorescence formation by simulating the wicking process, but not to reproduce the frequent absorption and drying episodes induced by naturally intermittent rainfall. Under such conditions the amount of water absorbed by a brick may be highly dependent on A_{cap}, in turn affecting the amount of dissolved gypsum source and accumulated gypsum efflorescence.

The field survey results showed that GE affects brick types covering the typical spectrum of brick moisture properties. The latter hence cannot be used as a factor for selecting brick types in order to limit GE risk (within the available range of commercial brick types). Also applying an extrusion manufacturing process to modify the pore structure does not seem to be an effective solution, as it yielded an unsightly shiny GE film. Nevertheless, the ATM test does not permit for a proper evaluation of the A_{cap} effect, and decreasing its level below the commonly found values may possibly lead to limiting GE extent by constraining the rainfall uptake and drying process.

7.4 Cement and brick as GE sources

Both brick and carbonated mortar joint may form a considerable GE source, as demonstrated in the field survey and cement carbonation chapters. On the other hand, gypsum appears to show a tendency for subsurface accumulation, and therefore even a presence of such significant GE source solely does not seem sufficient to generate abundant GE formation. While the latter was demonstrated on a simplified test applied to gypsum solution, this has not yet been confirmed for masonry components as GE sources. Four carbonated cement pastes and two bricks were hence ATM-tested to resolve whether the form of GE source has an effect on the GE risk. In addition, a single test was also applied to a sample composed of both components.

7.4.1 Carbonated cement paste

Four different commercial cement pastes were carbonated and tested as GE sources (Table 7.13), which in all cases led to a major DR drop (Figure 7.2), similar to the reference gypsum (G) setup (Figure 6.11 B). The mechanism appeared to be identical and related to the gypsum pore clogging, as both the efflorescence appearance (slight intergrain) and composition (gypsum) were similar. The only difference was the source abundance, which for cement pastes was limited to the amount of gypsum released upon carbonation: ranging from 1.20g to 2.94g of gypsum per brick (Table 7.14).

Nevertheless, this amount proved sufficient to yield gypsum pore clogging which effectively hindered moisture transport and thus GE accumulation. It shows that the subflorescing propensity of gypsum does not seem to depend on its source: either when it comes from carbonated cement paste or from pure gypsum solution (G in Section 6.3.2), gypsum accumulates under the surface. For the gypsum setups it took six wick phases to accomplish a major DR drop (Figure 6.11 B and Figure 9.4 A). This translated into an accumulation of 0.67-1.16g gypsum per brick, calculated from the amount of water evaporated during the six wick phases (Equation 6.6) for 35 samples (G1-10 sets) tested with gypsum solution (Figure 6.17 describes the tested setups, while Figure 9.4 A depicts their DR evolution). This range can be hence considered as a threshold for GE source content leading to the pore clogging and a major DR drop. The gypsum amount formed upon cement paste carbonation was considerably higher, demonstrating that indeed it could be held responsible for the observed major DR drop.

Cement B4 yielded slightly less intergrain GE than other setups, as reflected by its lower efflorescence coverage ($2 \pm 0\%$) and visual appearance. It behaved similar to the other setups in terms of DR evolution (Figure 7.2), but contained substantially more GE source than the other cement pastes (Table 7.14). However, the latter does not seem to explain the observed lower GE extent by e.g. more extensive pore clogging, as gypsum setups (containing unlimited GE source) yielded higher surface discoloration ($13 \pm 4\%$, Table 6.4). The anhydrous B4 cement (CEM IV / B-P 32.5) differs from the other tested cements by particularly high replacement of clinker with natural pozzolana component (45-64% clinker), however its potential effect on gypsum efflorescence formation after its hydration and carbonation is not evident.

Table 7.13   Overview of the ATM experiment variations and their settings, see Table 7.10 for the explanation of the setups' codes.

Code	B1	B2	B3	B4
Brick core	BR1	BR1	BR1	BR1
Test solution	Carbonated cement paste (B1-4) powder + water			
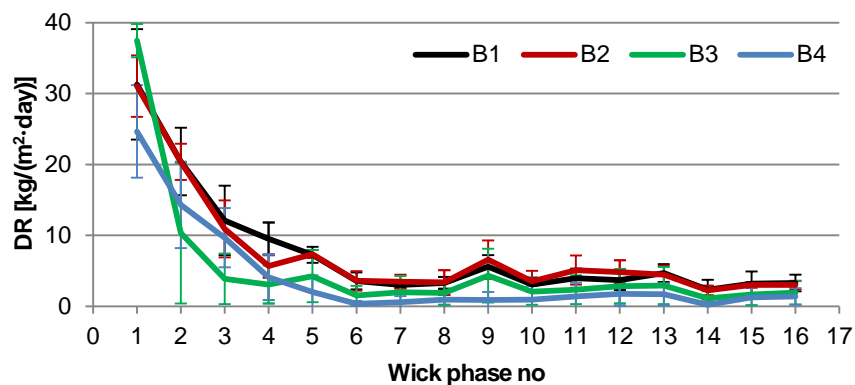
Figure 7.2 Drying rate evolution of ATM setups applied to carbonated cement paste as a GE source.

Table 7.14   Summary of ATM experiments, the table layout is explained in Table 6.2. The table contains an extra row 'Gypsum/brick' which provides an estimation of the amount of gypsum which can be derived from a GE source: brick powder or carbonated cement paste. It was calculated from their total water soluble SO_4^{2-} content determined according to '3.5.1 Leaching test' and normalised per a standard WF brick based on Table 7.4 and Table 7.5 data.

Setup's code	B1	B2	B3	B4
Efflorescence coverage	6 (7 ± 6) %	8 (6 ± 1) %	3 (6 ± 3) %	1 (2 ± 0) %
XRD	+ + + Gypsum	+ + Gypsum	+ + + Gypsum	+ + + Gypsum
HCl test	− HCl	− HCl	− HCl	− HCl
Efflorescence composition	Gypsum	Gypsum	Gypsum	Gypsum
Drying rate	DR drop	DR drop	DR drop	DR drop
Gypsum/brick [g]	1.20g gypsum	1.41g gypsum	1.97g gypsum	2.94g gypsum
Overview photography				
Magnified photography				

7.4.2 Brick

Bricks contain water soluble sulphate, whose source can be anhydrite and/or alkali sulphate(s). However, on the one hand their amounts may be too low for identification with XRD, and on the other hand the sources are in anhydrous form, what makes it difficult to identify them with TG. Similar as for carbonated cement paste, a simple dissolution monitoring experiment can aid in distinguishing between the two sources and in judging which one contributes most to the GE source (Section 5.3.1).

Figure 7.3 shows the result of a dissolution monitoring experiment applied to BR1 and BR2 brick powders. The plot indicates a strong correlation between the release of water soluble SO_4^{2-} and Ca^{2+}, as the 'SO_4^{2-} vs Ca^{2+}' trend lines show slopes (a_{BR1}=1.139 and a_{BR2}=0.939) and R^2 values (R^2_{BR1}=0.9983 and R^2_{BR2}=0.9356) close to 1. This in turn demonstrates that the main source of the leached Ca and SO_4^{2-} was a single compound characterized by $Ca^{2+}/SO_4^{2-} = 1$. Clay bricks are fired at temperatures far higher than gypsum and hemihydrate dehydration temperatures, which suggests that the source was mainly in form of anhydrous calcium sulphate - anhydrite.

Unlike for cement paste, the ATM test applied to two brick powders (Table 7.15) did not lead to a major DR drop, instead the DR stayed at an elevated level throughout the test duration, see Figure 7.4. Table 7.16 shows that besides gypsum, a considerable amount of calcite was detected in the efflorescence as well. The HCl test left behind only slight intergrain GE, thus no characteristic abundant GE was formed. The amount of GE source for BR1 and BR2 was lower than required to induce pore clogging (0.67-1.16g), what explains no major DR drop. Instead, the high DR maintained over the course of experiment allowed for a gradual accumulation of calcite. It resulted in an overall more pronounced surface discoloration than for the carbonated cement setups. However, it does not need to be the case for other brick types, as commercial bricks may contain GE source in much higher amounts, i.e. up to even 7.25g gypsum/brick (Table 4.3). The ATM results on carbonated cements indicated that the subflorescing propensity of gypsum does not depend on the chemistry of its source, and then it is expected that the

same behaviour would be observed for these anhydrite-rich brick types. It indeed finds confirmation in the (water) impregnation & drying test applied to anhydrite-rich Fletton brick types (Bowler and Winter, 1997). Their test was run for over a year and its efficacy was confirmed by yielding GE on the same brick types with addition of GE-triggering products, what has also demonstrated that such bricks contain a sufficient GE source. Nevertheless, when tested with water only, no GE was formed on their surface. While the drying process was not monitored, and the samples were neither analysed for subsurface salts accumulation, such results suggest subsurface gypsum pore clogging taking place. These results showed also that anhydrite, regardless of its very low dissolution rate (Jeschke and Dreybrodt, 2002), can be sufficiently dissolved and transported, to eventually accumulate as GE.
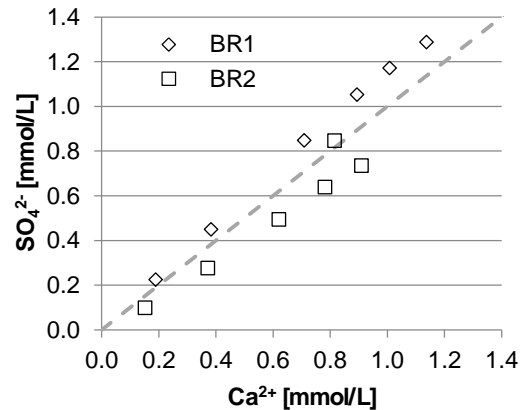
Figure 7.3   Correlation between leaching of SO_4^{2-} and Ca^{2+} ions from BR1 and BR2 brick powders. The six points for each brick type correspond to sampling at different time intervals (1hr, 6hr, 1d, 2d, 3d and 7d). The dotted line represents a y=x equation.

Table 7.15   Overview of the ATM experiment variations and their settings, see Table 7.10 for the explanation of the setups' codes.

Code	BR1	BR2
Brick core	BR1	BR1
Test solution	Brick (BR1 or BR2) powder + water	
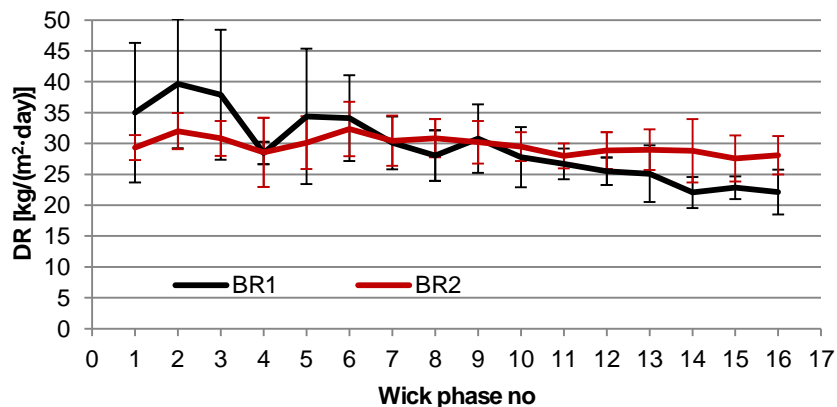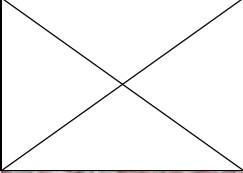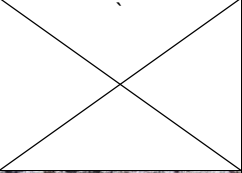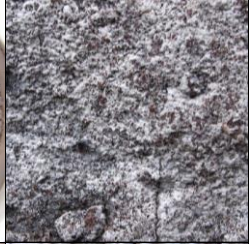
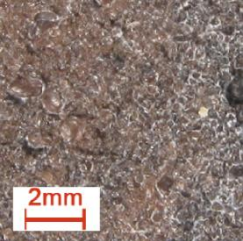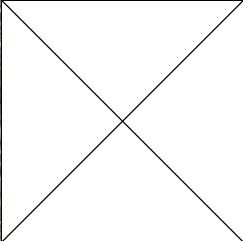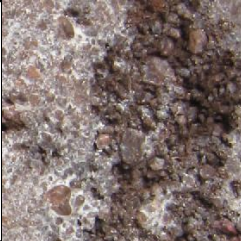Figure 7.4 Drying rate evolution of ATM setups applied to brick powder as a GE source.

Table 7.16   Summary of ATM experiments, the table layout is explained in Table 6.2. The last text row provides estimation of the amount of gypsum which can be possibly derived from the tested GE source (see Table 7.14 for explanation). In addition, field survey photographs of buildings constructed with BR1 and BR2 brick types are shown.

BR1		BR2	
ATM	Field survey (FS19)	ATM	Field survey (FS16)
28 (41 ± 10) %		37 (37 ± 2) %	
+ + Gypsum		+ Gypsum	
+ + HCl		+ + HCl	
Gypsum & calcite		Gypsum & calcite	
High DR		High DR	
0.42g gypsum		0.61g gypsum	

The BR1 and BR2 brick types were identified among the field survey cases and their photographs in Table 7.16 demonstrate the presence of the characteristically abundant GE. Its formation requires both an additional GE source (apart from the anhydrite-poor brick types BR1 and BR2) and a factor triggering its formation (instead of subsurface accumulation). Both can possibly originate from a carbonated mortar joint in masonry. Formation of a considerable gypsum source in the mortar joints was demonstrated in the previous section, while the GE triggering effect of mortar admixtures is discussed in the following ones. While GE is most pronounced on the brick surface (often leading to blaming the brick manufacturers for this surface blemish), the GE source and its trigger may actually originate from the mortar joint.

7.4.3 Brick and carbonated cement paste

The BR1 & B2+A3 setups contained both brick powder and a carbonated cement paste, see Table 7.17. The latter was prepared with an admixture, which turned out to be inert as it performed similarly to a pure B2 cement paste (Section 7.5.2), hence the effect of the admixture is not considered here. The test quickly yielded a major DR drop (Figure 7.5), accompanied by only negligible intergrain GE (Table 7.18), similar to the setup containing the cement paste only. This can likely be attributed solely to the GE source content (1.84g) being above the threshold range required to induce pore clogging (0.67-1.16g). The setup with the brick powder only (BR1 set in Table 7.16) yielded more surface discoloration due to calcite efflorescence formation, but here the additional GE source from the B2+A3 cement paste prevented this by quickly inducing pore clogging. It turns out then that the presence of a sufficient gypsum source in masonry, i.e. above the pore clogging threshold, may help avoiding formation of other types of efflorescences. A similar conclusion was reached for the gypsum setups (Section 6.4.4), where gypsum pore clogging hampered the surface accumulation of other sample-derived species.

Table 7.17   Overview of the ATM experiment variations and their settings, see Table 7.10 for the explanation of the setups' codes.

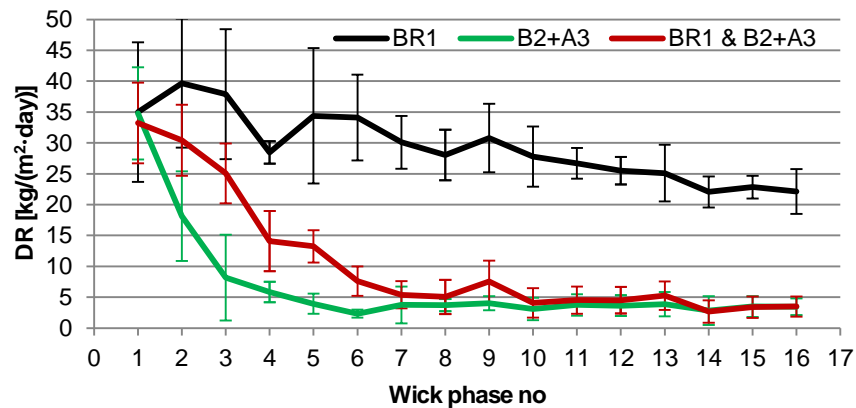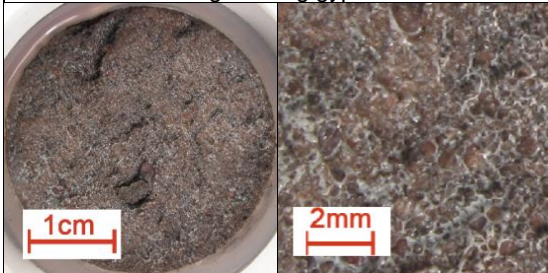| Code	BR1 & B2+A3
Brick core	BR1
Test solution	BR1 brick powder + carbonated cement (B2+A3) powder + water

Figure 7.5 Drying rate evolution of ATM setups applied to evaluating brick powder and cement paste as GE sources, separately (BR1, B2+A3) and combined (BR1 & B2+A3).

Table 7.18   Summary of ATM experiments, the table layout is explained in Table 6.2. The last text row provides estimation of the amount of gypsum which can be possibly derived from the tested GE sources, which in this case is a sum of sources derived from combined brick and cement samples (Table 7.14 for explanation).

BR1 & B2+A3
13 (15 ± 5) %
+ + + Gypsum
− HCl
Gypsum
DR-drop
0.42g + 1.42g gypsum

7.4.4 Discussion

The GE source may be either in the form of anhydrite contained within the brick, or may be formed by carbonation of the mortar joint. The presence of a considerable gypsum source and conditions promoting efflorescence formation are however insufficient to always result in the characteristic abundant GE formation observed in the field survey. It was not obtained either for the ATM applied to carbonated cement paste or to brick powder. In case of the latter, it appears that anhydrite's exceptionally low dissolution rate is not a constraint for GE formation on masonry. However, the brick types selected in this exploratory study were deficient in anhydrite, which led to neither pore clogging nor considerable GE formation. This actually demonstrates that some existing brick types contain sulphate at levels which do

not contribute considerably to the GE risk, even though GE develops always preferentially on their surface. It is hence feasible to reduce the GE risk on the level of bricks manufacturing by minimizing the content of sulphate in the clay mix composition. That can possibly be achieved by the choice of low sulphur clays and fuels, and/or binding the sulphate present in clay mix into virtually insoluble $BaSO_4$ by means of $BaCO_3$ addition (Kindrick and Harrison, 1980; MacGregor Miller and Melander, 2003). While the latter approach allows for immobilising water soluble sulphates, it is not effective against virtually insoluble pyrite (FeS_2), which may be possibly present in clay mix and give rise to water soluble sulphates after brick firing due to pyrite oxidation (Vogt and Tatarin, 2013). Conversely, carbonation of the tested commercial cements supplied sufficient amount of gypsum to induce pore clogging, and thus the subflorescing propensity of gypsum prevented abundant GE formation. Moreover, it appears to hinder formation of other types of efflorescence as well, and thus it might be hypothesised that a sufficient GE source content in masonry components may be actually recommended. This finds confirmation in the British experience, where thousands of millions of bricks with high anhydrite content were produced and used for construction with no history of considerable surface blemish for more than a century (Butterworth, 1957; Bowler and Fisher, 1989; Bowler and Winter, 1996). On the other hand, gypsum formation in mortars could have taken place as long as cement has been used for their preparation and in the case of Belgium pure cement mortars have been commonly used since the 1950's. In both cases, the GE sources were present in masonry far earlier than the first alarming reports on GE from 1980's in the UK and 1990's in Belgium. The apparent tendency of gypsum to crystallise under the surface may possibly explain the lack of GE on masonry over decades, regardless of its source presence either in a brick or mortar.

The production of Portland cement requires intensive grinding of its components, and grinding aids are used to facilitate this process. The British study on GE (Bowler and Winter, 1997) suggested that some of these substances might have triggered GE formation similarly to mortar admixtures. However, the tests applied to the selected Belgian cements demonstrate that in their case the used substances did not bring such a risk.

The ATM experiments on carbonated cement, brick powder and their mixture, combined with the literature data demonstrate that a presence of a GE source in masonry is indeed a necessary but not a sufficient condition to yield abundant GE (as found in the field survey). Instead, regardless of the GE source, gypsum shows a specific tendency for subsurface accumulation, which yields slight intergrain GE at most. The next section therefore investigates the effect of admixtures, which both in Belgium and in the UK have been recently introduced to mortar formulations, and can therefore shed light on the genesis of this problem.

7.5 Mortar admixtures

The experiments applied to carbonated cement confirmed that gypsum exhibits a subflorescing propensity regardless of its source, and hence that a GE source present in masonry alone does not necessarily result in the formation of abundant GE. It therefore requires an additional factor, pointing at mortar admixtures which were suspected previously of triggering GE (Bowler and Winter, 1997). In the following sections we focus on their effect on the GE risk by applying the ATM methodology. First, the common Belgian admixture products were benchmarked with a simplified test setup, and next the effect of two selected products was evaluated under more realistic conditions: together with a brick powder and as a carbonated cement paste component.

7.5.1 Admixtures benchmarking

The common British mortar admixtures (suspected for triggering GE) are reported to be surfactant based, hence significantly reducing the surface tension (Bowler and Winter, 1997). We therefore tested whether the selected common Belgian products also exert a similar effect, see the list of setups in Table 7.19. Table 7.20 confirms this for the selected admixtures (A1-A4), indicating that their active compound is a surfactant. The same test was also applied to a concrete superplasticizer A5, which in contrast did not alter significantly the surface tension.

Table 7.19 Overview of the ATM experiment variations and their settings, see Table 7.10 for the explanation of the setups' codes.

Code	G+A1	G+A2	G+A3	G+A4	G+A5
Brick core	BR1 saturated in gypsum and admixture solution (G+A1 – G+A5)				
Test solution	$CaSO_4 \cdot 2H_2O$				

Table 7.20 Surface tension (average ± SD) of gypsum solution (G), water and admixture & gypsum (G+A1 – G+A5) solutions.

Solution	Surface tension [mN/m^2]		
G	70.7	±	0.7
Water	70.0	±	0.1
G+A5	69.4	±	0.2
G+A3	29.2	±	0.4
G+A2	28.9	±	0.2
G+A4	25.8	±	0.0
G+A1	24.0	±	0.0

Influence on the GE risk

The introduction of mortar admixtures (A1-4) to the ATM gypsum setup led to overcoming the typical major DR drop, see Figure 7.6. Moreover, the A3 product resulted in a DR even higher than for water setups (43 kg/(m²·day) on average, see W set in Figure 6.11 A) owing to the formation of abundant dendritic surface efflorescence (Table 7.21), which enlarged the drying surface area and consequently the DR as well. Out of the four admixtures, the A4 altered the DR the least, resulting in a moderate DR, which eventually showed a major drop. The high DR translated into an efficient transport of gypsum solution and gypsum precipitation on the surface, what resulted in formation of abundant GE, see G+A1-4 in Table 7.21. The formed efflorescence was very abundant. The A1-4 admixtures composition is based on surfactants, as demonstrated by their crucial reduction of the surface tension (Table 7.20). This suggests that the presence of surfactants changed the gypsum propensity from subsurface accumulation into surface efflorescence. In the absence of surfactants gypsum accumulated below the sample surface, what might be possibly explained by the gypsum's propensity for crystallisation at a solid-liquid interface, hence also within the brick pores (Section 6.3.2). On the other hand, surfactants accumulate at a liquid-air interface, where they can prompt nucleation and crystallisation (Canselier, 1993), and in this way promote crystallisation at the brick surface instead, resulting in efflorescence formation. Gypsum efflorescence formed in the presence of admixtures was initially in the form of complex dendritic structures, which upon frequent wetting cycles recrystallized into more bulky forms, but nevertheless their initial dendritic structure was often still partly preserved what can be noticed on the magnified pictures in Table 7.21. In contrast, in absence of admixtures gypsum crystallised as densely packed stacks of plates (Figure 6.8). The different crystal habits could be also possibly explained by the effect of surfactants: their adsorption onto crystalline faces alters the crystal growth process and in turn modifies both habit and size distribution of crystal products (Canselier, 1993). These effects could be possibly investigated by crystallisation experiments carried out in glass capillaries (Rodriguez-Navarro and Doehne, 1999; Shahidzadeh-Bonn et al., 2008), by e.g. comparing behaviour of gypsum solution with addition of admixture to a pure one. Gypsum efflorescence found on actual constructions was also in form of local thick accumulations, though less abundant and without the dendritic shape aspect (Table 4.1). The particular abundance of laboratory simulated GE is attributed to both unlimited gypsum source supplied at a relatively high concentration (2.2 g/L gypsum solution, equivalent of 85% gypsum saturation at 20°C) and to drying conditions optimised for promoting efflorescence growth (35°C, 21% RH, continuous air flow). The lack of dendritic aspect on field survey cases is likely related to the fact that over years the developing GE was subjected to hundreds of intensive wetting episodes, upon which the forming deposit recrystallized. Under the ATM conditions the wetting water was completely absorbed by a brick within less than 50 minutes, what yielded only its partial recrystallization, in some cases still preserving its initial dendritic aspect.

The concrete superplasticizer A5 did not alter the gypsum crystallisation behaviour and the setups performed similarly to the ones with gypsum solution only (G in Table 6.4). DR drop was quickly generated by pore clogging, accompanied by a scarce intergrain GE, albeit even less pronounced than for the reference gypsum setups. The A5 product is a concrete superplasticizer (sulphonated melamine formaldehyde condensate, Table 7.6) which in contrast to surfactant based products does not alter the surface tension (Table 7.20). The sulphonated melamine superplasticizers are reported to have no substantial effect on gypsum crystallisation (Middendorf and Budelmann, 1995), what is in line with the present results.
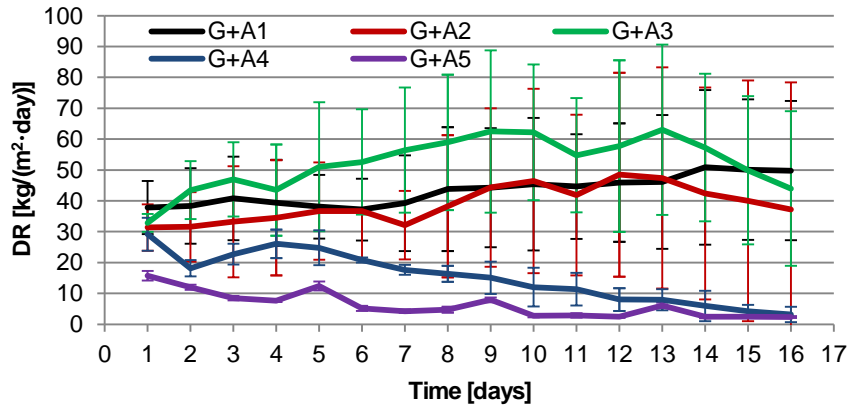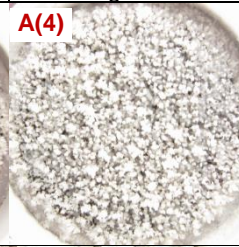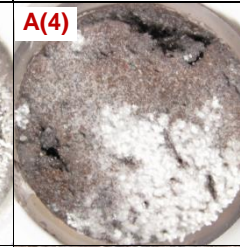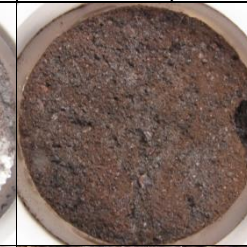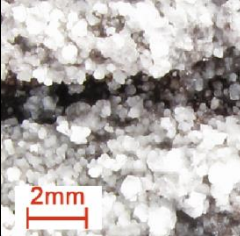

Figure 7.6 Effect of addition of mortar admixtures (A1-4) and concrete superplasticizer (A5) to the test solution (gypsum) on the drying rate evolution.

Table 7.21   Summary of ATM experiments, the table layout is explained in Table 6.2. The A(X) symbol identifies sets within which abundant GE was found, while X stands for the number of affected samples out of four.
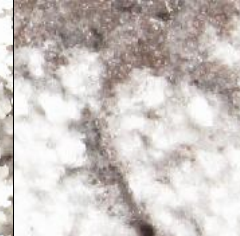
G+A1	G+A2	G+A3	G+A4	G+A5
77 (81 ± 6) %	83 (88 ± 9) %	92 (90 ± 5) %	72 (57 ± 20) %	1 (1 ± 2) %
+ + + Gypsum	+ + + Gypsum	+ + + Gypsum	+ + + Gypsum	+ + Gypsum
− HCl	− HCl	− HCl	− HCl	− HCl
Gypsum	Gypsum	Gypsum	Gypsum	Gypsum
High DR	High DR	High DR	Moderate DR	DR drop

Influence on the wick performance

Based on the benchmarking results, the A3 and A5 admixtures were selected for further evaluation. The former triggered the most abundant GE, while the latter was the only one that did not alter the

subflorescing propensity of gypsum. In the first step the above experiment was modified by replacing gypsum solution with distilled water (Table 7.22) to investigate the effect on the wick process only, see Figure 7.7. The results for the setups with A3 addition (W+A3) and water setups (W) show considerable scatter and overlap, thus it cannot be judged whether they differ significantly regardless of a major difference in their average DRs. The average DR for the W+A3 is lower than for the W setups, hence there is no indication of a beneficial effect of the A3 admixture on the efflorescence formation by e.g. enhancing the wick process. The GE triggering effect thus appears to work through altering gypsum crystallisation behaviour only. In contrast, the setups with addition of the A5 concrete superplasticizer (W+A5) showed very repeatable DR, which on average was substantially lower than for the water setups (W). However, the reason for this effect cannot be explained from the available data.

Table 7.22   Overview of the ATM experiment variations and their settings, see Table 7.10 for the explanation of the setups' codes.

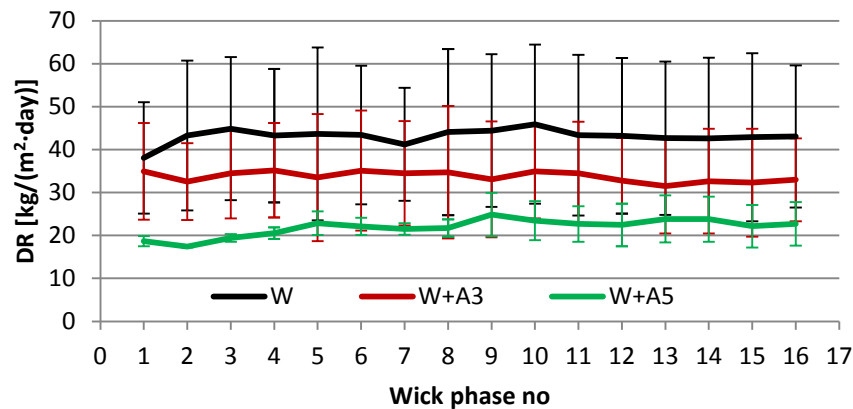| Code	W+A3	W+A5
Brick core	BR1 saturated in water-admixture solution (W+A3 or W+A5)	
Test solution	Water	

Figure 7.7   Effect of addition of mortar admixture (A3) and concrete superplasticizer (A5) to the test solution (water) on the drying rate evolution.

7.5.2 Carbonated cement & admixture paste

The ATM test applied to carbonated cement pastes containing admixtures yielded controversial results. While addition of the A3 admixture resulted in overcoming gypsum pore clogging and consequently generated high DR when tested with gypsum solution, its addition to B1 and B2 cement pastes (Table 7.23) did not yield such effect anymore. Instead, in both cases a major DR drop took place (Figure 7.8), similar as for pure carbonated cement pastes (Figure 7.2), and was accompanied by a slight intergrain GE (Table 7.24). The reason for the lack of the expected admixture effect is not clear, it might be possibly explained by its encapsulation in a complex structure of cement paste, or another type of immobilising interaction. This hypothesis can be assessed in future by determining the amount of admixture leached from a carbonated cement sample (estimated from the measurement of total organic carbon in leachate (Dransfield, 2007)) and comparing it to the amount of admixture added during cement paste preparation.

In contrast, the superplasticizer A5 led to a major DR drop when tested in the gypsum ATM setup, but its addition to both cement pastes resulted in a high DR maintained over the test duration (Figure 7.8), accompanied by a pronounced calcite efflorescence (B1+A5) or abundant gypsum and calcite efflorescence (B2+A5) formation (Table 7.24). Carbonation of the B1+A5 cement paste did not result in gypsum formation, which explains the lack of gypsum in the deposit. The A5 superplasticizer thus

retarded cement carbonation, which is further supported by the development of calcite efflorescence originating from the noncarbonated portlandite. No such effect was observed for the composition with the B2 cement paste. A significant amount of gypsum was formed upon carbonation, and abundant GE formation was observed. Even though A5 superplasticizer did not alter gypsum's subflorescing tendency in experiments with gypsum solution, it showed specific interaction effects with cement, which led either to limiting of the GE risk, or alternatively its enhancement. While these preliminary results demonstrate the complex chemistry of cement systems and its interactions with mortar admixtures and superplasticizers, they are not sufficient to explain the underlying mechanisms. Investigating the nature of these specific interactions between admixtures and hydrated Portland cement may pose a difficult analytical problem. It can be attributed to very low dosage of admixtures (Ramachandran, 1995) and the fact that their interactions involve a wide diversity of phenomena, resulting from the reaction between two complex chemical systems: multi-phasic hydrated Portland cement and multi-component commercial admixtures formulations (Jolicoeur and Simard, 1998).

Table 7.23   Overview of the ATM experiment variations and their settings, see Table 7.10 for the explanation of the setups' codes.

Code	B1+A3	B2+A3	B1+A5	B2+A5	B5
Brick core	BR1	BR1	BR1	BR1	BR1
Test solution	Powder of carbonated 'cement and admixture' paste + water				
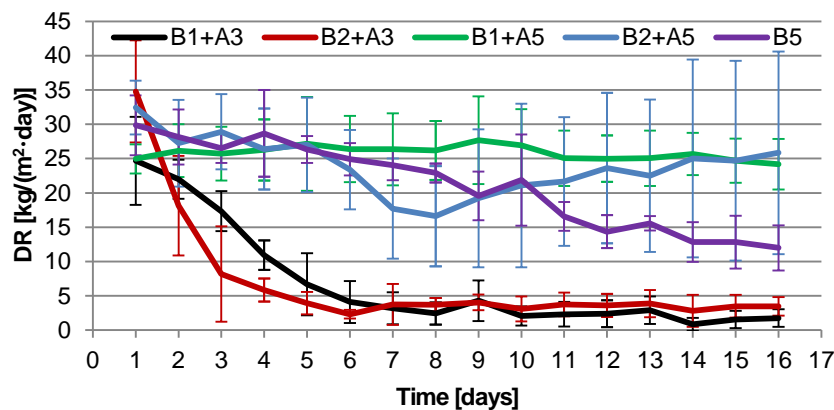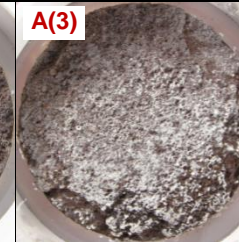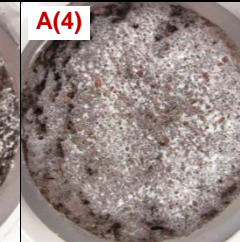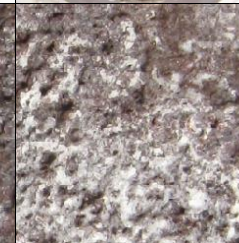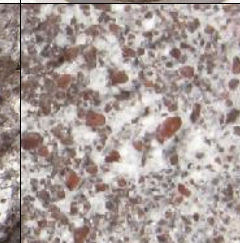
Figure 7.8 Drying rate evolution of ATM setups applied to carbonated cement pastes containing admixtures.

Carbonation of the commercial premixed formulation B5 led to a formation of the most abundant GE source (compare Table 7.14 and Table 7.24). All samples were considerably covered with gypsum deposit, reminiscent of GE cases identified during field survey. At the same time gypsum crystallisation did not constrain surface evaporation as reflected by a high DR (Figure 7.8). This shows both that (i) commercial mortar formulations can supply sufficient amount of gypsum after their carbonation and (ii) may contain components triggering abundant GE formation at the masonry surface. The admixture component of B5 formulation appears to maintain its GE triggering properties even after its incorporation in a cement paste, followed by its hydration (28 days) and carbonation (70 days). The experiments on masonry wallettes (Bowler and Sharp, 1998) demonstrated that this can hold true even after a couple of years after their construction. Moreover, while the admixtures A3 and A5 were overdosed at a three times surplus (as an initial attempt to reflect common practice), the B5 mortar is a premixed composition and its admixture content was not increased. It shows that the actual admixtures levels in commercial premixed products might be sufficient to trigger GE formation.

Table 7.24 Summary of ATM experiments, the table layout is explained in Table 6.2. The last text row provides estimation of the amount of gypsum which can be possibly derived from the tested GE source (see Table 7.14 for explanation). The A(X) symbol identifies sets within which abundant GE was found, while X stands for the number of affected samples out of four.

B1+A3	B2+A3	B1+A5	B2+A5	B5
5 (9 ± 5) %	6 (6 ± 2) %	16 (10 ± 4) %	47 (52 ± 20) %	58 (44 ± 15) %
+ + + Gypsum	+ + + Gypsum	+ Calcite	+ + + Gypsum	+ + + Gypsum
− HCl	− HCl	+ + + HCl	+ HCl	− HCl
Gypsum	Gypsum	Calcite	Gypsum & Calcite	Gypsum
DR drop	DR drop	High DR	High DR	High DR
1.51g gypsum	1.42g gypsum	0.04g gypsum	1.32g gypsum	5.15g gypsum

7.5.3 Brick & admixture

Addition of the A3 mortar admixture to the BR1 brick powder (Table 7.25) resulted in inconsistent outcomes. Three setups performed similarly in terms of DR evolution (BR1+A3 (3s) in Figure 7.9) and efflorescence formation (Table 7.26) to the ones with brick powder only (BR1 in Table 7.16). In both (BR1 and BR1+A3) tests the brick powder supplied the same low amount of gypsum, and the results showed that it is insufficient to either cause pore clogging or accumulate as abundant GE. On the other hand, a single setup showed exceptionally high DR (BR1+A3 (1s) in Figure 7.9) accompanied by abundant GE, similarly to the A3 admixture performance in the benchmarking test (Section 7.5.1). The tested brick powder was fine and homogenous, and it is hence improbable that the brick powder sample in one setup contained more GE source. Another possibility is that a single brick core was enriched in calcium sulphate (e.g. in form of coarser grains) which was not completely extracted during the leaching procedure. Regardless of the origin of GE, this single experiment demonstrated that the admixture addition triggered abundant GE formation. In contrast, the addition of the A5 superplasticizer did not alter the DR evolution (Figure 7.9), but led apparently to a less pronounced efflorescence than for the brick powder only (BR1 in Table 7.16).

The ATM tests applied to brick powder, with and without the GE-triggering A3 admixture, resulted in a slight GE only and no gypsum pore clogging in all cases (but a single one). It demonstrated that these brick types do not contribute to the GE risk due to the very low GE source content (0.42-0.61g gypsum), what is not necessarily the case for other commercial brick types containing as much 7.25g GE source/brick. Bowler and Winter's efflorescence test applied to bricks rich in anhydrite in presence of mortar admixtures did indeed yield the characteristic GE formation (Bowler and Winter, 1997). It would be then of benefit to repeat the ATM tests, and apply them to brick types containing more abundant GE source, which could lead either to a measurable DR drop (via gypsum pore clogging) or abundant GE formation.

Table 7.25   Overview of the ATM experiment variations and their settings, see Table 7.10 for the explanation of the setups' codes.

Code	BR1+A3	BR1+A5
Brick core	BR1	BR1
Test solution	BR1 brick powder + water + admixture	
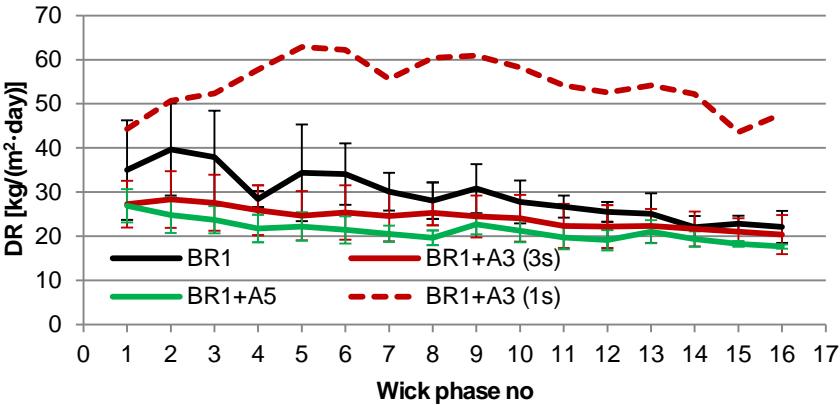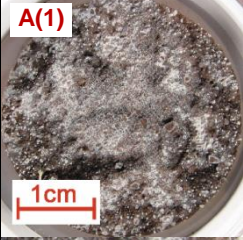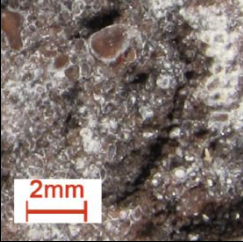
Figure 7.9 DR evolution of ATM setups applied to evaluation of a brick (BR1) with addition of admixtures (A3 and A5). The results for the BR1+A3 set is split into two plots: the average for three samples BR1+A3(3s), and a single result BR1+A3(1s) for an outstanding setup (which yielded abundant GE).

Table 7.26   Summary of ATM experiments, the table layout is explained in Table 6.2. The last text row provides estimation of the amount of gypsum which can be possibly derived from the tested GE source (see Table 7.14 for explanation). The A(X) symbol identifies sets within which abundant GE was found, while X stands for the number of affected samples out of four

BR1+A3	BR1+A5
38 (36 ± 12) %	15 (12 ± 4) %
+ + + Gypsum	? Gypsum
+ HCl	+ + HCl
Gypsum & Calcite	Calcite & Gypsum?
High DR	High DR
0.42g gypsum	0.42g gypsum

7.5.4 Discussion

The role of admixtures in the recent GE outbreak

Abundant GE formation was triggered by all tested surfactant-based admixtures in the benchmarking test. The tests applied to cement paste and brick powder yielded inconsistent results, but nevertheless confirmed that this can also hold for triggering GE from masonry components. The characteristic abundant GE form was obtained only for the setups containing admixtures; otherwise the tests led to a scarce GE, in some cases accompanied by calcite efflorescence. These findings are in line with the Bowler *et al.* (1997, 1998) results, as they similarly succeeded to simulate GE formation only by implementing admixtures in their (i) impregnation & drying test and the (ii) masonry wallette testing. The major role of mortar admixtures is further supported by the fact that their increasing use starting from the 80's coincides with the outbreak of GE cases in both Belgium and the UK. This correlation together with the experimental data strongly suggests that the use of mortar admixtures is responsible for the recent GE onset.

ATM applied to admixtures evaluation

The GE risk is a function of the GE source availability, the presence of admixtures, and their interaction with hydrating cement. An exploratory admixture benchmarking test can identify products which can trigger abundant GE. However, this capability can be hindered by admixture entrapment in a hardened cement paste or by an insufficient GE source. The choice of a test should be hence motivated by a well-defined research question.

The effect of a superplasticizer

The commercial plasticizers sufficiently reduce the requirement for water addition to masonry mortars, hence up till now there was no significant demand for applying more specialised and expensive superplasticizer products. However, the common plasticizers are surfactant based, what apparently may trigger abundant GE formation. The tested superplasticizer A5 did not affect the surface tension, and the benchmarking test revealed that it neither led to abundant GE, what makes it a potential replacement for plasticizers. However, the preliminary results showed that its interaction with cement paste may nevertheless lead to abundant GE. It further demonstrates, that the simple benchmarking test may not be sufficient to predict their performance, hence it appears necessary to evaluate them as a cement paste components. Moreover, sulponate-type superplasticizers do not induce air entrainment (Mosquet, 2003), and thus cannot be considered as an air-entrainer substitute.

7.6 Conclusions

The present study was designed to adapt the developed ATM for evaluating masonry components. It required determining a representative sample amount to assure the test reliability and adjusting the cement carbonation procedure. A series of tests were realised using the optimised methodology and they yielded formulation of numerous conclusions, which may help avoiding the GE problem and set directions for future research.

The ATM results confirm the field survey findings, suggesting that the GE risk is independent of the moisture properties of commercial hand moulded bricks. Application of an extruded brick did not bring any advantage either. Moreover, it yielded a considerable shiny GE film due to its specific surface properties, while the hand moulded bricks developed negligible intergrain GE under the same experimental conditions.

Both brick and mortar can be the sources of calcium sulphate(s), via respectively the dissolution of anhydrite or the carbonation of ettringite. And despite their low solubility, calcium sulphate(s) can be dissolved in the pore water, and transported via diffusion and advection. All the mechanisms related to sources, transport and crystallisation are equally active in older cement-based masonry, contrary to the more recent nature of the gypsum efflorescence problem. The lack of GE on older masonry buildings is likely attributed to gypsum's tendency to crystallize below the surface, leading to subflorescence instead of

efflorescence. This phenomenon was demonstrated both on tests applied to gypsum solution and carbonated cement paste, what contributes to the existing knowledge on salt crystallisation behaviour. On the other hand, the selected brick types contained insufficient GE source to yield either pore clogging or abundant GE. It implies that among the commercial clay bricks there are types which do not likely contribute to the GE risk owing to their very low GE source content, and hence possibly also other brick types can be possibly optimised in this direction.

Gypsum efflorescence has sprung up during the last three decades, what apparently coincides with the increased use of admixtures as components of mortar formulations. The present study provides additional evidence for the crucial role of surfactant based products. Indeed, abundant GE was obtained only for the setups where mortar admixtures were applied. The test on masonry mortar formulation demonstrated that the mortar joint may supply both a sufficient GE source and admixtures triggering abundant GE formation. The latter may stay active even after a long period of cement paste hydration and carbonation. The experimental and literature data suggest that mortar admixtures are responsible for the recent GE outbreak and therefore they should be avoided in mortar formulations.

The superplasticizers show potential for providing sufficient mortar mix workability without inducing GE formation, as they may decrease water demand of mortar without affecting the surface tension. It needs to be noted though, that they cannot be considered as replacement for air-entraining agents, while a lack of the latter may result in insufficient freeze-thaw durability of hardened mortar. Moreover, the preliminary test revealed that they may yield a specific interaction with cement resulting in abundant GE formation. The nature of the interaction is not known and hence further research is required to optimise them for application in masonry mortars.

One of the more significant findings to emerge from this study is that in the absence of surfactant based admixtures, the presence of a considerable GE source does not lead to GE formation owing to the gypsum subflorescing tendency. Moreover, gypsum pore clogging appears to prevent from formation of other types of efflorescence. The efflorescence free, old masonry buildings demonstrate that avoiding this problem in future is possible. Our findings enhance understanding of the GE genesis, and indicate that this problem can be possibly solved without limiting the GE source content in masonry, but rather by finding an inert replacement for mortar admixtures.

8 Conclusions and perspectives

8.1 General conclusions

Even though persistent efflorescence on Belgian masonry has been recognised for the last two decades, little was known about its composition, nature, and origin. Over the last years the number of reported cases was growing progressively, to an extent which created a considerable threat for a ceramic industry. This PhD project was initiated in response to this increasing problem, to enhance our understanding of this puzzling phenomenon, but also to provide tools allowing avoiding it in future. Both aims were successfully fulfilled. For the first time a detailed field study has been realised to investigate the Belgian cases, what allowed establishing the composition of persistent efflorescence and identifying its sources. A particular attention was paid to demonstrate the formation of efflorescence source in mortar, by designing and carrying out a tailored cement paste carbonation experiment. The main findings of these two studies helped defining requirements for designing an efflorescence test method. The developed method solved the shortcomings of the existing ones, by being versatile and significantly faster. Its application to a range of masonry components: bricks, cements and admixtures, yielded first insights on their contribution to the efflorescence risk and shed light on the possible solutions to the problem. The intermediate results and findings presented in this thesis allow answering the main research questions (Section 1.2), and they are addressed below.

1. **GE characteristics, mechanism and sources**
   The field survey of the GE cases in Belgium enabled a comparison of its characteristic features with other studies, and shed light on the mechanism and source of GE. The analysed data complemented by results from the cement paste carbonation and accelerated test method studies allowed answering the following two questions:
   1.1. *What is the composition of persistent efflorescence in Belgium? What are its characteristic features and how do they relate to the British and Dutch cases?*
      The efflorescence composition was determined in 19 out of 28 cases. In 13 of these gypsum was identified as the only or predominant component, while in 5 more cases it was accompanied by calcite. Persistent efflorescence develops exclusively on constructions erected within the last two decades, affecting mostly bricks on facades exposed to wind-driven rain (SW), and locally takes the form of abundant crusts. The property owners often reported that they perceived the efflorescence only after a couple of years, but it is not clear whether it was due to a delayed or slow development. The Belgian efflorescence cases share the same characteristics as the reported British (Bowler and Winter, 1996) and Dutch ones (Brocken and Nijland, 2004), thus it is likely that the same mechanism is responsible for their recent occurrence.
   1.2. *Are the GE components derived from internal or external sources?*
      Gypsum crusts typically formed on calcareous stones have a blackish appearance and develop on sheltered parts of a building (Steiger *et al.*, 2011). In contrast, the recent GE cases have a grey-white appearance and develop on the walls facing the prevailing wind-driven rain loads. The latter underlines the major role of wetting and drying conditions, implying that moisture transfer inside the masonry (facilitating the dissolution, transport and precipitation of gypsum) is a crucial factor. GE components are hence derived exclusively from the masonry components, and not from external sources like polluted air. Both masonry components can be direct sources of GE. Gypsum formation upon cement paste carbonation was demonstrated with a dedicated static dissolution monitoring experiment. The same experiment applied to brick moreover confirmed the presence of anhydrite in tested bricks. Finally, the ATM tests applied to brick and carbonated cements produced different degrees of GE, clearly demonstrating that these GE sources can lead to the GE formation.

2. **Aim: development of a fast and versatile efflorescence test method**
   The field survey enhanced our understanding of GE and processes leading to its formation, what set a direction for developing an accelerated efflorescence test method.
   An accelerated test method for assessing GE risk was successfully developed. The method was validated in three ways: under laboratory climate conditions, with an alternative NaCl test solution

and with respect to the effect of position in the climate cabinet. The developed methodology allows for an independent evaluation of (i) brick and cement as GE sources, (ii) the effect of brick moisture properties, and (iii) the effect of mortar admixtures. If required, the test can be applied to multiple factors at once. When applied to the evaluation of masonry components, the ATM test in many cases produced abundant GE, reminiscent of GE found on buildings investigated during the field survey. Moreover, while the Bowler and Winter (1997) efflorescence tests took at least one year (for brick only) or a couple of years (for masonry wallettes), the ATM shortens the test duration significantly: down to four weeks when applied to the brick or admixtures, and down to four months when cement paste carbonation was included.

3. GE genesis

The ATM test was applied to investigate the gypsum crystallisation behaviour. The experimental data supported by field survey observations and literature data contributed to elucidating the genesis of the recent GE occurrence.

3.1. Why did GE not occur before 80-90's and what triggered its formation later on?

The ATM tests have confirmed that gypsum exhibits an intrinsic subflorescing property, which results in its accumulation just beneath the drying surface, instead of forming the usual surface efflorescence typical for many common salts. It means that the presence of a considerable GE source in masonry is not solely sufficient to yield abundant GE as observed in the field survey cases. This was indeed experimentally observed in our ATM tests applied to carbonated cement as well as in Bowler and Winter's tests applied to anhydrite-rich bricks (Bowler and Winter, 1997). Moreover, when the GE source is present in a sufficient amount, its subsurface accumulation may lead to pore clogging, virtually arresting moisture transport to the surface. The threshold of the GE source content inducing pore clogging was estimated at 0.67-1.16g gypsum/brick. The ATM experiments have actually demonstrated that this pore clogging prevents the formation of other types of efflorescence, and could hence be considered desirable. This phenomenon may explain the British experiences: no GE was observed for tens of years regardless of a wide use of traditional Fletton bricks rich in anhydrite (Bowler and Fisher, 1989). This inference can probably also be extrapolated to the Belgian and Dutch GE cases, because bricks containing considerable amount of anhydrite have not been uncommon in the range available on the market. However, while gypsum pore clogging was demonstrated experimentally, no investigation has yet addressed its actual occurrence in older masonry constructions.

A considerable GE source presence is necessary, but not sufficient solely, to yield abundant GE, owing to gypsum's subflorescing propensity. Accumulation of gypsum on the surface of a drying porous medium hence requires the presence of an additional factor. Mortar admixtures turned out to trigger abundant GE when ATM-tested with gypsum solution, and in some cases when tested together with brick powder or as component of carbonated cement paste. This is in line with the results of Bowler and Winter (1997), who reproduced abundant GE formation only in cases where the admixtures were implemented in tests. Both in Belgium and in the UK the onset of GE cases correlates with an increased use of mortar admixtures, indicating them as the reason for the recent outbreak of persistent efflorescence.

4. GE risk

The developed ATM test was applied to separately evaluate the contribution of different masonry components towards the GE risk. A versatile test design allowed addressing and answering the following specific questions:

4.1. Can brick provide a sufficient amount of the GE source?

Bricks may contain anhydrous calcium sulphate (anhydrite), characterised by a particularly low solubility and slow dissolution. In ATM tests anhydrite-poor bricks (0.42-0.61g gypsum/brick) were used, which produced only slight GE formation, but these nevertheless confirmed that the particularly low solubility or slow dissolution of anhydrite does not preclude its contribution to GE formation. Nevertheless, due to their very low GE source content, an abundant GE was not obtained. On the other hand, GE formation from the British anhydrite-rich bricks was clearly demonstrated experimentally in other studies (Bowler and Winter, 1997). Bricks with a sizeable

anhydrite content are also commercially available in Belgium, one type of which (with about 7g gypsum/brick) was identified among the field survey cases.

4.2. Can mortar provide a sufficient amount of the GE source?

GE was identified in field survey cases on facades, where bricks deficient in anhydrite were used (e.g. 0.19g gypsum/brick), what showed that gypsum was derived from the mortar joints. Indeed, gypsum formation upon cement paste carbonation was demonstrated with a tailored dissolution monitoring experiment. Its formation takes place after an induction period required for sufficient cement paste carbonation, what may be reflected in the reported delayed GE occurrence. The ATM test applied to a carbonated binder (from the premixed mortar) confirmed that it can yield abundant GE, reminiscent of the GE found during field survey, owing to both a sufficient GE source (5.15g gypsum/brick) and the presence of mortar admixtures. On the other hand, the same test applied to four commercial cements resulted in a negligible GE only. Even though the GE source content (1.20-2.94g gypsum/brick) could have been sufficient to yield considerable GE, its formation was inhibited by pore clogging (threshold at 0.67-1.16g gypsum/brick), in absence of any GE triggering mortar admixtures.

4.3. Is it possible to limit the brick contribution to the GE risk by limiting its GE source?

Anhydrite in bricks originates either from calcium sulphate(s) present in clay mix, or is formed upon reaction of calcium compounds with other sulphates originating from clay components or from burnt fuel (Vogt and Tatarin, 2013). The anhydrite content can thus be limited by using low sulphur clays and fuels. On the other hand, the water soluble sulphate present in the clay mix can be bound into virtually insoluble compounds by addition of $BaCO_3$ during the production process. However, this procedure is not effective in case of presence of virtually insoluble pyrite in clay mix, which can give rise to water soluble sulphates upon its oxidation during brick firing (Vogt and Tatarin, 2013). Bricks particularly deficient in anhydrite are commercially available in Belgium, and two types were ATM tested. The tests yielded negligible GE, regardless whether admixtures were used or not, what demonstrated that brick's contribution to GE can be limited at the level of its source abundance. On the other hand, the tests demonstrated that in absence of a sufficient GE source no gypsum pore clogging takes place (threshold at 0.67-1.16g gypsum/brick), what may lead to formation of other type of persistent efflorescence (calcite).

4.4. Is it possible to limit the brick contribution to the GE risk by optimizing its moisture properties?

The analysis of field survey cases did not reveal any correlation between the GE risk and brick moisture properties (within the range found for commercial products). This was further supported by an exploratory ATM test applied to two brick types characterised by significantly different A_{cap}. Nevertheless, limiting the A_{cap} below the commonly found values may possibly limit the GE risk by constraining the water uptake and drying processes. Testing an extruded brick type did not reveal an advantage either, instead it apparently yielded a considerable shiny GE film.

4.5. Is it possible to limit the mortar contribution to the GE risk by reducing the calcium sulphate(s) addition to cement?

A surplus of calcium sulphate(s) is added to cement for economic reasons (Škapa, 2009). On the other hand, a recent study (Tsamatsoulis and Nikolakakos, 2013) demonstrated that even without their addition cements can yield 85-90% of their optimised strength, as already considerable amounts of sulphate may be present in cement clinker. The amount of sulphate in cement can be further decreased by diluting the ground clinker by addition of SCMs (Ghosh, 2003). While it shows a potential for major reduction of calcium sulphate(s) addition, it needs to be seen though whether this would not compromise other important cement properties (e.g. setting properties).

4.6. Is it possible to limit the mortar contribution to the GE risk by inhibiting gypsum formation in a cement paste?

The carbonation monitoring study confirmed that the decomposition of ettringite and monosulphate to gypsum was delayed due to a stabilising effect of CH, and thus could be also possibly arrested by maintaining a sufficient CH content in a cement paste. Pozzolanic SCMs consume the formed CH, hence seemingly their reduction or elimination could potentially retard gypsum formation in mortar. However, while this study has confirmed the accelerating effect of fly ash and granulated blast furnace slag on the process of cement paste carbonation (Šavija and Luković, 2016), these two did not advance the major gypsum release, as it actually took place with similar delay for both pure and SCM blended cements. On the other hand, part of Portland

cement in mortar could be possibly substituted by CH (cement-lime mortar), what may hinder the process of gypsum release owing to a formation of a dense carbonated zone (Brocken *et al.*, 2000). This concept was however not addressed in this study and requires further research.

4.7. *Is it possible to limit the GE risk by eliminating the surfactant-based mortar admixtures?*
In absence of GE triggering admixture products gypsum accumulates below the surface, and hence does not spoil its appearance. A sufficient GE source content, i.e. above the threshold level for pore clogging (0.67-1.16g gypsum/brick) may also reduce a risk of other types of efflorescence. Such level could be possibly supplied by both cement and brick: the tested commercial cements proved to release a sufficient amount of gypsum upon carbonation (1.20-5.15g gypsum/brick), while there are commercial brick types containing enough of the GE source (e.g. 7.16g gypsum/brick, as identified within the field survey cases). Elimination of the admixtures may hence potentially solve the GE problem without a need for limiting the GE source content in mortar or brick.

Gypsum efflorescence emerges as an extraordinarily complex phenomenon, as its genesis relates to such aspects as (among others) carbonation and decomposition of hydrated cement phases, specific crystallisation behaviour of gypsum, and its alteration by a distinct interaction with surfactant compounds. Revealing these mechanisms was possible only on account of a comprehensive approach including field and laboratory studies.

8.2 Research perspectives

This study explored the genesis of GE cases in Belgium and owing to the developed accelerated efflorescence test it provided recommendations aiming at limiting the GE occurrence in the future. While these have enabled us to answer the above questions, some aspects remain to be addressed, and are explained in the following sections.

Subflorescing propensity of gypsum

The particular behaviour of gypsum – its tendency for accumulation beneath the surface under conditions promoting efflorescence formation – has been reported previously for a variety of materials: bricks (Franke and Grabau, 1994, 1998), limestone (Cardell et al., 2008), sandstones (Snethlage and Wendler, 1997), granites (Charola et al., 2006), gypsum plaster (Seck et al., 2015), and has been confirmed in this study for an exemplary commercial Belgian clay brick. These studies suggest that gypsum's subflorescing propensity is not related to particular properties of a transport medium, neither to drying conditions, as demonstrated on the example of ATM test carried out under laboratory (24 ± 2°C, 53 ± 7% RH) and accelerated conditions (35 ± 2°C and 21 ± 4% RH) (Section 6.4.3). The effect of the brick moisture properties was preliminarily assessed on two hand-moulded brick types. It would be also of interest to establish a relation between the brick's porosity (e.g. pore size distribution) and the pore clogging (e.g. amount of accumulated gypsum) for a wider range of brick types.

The observed gypsum subsurface accumulation might indicate that it exhibits particularly strong preference for crystallisation at the solid-liquid interface (e.g. subflorescence in the brick's porosity) over the liquid-air one (efflorescence at the drying front on the brick surface). This hypothesis may be possibly tested with crystallisation experiments carried out in glass capillaries (Rodriguez-Navarro and Doehne, 1999; Shahidzadeh-Bonn et al., 2008), which allow observing initiation of the crystallisation process and precisely identifying the crystallisation location, taking advantage of observation under an optical microscope. These experiments would possibly increase our understanding of the pore-clogging phenomenon and enable us to model better the underlying processes (Todorovic and Janssen, 2014, 2015).

One of the key findings is linking the lack of GE on older masonry with gypsum's subflorescing tendency and the ensuing pore clogging. While this phenomenon was demonstrated experimentally, no investigation has yet targeted examining older unblemished masonry constructions for its actual occurrence. Attempts were made in this project to get permission for sampling masonry cores from selected masonry constructions, but the construction owners were always reluctant, mostly due to fear of damaging their facades.

The GE triggering effect of admixtures

The ATM test applied to gypsum solution yielded subflorescence formation, but addition of a slight amount of surfactant-based mortar admixtures triggered formation of abundant efflorescence under the same experimental conditions. This exceptional effect may be possibly explained by accumulation of surfactants at the liquid-air interface (drying front on the brick surface), where they can induce nucleation and salts crystallisation (Canselier, 1993). This effect, similarly as for gypsum's subflorescing propensity, could be investigated be means of a crystallisation test carried out in glass capillaries (Rodriguez-Navarro and Doehne, 1999; Shahidzadeh-Bonn et al., 2008) on solutions of gypsum and admixture products.

Cement-admixtures interaction

All the tested surfactant-based admixtures (A1-4) triggered abundant GE formation from gypsum solution (Section 7.5.1). However, when a single product (A3) was tested as a component of a cement paste, no such effect was observed anymore (Section 7.5.2). This suggests that it might have been immobilised in a complex structure of hydrated cement paste. This hypothesis could be tested by subjecting a carbonated cement paste sample to a leaching test and estimating the content of dissolved admixture by measuring the content of total organic carbon in the leachate (Dransfield, 2007). Its comparison with the amount of admixture added to the cement paste sample would allow assessing the extent of the immobilising effect.

The effect of admixture on formation of GE from brick

The ATM test on brick and admixture used a brick type deficient in anhydrite, and this already could prevent from observing the GE triggering effect induced by the added mortar admixtures. It would be then of interest to repeat these tests with bricks containing more elevated levels of anhydrite, similar to Bowler and Winter (1997).

Admixtures replacement

The ultimate goal of the brick industry is to eliminate the GE problem. This research indicated that this can be achieved by eliminating the GE-triggering mortar admixtures, and finding an inert substitute is hence a necessary and final step. The tested superplasticizer yielded promising results in the benchmarking tests, but showed unsatisfactory results in combination with cement paste due to an interaction effect. While the lack of reducing effect on surface tension explains no GE triggering effect in the benchmarking tests, this also results in no air-entraining capability. Such superplasticizer products cannot hence substitute the air-entraining agents, which have a beneficial effect on the freeze-thaw resistance of cement mortar.

In this exploratory study four (surfactant-based) commercial admixtures were tested. Their composition was not known, while as an initial attempt their concentration during the test was increased three fold due to a general practice of admixture overdosing at the construction site. In the next step a more systematic approach should be implemented to investigate the effect of composition and concentration on the GE risk. A molecule of surfactant is composed of the polar head and the nonpolar tail, and the former may play an important role in triggering GE formation. Surfactants may induce crystallisation at the liquid-air interface and a critical parameter in this process is the compatibility between certain crystal faces and the arrangement of surfactant's polar groups at the interface (Canselier, 1993). It would then be worth focusing on investigating how the GE triggering effect depends on the charge (anionic, cationic, non-ionic) and type (e.g. carboxylate COO^-, sulphonate SO_2O^-) of the surfactant's polar group (Ramachandran, 1995). This could be possibly realised in a similar way as the admixture benchmarking test (Section 7.5.1), by applying ATM method to a solutions of gypsum and selected surfactants.

Alternatively, the desired workability of mortar could possibly also be achieved by formulating a cement-lime mortar without the need for air-entrainer addition (Tate and Thomson, 2001). Moreover, lime, besides providing good plasticity to the mix, may as well inhibit ettringite decomposition and thus gypsum formation in the mortar joint (Brocken *et al.*, 2000). One needs to remember though, that a masonry mortar, besides providing GE free masonry, should also respect a number of mechanical requirements defined in European and national normatives.

93

Carbonation duration

The ATM test duration has been shortened significantly, but still it takes four months when applied to the evaluation of carbonated cement paste. It stems from the long duration required for cement paste curing (28d) and cement paste carbonation (70d). The latter could possibly be accelerated by further reducing the grain size of the cement paste powder (0.5-2mm in this project), but this on other hand may bring a risk of insufficient powder permeability (for CO_2) and thus uneven carbonation progress. The alternative approach could be to realise the carbonation phase on mortar grains instead of cement paste, which are characterised by a higher and coarser porosity, and thus should possibly carbonate more effectively.

9 Appendices

9.1 Appendices

9.1.1 Appendix A: Repeatability

Table 9.1 shows the results of repeated analyses performed on hydrated cement samples subjected to the same duration of carbonation test. The cement paste grains were separately sampled and prepared for each analysis. The results show that the amounts of CH and water soluble sulphate were determined with a very high repeatability (RSD=1-2%). On the other hand, the QPA results for AFm were markedly less repeatable (RSD at 22% and 77%), what was likely attributed to their content being at the edge of the detection limit. The QPA results for the AFT showed also increased variability (RSD at 6% and 22%). Both AFt and AFm phases are particularly sensitive to the sample preparation conditions: drying, grinding and storage (Snellings, 2016), what may explain the observed variation.

Table 9.1 Results of the repeatability analysis. For convenience, the monosulphate and ettringite names are shortened to their respective mineral group names: AFm and AFt. Minerals' content is expressed in g/100g anhydrous, while the extracted water soluble SO_4^{2-} in mmol/100g anhydrous. Next to the average a standard deviation (SD) and a relative standard deviation (RSD) is calculated. NA stands for not analysed.

Sample	AFt (QPA)	AFm (QPA)	CH (TG)	SO_4^{2-} (ICP-OES)
CEM I 0d	3.06	0.55	12.81	NA
CEM I 0d	3.25	0.40	13.22	NA
CEM I 0d	4.51	0.37	12.71	NA
Average	**3.61**	**0.44**	**12.91**	-
SD	**0.79**	**0.09**	**0.27**	-
RSD	**22%**	**22%**	**2%**	-
CEM I 18d	4.79	0.29	6.89	NA
CEM I 18d	4.41	0.04	6.89	NA
CEM I 18d	4.32	0.19	6.79	NA
Average	**4.51**	**0.18**	**6.86**	-
SD	**0.25**	**0.12**	**0.05**	-
RSD	**6%**	**70%**	**1%**	-
CEM I 155d	NA	NA	NA	13.72
CEM I 155d	NA	NA	NA	13.88
CEM I 155d	NA	NA	NA	14.05
Average	**-**	**-**	**-**	**13.88**
SD	**-**	**-**	**-**	**0.17**
RSD	**-**	**-**	**-**	**1%**

9.1.2 Appendix B: Summary of initial and final DR, and final %E

The scatter graphs below (Figure 9.1 and Figure 9.2) summarize the key parameters: the initial and final DRs, and the final %E values, displaying the parameter's value for each individual setup. The arrows indicate outlier cases, which are further addressed in the '9.1.3 Appendix C: ATM outliers' appendix.
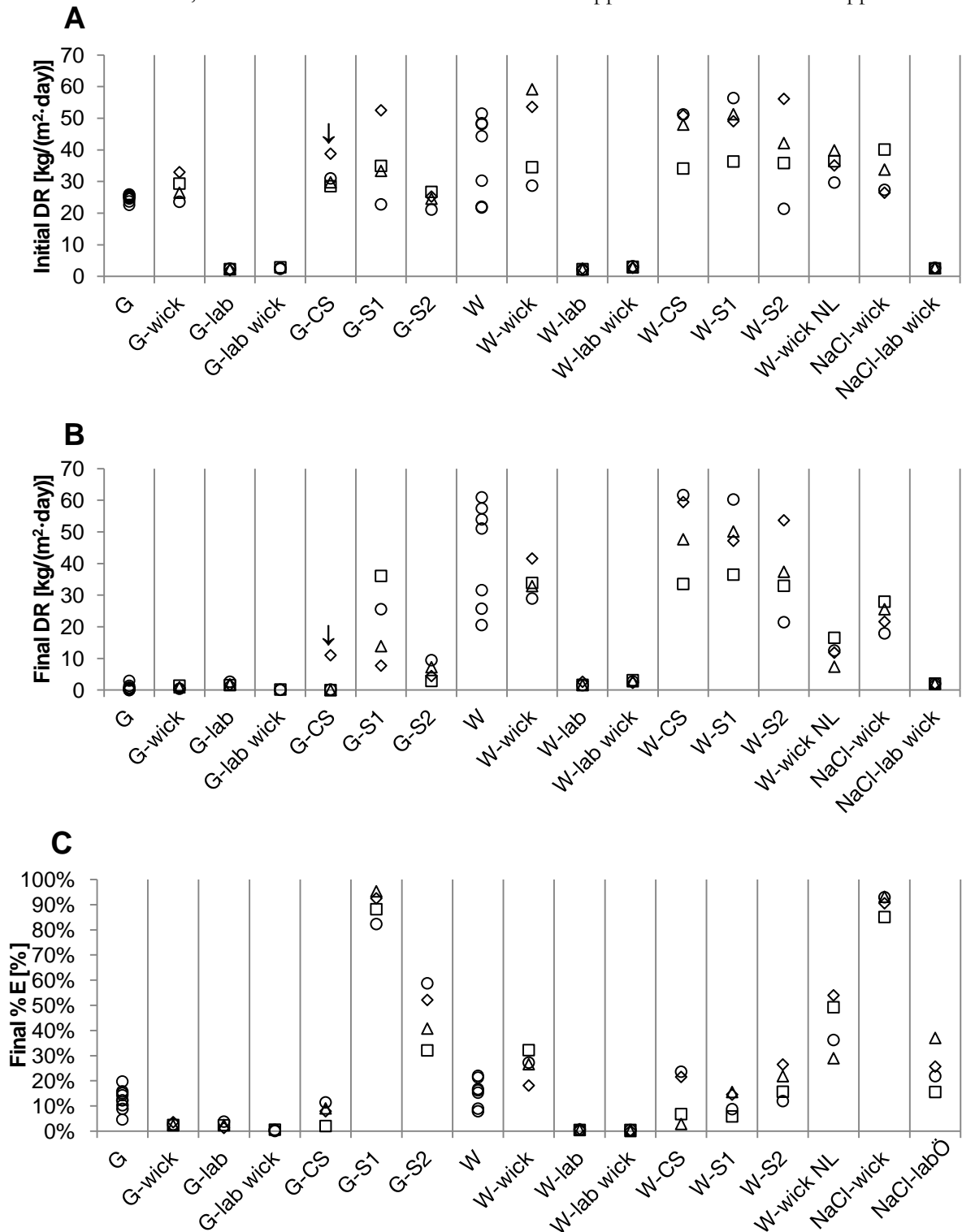

Figure 9.1   A comparison of the initial (A) and the final drying rates (B), and the final efflorescence coverage (C). The arrows indicate an outlier case.
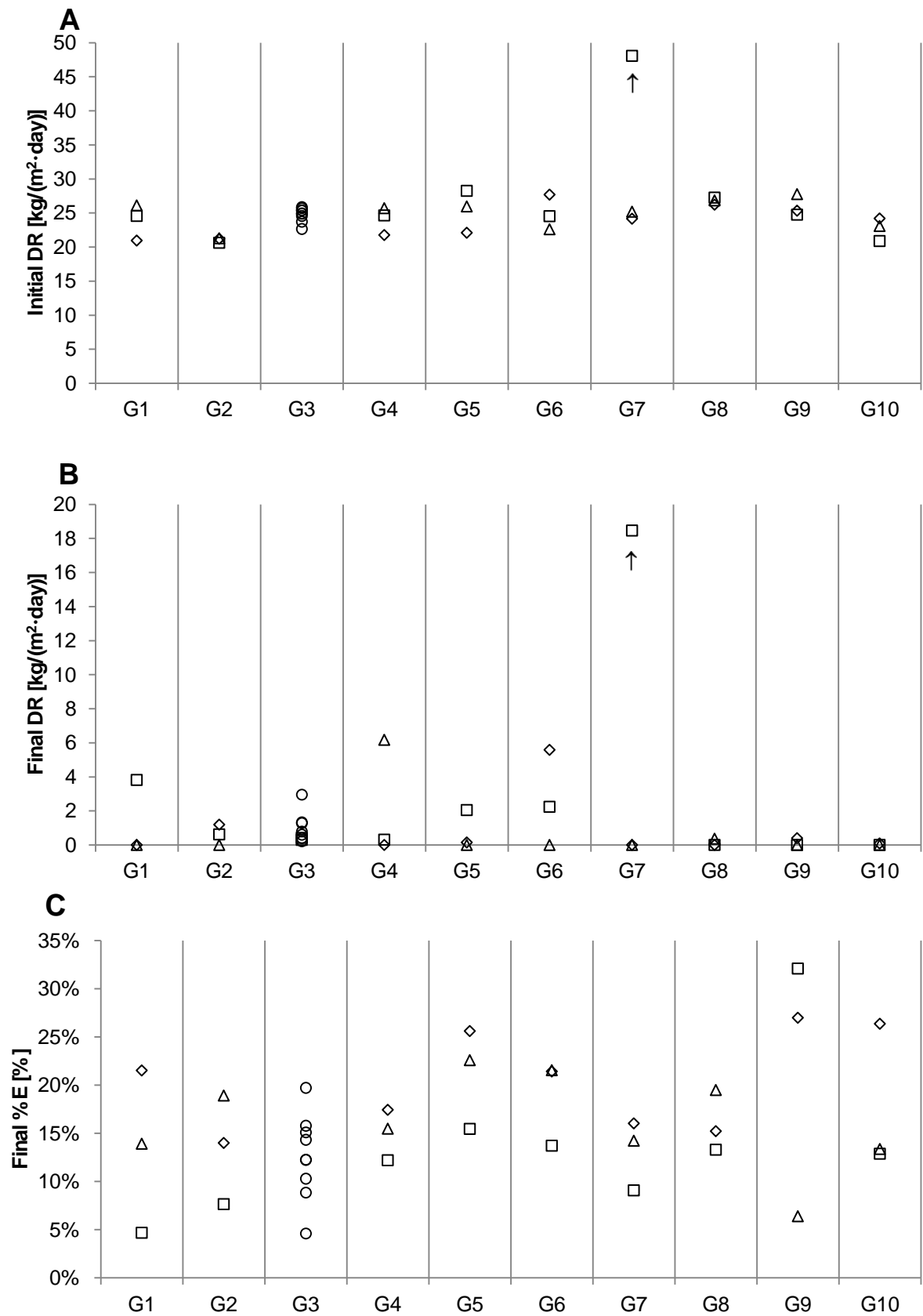
Figure 9.2   A comparison of the initial (A) and the final drying rates (B), and the final efflorescence coverage (C) for the effect of location study. The arrows indicate an outlier case.

9.1.3 Appendix C: ATM outliers

The drying rate evolution plots for the G-CS 58 and G7-25 setups showed a major deviation from the behaviour of other setups from the same set, see the dashed line plot in Figure 9.3 A and Figure 9.4 A, respectively. This was likely attributed to the setup's leakage. The two results were hence regarded as outliers. Nevertheless, the efflorescence evolution (Figure 9.3 B and Figure 9.4 B) appeared to be not affected by the leakage and therefore it was considered as a valid result.
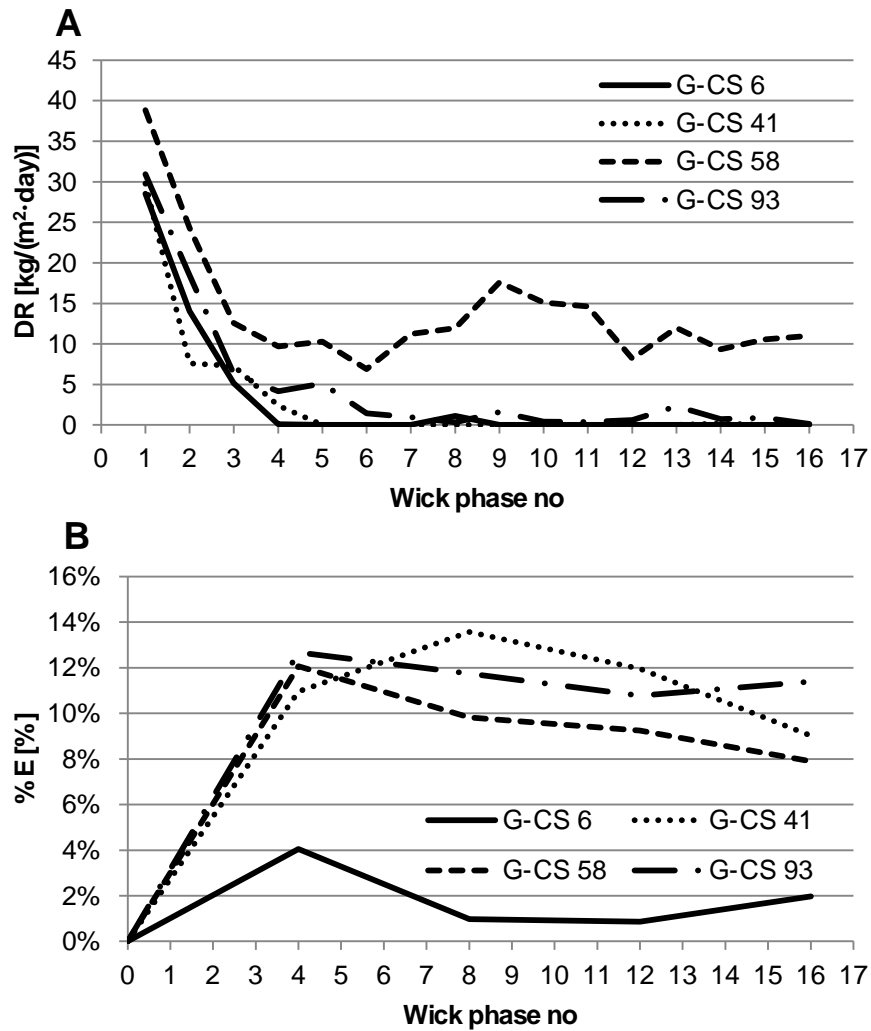

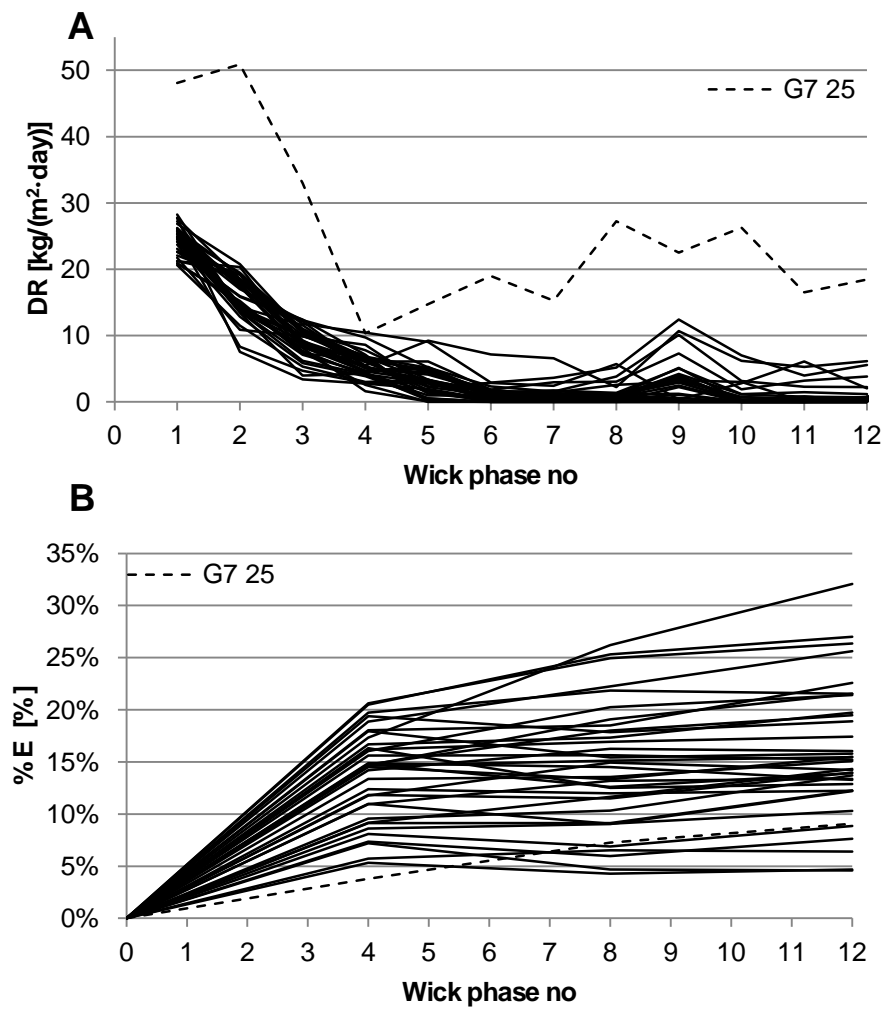Figure 9.3 The drying rate (A) and the efflorescence coverage (B) evolutions for the G-CS setups.

Figure 9.4   The drying rate (A) and the efflorescence coverage (B) plots for the G1-9 setups (the effect of location study).

9.2 Bibliography

Allman, R., 1977. "Refinement of the Hybrid Layer Structure (Ca2Al(OH)6)+ (0.5SO4·3H2O)–."*Neues Jahrbuch Für Mineralogie Monatshefte* 4: 136–44.

Anstice, D.J., 2000. "Corrosion Inhibitors for the Rehabilitation of Reinforced Concrete." Ph.D. thesis, Aston University.

Anstice, D.J., Page C.L., Page M.M., 2005. "The Pore Solution Phase of Carbonated Cement Pastes." *Cement and Concrete Research* 35 (2): 377–83. doi:10.1016/j.cemconres.2004.06.041.

ASTM C67-07, 2007. "ASTM C67-07 Standard Test Methods for Sampling and Testing Brick and Structural Clay Tile."

Badens, E., Veesler, S., Boistelle, R., 1999. "Crystallization of Gypsum from Hemihydrate in Presence of Additives." *Journal of Crystal Growth* 198–199, Part 1 (0): 704–9. doi:10.1016/S0022-0248(98)01206-8.

Barozzi, G. S., Angeli, D., 2014. "A Note on Capillary Rise in Tubes" *Energy Procedia* 45, 548–557.

Bettzieche, H., 1994. "Influence of Cements and Ready-Mixed Mortars on the Efflorescence of Fairfaced Masonry = Einfluss von Zementen Und Fertigmörteln Auf Die Ausblühungen von Sichtmauerwerk." *ZI International* 47 (6): 397–408.

Boeyens, J.C.A., Ichharam, V.V.H., 2002. "Redetermination of the Crystal Structure of Calcium Sulphate Dihydrate, CaSO4·2H2O." *Zeitschrift Für Kristallographie - New Crystal Structures* 217 (JG). doi:10.1524/ncrs.2002.217.jg.9.

Bowler, G.K., Fisher, K., 1989. "Soluble Salt Analysis and Indexation of Sulphation Risk." *Masonry International - Journal of the British Masonry Society* 3 (2): 62–67.

Bowler, G.K., Sharp, R.H., 1998. "Testing of Various Brick/Mortar Combinations for Mortar Durability, Efflorescence Potential and Resistance to Rain Penetration." *Proc Br Masonry Soc*, 8:31–36.

Bowler, G.K., Winter, N.B., 1996. "New Form of Salt Staining on External Masonry." *British Ceramic Transactions* 95 (2): 82–86.

Bowler, G.K., Winter, N.B., 1997. "Investigation into Causes of Persistent Efflorescence on Masonry." *Masonry International* 11 (1): 15–18.

Brocken, H., Nijland, T.G., 2004. "White Efflorescence on Brick Masonry and Concrete Masonry Blocks, with Special Emphasis on Sulfate Efflorescence on Concrete Blocks." *Construction and Building Materials* 18 (5): 315–23. doi:16/j.conbuildmat.2004.02.004.

Brocken, H.J.P., van der Pers, N.M., Larbi, J.A., 2000. "Composition of Lime-Cement and Air-Entrained Cement Mortar as a Function of Distance to the Brick-Mortar Interface: Consequences for Masonry." *Materials and Structures* 33 (10): 634–46. doi:10.1007/BF02480603.

BS 3921:1985, 1985. "BS 3921:1985 British Standard Specification for Clay Bricks", *British Standards Institution*

Buck, A.L., 1981. "New Equations for Computing Vapor Pressure and Enhancement Factor." *Journal of Applied Meteorology* 20 (12): 1527–32.

Bueger, C., de Barquin, F., Malengreau, N., Tirlocq, J., 2005. "Efflorescence on Clay Bricks Masonry: Towards a New Test Method." *10DBMC International Conference On Durability of Building Materials and Components,* Lyon

Butterworth, B., 1957. "Efflorescence and Staining of Brickwork." *The Brick Bulletin* 3 (5): 3–10.

Canselier, J.P., 1993. "The effects of surfactants on crystallization phenomena" *Journal of Dispersion Science and Technology* 14 (6): 625–44. doi:10.1080/01932699308943435.

Cardell, C., Benavente, D., Rodríguez-Gordillo, J., 2008. "Weathering of Limestone Building Material by Mixed Sulfate Solutions. Characterization of Stone Microstructure, Reaction Products and Decay Forms." *Materials Characterization* 59 (10): 1371–85. doi:10.1016/j.matchar.2007.12.003.

Caspi, E.N., Pokroy, B., Lee, P.L., Quintana, J.P., Zolotoyabko, E., 2005. "On the Structure of Aragonite." *Acta Crystallographica Section B Structural Science* 61 (2): 129–32. doi:10.1107/S0108768105005240.

Chaix-Pluchery, O., Pannetier, J., Bouillot, J., Niepce, J.C., 1987. "Structural Prereactional Transformations in Ca(OH)2." *Journal of Solid State Chemistry* 67 (2): 225–34. doi:10.1016/0022-4596(87)90358-6.

Charola, A.E., Centeno, S.A., 2002. "Analysis of Gypsum-Containing Lime Mortars: Possible Errors Due to the Use of Different Drying Conditions." *Journal of the American Institute for Conservation* 41 (3): 269–78. doi:10.2307/3179923.

Charola, A.E., Pühringer, J., Steiger, M., 2006. "Gypsum: A Review of Its Role in the Deterioration of Building Materials." *Environmental Geology* 52 (2): 339–52. doi:10.1007/s00254-006-0566-9.

Cheng, G.C.H., Zussman, J., 1963. "The Crystal Structure of Anhydrite (CaSO₄)." *Acta Crystallographica* 16 (8): 767–69. doi:10.1107/S0365110X63001997.

Chin, I.R., Behie, B., 2010. "Efflorescence: Evaluation of Published Test Methods for Brick and Efforts to Develop a Masonry Assembly Test Method." In *Symposium on Masonry*, edited by J. Farny and W.L. Behie, 3-3–11. 100 Barr Harbor Drive, PO Box C700, West Conshohocken, PA 19428-2959: ASTM International.

Conley, R., Bundy, W., 1958. Mechanism of gypsification. *Geochimica et Cosmochimica Acta* 15, 57–72.

CSTC, 2009. "Spécifications Européennes Sur La Résistance En Compression Des Produits de Maçonnerie (N° 4/2009 – Cahier N° 3)." Les Dossiers du CSTC. http://www.cstc.be/homepage/download.cfm?dtype=publ&doc=cstc_artonline_2009_4_no3.pdf&lang=fr [Accessed 14 March 2017].

Derluyn, H., Janssen, H., Carmeliet, J., 2011. "Influence of the Nature of Interfaces on the Capillary Transport in Layered Materials." *Construction and Building Materials* 25 (9): 3685–93. doi:10.1016/j.conbuildmat.2011.03.063.

Dollase, W.A., 1986. "Correction of Intensities for Preferred Orientation in Powder Diffractometry: Application of the March Model." *Journal of Applied Crystallography* 19 (4): 267–72. doi:10.1107/S0021889886089458.

Dow, C., Glasser, F.P., 2003. "Calcium Carbonate Efflorescence on Portland Cement and Building Materials." *Cement and Concrete Research* 33 (1): 147–54. doi:10.1016/S0008-8846(02)00937-7.

Dransfield, J., 2007. "Leaching of admixtures from concrete." *UK Cement Admixtures Association Admixtures Environmental Sheet.*

Eloukabi, H., Sghaier, N., Ben Nasrallah, S., Prat, M., 2013. "Experimental Study of the Effect of Sodium Chloride on Drying of Porous Media: The Crusty–patchy Efflorescence Transition." *International Journal of Heat and Mass Transfer* 56 (1–2): 80–93. doi:10.1016/j.ijheatmasstransfer.2012.09.045.

EN 771-1, 2011. "Specification for Masonry Units - Part 1: Clay Masonry Units." *European Committee for Standardization*

EN 772-5, 2002. "Methods of Test for Masonry Units - Part 5: Determination of the Active Soluble Salts Content of Clay Masonry Units." *European Committee for Standardization*

EN 772-11, 2000. "Methods of Test for Masonry Units - Part 11: Determination of Water Absorption of Aggregate Concrete, Manufactured Stone and Natural Stone Masonry Units due to Capillary Action and the Initial Rate of Water Absorption of Clay Masonry Units." *European Committee for Standardization*

Espinosa-Marzal, R.M., Scherer, G.W., 2010. "Mechanisms of Damage by Salt." *Geological Society, London, Special Publications* 331 (1): 61–77. doi:10.1144/SP331.5.

François, M., Renaudin, G., Evrard, O., 1998. "A Cementitious Compound with Composition $3CaO.Al_2O_3.CaCO_3.11H_2O$." *Acta Crystallographica Section C Crystal Structure Communications* 54 (9): 1214–17. doi:10.1107/S0108270198004223.

Franke, L., Grabau, J., 1994. "Transport of Salt Solutions in Brickwork." In *Conservation of Historic Brick Structures*, Baer N. S., Fitz S, Livingston R.A., 167–72. Donhead.

Franke, L., Grabau, J., 1998. "Influence of Salt Content on the Drying Behavior of Brick." In *Conservation of Historic Brick Structures*, Baer N. S., Fitz S, Livingston R.A., 59–68. Donhead.

Franke, L., Schumann, I., 1998. "Causes and Mechanisms of the Decay of Historic Brick Buildings in Northern Germany." In *Conservation of Historic Brick Structures*, Baer N. S., Fitz S, Livingston R.A., 25–34. Donhead.

Freyer, D., Voigt, W., 2003. "Crystallization and Phase Stability of CaSO4 and CaSO4 – Based Salts." *Monatshefte Für Chemie / Chemical Monthly* 134 (5): 693–719. doi:10.1007/s00706-003-0590-3.

Fu, Y., Xie, P., Gu, P., Beaudoin, J. J., 1994. "Effect of temperature on sulphate adsorption/desorption by tricalcium silicate hydrates." *Cement and Concrete Research* 24, 1428–1432.

Gabrisová, A., Havlica, J., Sahu, S., 1991. "Stability of Calcium Sulphoaluminate Hydrates in Water Solutions with Various pH Values." *Cement and Concrete Research* 21 (6): 1023–27. doi:10.1016/0008-8846(91)90062-M.

Garrabrants, A.C., Sanchez, F., Kosson, D.S., 2004. "Changes in Constituent Equilibrium Leaching and Pore Water Characteristics of a Portland Cement Mortar as a Result of Carbonation." *Waste Management* 24 (1): 19–36. doi:10.1016/S0956-053X(03)00135-1.

Ghosh, S. N., 2003. *Advances in Cement Technology: Chemistry, Manufacture and Testing*. CRC Press.

Goetz-Neunhoeffer, F., Neubauer, J., 2006. "Refined Ettringite $(Ca_6Al_2(SO_4)_3(OH)_{12}\cdot26H_2O)$ Structure for Quantitative X-Ray Diffraction Analysis." *Powder Diffraction* 21 (01): 4–11. doi:10.1154/1.2146207.

Goudie, A.S., 1986. "Laboratory Simulation of 'the Wick Effect' in Salt Weathering of Rock." *Earth Surface Processes and Landforms* 11 (3): 275–85. doi:10.1002/esp.3290110305.

Grounds, T., Midgley, H.G., Novell, D.V., 1988. "Carbonation of Ettringite by Atmospheric Carbon Dioxide." *Thermochimica Acta* 135: 347–52. doi:10.1016/0040-6031(88)87407-0.

Hendrickx, R., 2009. "The Adequate Measurement of the Workability of Masonry Mortar." Ph.D. thesis, KU Leuven.

Hewlett, P., 2004. *Lea's Chemistry of Cement and Concrete, Fourth Edition*. 4th ed. Butterworth-Heinemann.

Holcim Belgique S.A., 2010. "Guide Du Macon Holcim Ciment Belgique." http://www.holcim.be/uploads/BE/Guide_du_Macon_Holcim_Ciment_Belgique.pdf [Accessed 14 March 2017].

Janssen, H., Blocken, B., Roels, S., Carmeliet, J., 2007. "Wind-driven rain as a boundary condition for HAM simulations: Analysis of simplified modelling approaches." *Building and Environment* 42, 1555–1567.

Jeschke, A.A., Dreybrodt, W., 2002. "Pitfalls in the Determination of Empirical Dissolution Rate Equations of Minerals from Experimental Data and a Way out: An Iterative Procedure to Find Valid Rate Equations, Applied to Ca-Carbonates and -Sulphates." *Chemical Geology* 192 (3–4): 183–94. doi:10.1016/S0009-2541(02)00135-3.

Kamhi, S.R., 1963. "On the Structure of Vaterite CaCO3." *Acta Crystallographica* 16 (8): 770–72. doi:10.1107/S0365110X63002000.

Kindrick, R.H., Harrison, B.C., 1980. Extended $BaCO_3$ for brick scum prevention. 4226635, filed June 4, 1979, and issued 1980.

Kraus, K., Droll, K., 2009. "Investigations of Soluble Salt Contents in Modern Hydraulic Lime Mortars - Test Method and First Results.", 207–13. http://www.rilem.org/images/publis/pro067-019.pdf [Accessed 14 March 2017].

Kumar, R., Bhattacharjee, B., 2003. "Porosity, Pore Size Distribution and in Situ Strength of Concrete." *Cement and Concrete Research* 33 (1): 155–64. doi:10.1016/S0008-8846(02)00942-0.

Kuntze, R.A., 2008. "4. Basic Properties." In *Gypsum: Connecting Science and Technology*, 23–36. R. A. K. Associates.

Kuzel, H.J., Pöllmann, H., 1991. "Hydration of C3A in the Presence of $Ca(OH)_2$, $CaSO_4 \cdot 2H_2O$ and $CaCO_3$." *Cement and Concrete Research* 21 (5): 885–95. doi:10.1016/0008-8846(91)90183-I.

Le Page, Y., Donnay, G., 1976. "Refinement of the Crystal Structure of Low-Quartz." *Acta Crystallographica Section B Structural Crystallography and Crystal Chemistry* 32 (8): 2456–59. doi:10.1107/S0567740876007966.

Lothenbach, B., Durdziński, P., De Weerdt, K., 2016. "Thermogravimetric Analysis." *A Practical Guide to Microstructural Analysis of Cementitious Materials*, 177-212.

Lubelli, B., Van Hees R.P.J., Nijland, T.G., 2014. "Salt Crystallization Damage: How Realistic Are Existing Ageing Tests?" In *AMS 2014: 1st International Conference on Ageing of Materials and Structures, Delft, The Netherlands, 26-28 May 2014*. DCMat Ageing Center.

MacGregor Miller, F., Melander, M.J., 2003. "Efflorescence - a Synopsis of the Literature." In *Proceedings, the Ninth North American Masonry Conference*, 11–24. Masonry Society.

Maslen, E.N., Streltsov, V.A., Streltsova, N.R., 1993. "X-Ray Study of the Electron Density in Calcite, $CaCO_3$." *Acta Crystallographica Section B Structural Science* 49 (4): 636–41. doi:10.1107/S0108768193002575.

McPolin, D., Basheer, P., Long, A., 2009. "Carbonation and pH in Mortars Manufactured with Supplementary Cementitious Materials." *Journal of Materials in Civil Engineering* 21 (5): 217–25. doi:10.1061/(ASCE)0899-1561(2009)21:5(217).

Mertens, G., 2009. "Characterisation of Historical Mortars and Mineralogical Study of the Physico-Chemical Reactions on the Pozzolan-Lime Binder Interface.", Ph.D. thesis, KU Leuven.

Middendorf, B., Budelmann, H., 1995. "Effects of Different Additives on Microstructural Development in Gypsum Based Building Materials." *Proc. 5th Euroseminar Microscopy Applied to Building Materials, (ed. J. Elsen), Leuven, Belgium*, 40–48.

Montagnino, D., Costa, E., Massaro, F.R., Artioli, G., Aquilano, D., 2011. "Growth Morphology of Gypsum in the Presence of Copolymers." *Crystal Research and Technology* 46 (10): 1010–1018. doi:10.1002/crat.201100131.

Mosquet, M., 2003. "Domieszki nowej generacji [The admixtures of new generation]", Budownictwo Technologie Architektura [Civil Engineering Technology Architecture] Special Issue: 21—23.

Mumme, W., Hill, R., Bushnellwye, G., Segnit, E., 1995. "Rietveld Crystal-Structure Refinements, Crystal-Chemistry and Calculated Powder Diffraction Data for the Polymorphs of Dicalcium Silicate and Related Phases." *Neues Jahrbuch Fur Mineralogie-Abhandlungen* 169 (1): 35–68.

Myneni, S.C.B., Traina, S.J., Logan, T.J., 1998. "Ettringite Solubility and Geochemistry of the $Ca(OH)_2$–$Al_2(SO_4)_3$–H_2O System at 1 Atm Pressure and 298 K." *Chemical Geology* 148 (1–2): 1–19. doi:10.1016/S0009-2541(97)00128-9.

Nachshon, U., Weisbrod, N., Dragila, M.I., Grader, A., 2011. "Combined Evaporation and Salt Precipitation in Homogeneous and Heterogeneous Porous Media." *Water Resources Research* 47 (3): W03513. doi:10.1029/2010WR009677.

Nishi, F., Takéuchi, Y., 1975. "The $A_{16}O_{18}$ Rings of Tetrahedra in the Structure of $Ca_{8.5}NaAl_6O_{18}$." *Acta Crystallographica Section B Structural Crystallography and Crystal Chemistry* 31 (4): 1169–73. doi:10.1107/S0567740875004736.

Nishikawa, T., Suzuki, K., Ito, S., Sato, K., Takebe, T., 1992. "Decomposition of Synthesized Ettringite by Carbonation." *Cement and Concrete Research* 22 (1): 6–14. doi:10.1016/0008-8846(92)90130-N.

Noirfontaine, M.N., Courtial, M., Dunstetter, F., Gasecki, G., Signes-Frehel, M., 2011. "Tricalcium Silicate Ca_3SiO_5 Superstructure Analysis: A Route towards the Structure of the M1 Polymorph." *Zeitschrift Für Kristallographie Crystalline Materials* 227 (2): 102–112. doi:10.1524/zkri.2012.1425.

Pade, C., Guimaraes, M., 2007. "The CO_2 Uptake of Concrete in a 100 Year Perspective." *Cement and Concrete Research* 37 (9): 1348–56. doi:10.1016/j.cemconres.2007.06.009.

Pagé, M., 2003. Superplasticizers for Concrete: Fundamentals, Technology, and Practice., Supplementary Cementing Materials for Sustainable Development, Incorporated.

Pajares, I., Martinez-Ramirez, S., Blanco-Varela, M.T., 2003. "Evolution of Ettringite in Presence of Carbonate, and Silicate Ions." *Cement and Concrete Composites* 25 (8): 861–65. doi:10.1016/S0958-9465(03)00113-6.

Parrott, L. J., 1987. *A Review of Carbonation in Reinforced Concrete*. Cement and Concrete Association.

Ramachandran, V. S., 1995. "Concrete Admixtures Handbook: Properties, Science, and Technology.", Elsevier Science Limited.

Redhammer, G., Tippelt, G., Roth, G., Amthauer, G., 2004. "Structural Variations in the Brownmillerite Series $Ca_2(Fe_2{-}xAl_x)O_5$: Single-Crystal X-Ray Diffraction at 25°C and High-Temperature X-Ray Powder Diffraction (25°C ≤ T ≤ 1000°C)." *American Mineralogist* 89 (2–3): 405–20. doi:10.2138/am-2004-2-322.

Renaudin, G., Filinchuk, Y., Neubauer, J., Goetz-Neunhoeffer, F., 2010. "A Comparative Structural Study of Wet and Dried Ettringite." *Cement and Concrete Research* 40 (3): 370–75. doi:10.1016/j.cemconres.2009.11.002.

Rodriguez-Navarro, C., Doehne, E., 1999. "Salt Weathering: Influence of Evaporation Rate, Supersaturation and Crystallization Pattern." *Earth Surface Processes and Landforms* 24 (3): 191–209.

Rodriguez-Navarro, C., Doehne, E., Sebastian, E., 2000. "Influencing Crystallization Damage in Porous Materials through the Use of Surfactants: Experimental Results Using Sodium Dodecyl Sulfate and Cetyldimethylbenzylammonium Chloride." *Langmuir* 16 (3): 947–54. doi:10.1021/la990580h.

Runčevski, T., Dinnebier, R.E., Magdysyuk, O.V., Pöllmann, H., 2012. "Crystal Structures of Calcium Hemicarboaluminate and Carbonated Calcium Hemicarboaluminate from Synchrotron Powder Diffraction Data." *Acta Crystallographica Section B Structural Science* 68 (5): 493–500. doi:10.1107/S010876811203042X.

Sanders, J.P., Brosnan, D.A., 2010. "Test Method for Determining the Efflorescence Potential of Masonry Materials Based on Soluble Salt Content." In *Symposium on Masonry*, edited by J. Farny and W.L. Behie, PA 19428-2959: ASTM.

Šavija, B., Luković, M., 2016. "Carbonation of Cement Paste: Understanding, Challenges, and Opportunities." *Construction and Building Materials* 117 (August): 285–301. doi:10.1016/j.conbuildmat.2016.04.138.

Scherer, G.W., 2004. "Stress from Crystallization of Salt." *Cement and Concrete Research*, H. F. W. Taylor Commemorative Issue, 34 (9): 1613–24. doi:10.1016/j.cemconres.2003.12.034.

Seck, M.D., Van Landeghem, M., Faure, P., Rodts, S., Combes, R., Cavalié, P., Keita, E., Coussot, P., 2015. "The Mechanisms of Plaster Drying." *Journal of Materials Science*, January, 1–11. doi:10.1007/s10853-014-8807-x.

Shahidzadeh-Bonn, N., Rafaï, S., Bonn, D., Wegdam, G., 2008. Salt Crystallization during Evaporation: Impact of Interfacial Properties. *Langmuir* 24, 8599–8605.

Singh, N. B., 2005. The Activation Effect of K_2SO_4 on the Hydration of Gypsum Anhydrite, $CaSO_4(II)$. *Journal of the American Ceramic Society* 88, 196–201.

Škapa, R., 2009. "Optimum Sulfate Content of Portland Cement." Ph.D. thesis, Aberdeen University.

Snellings, R., Mertens, G., Elsen, J., 2012. "Supplementary Cementitious Materials." *Reviews in Mineralogy and Geochemistry* 74 (1): 211–78. doi:10.2138/rmg.2012.74.6.

Snellings, R., 2016. "X-Ray Powder Diffraction Applied to Cement." *A Practical Guide to Microstructural Analysis of Cementitious Materials*, 107.

Snethlage, R., Wendler, E., 1997. "Moisture Cycles and Sandstone Degradation.". Baer NS, Saving Our Architectural Heritage: The Conservation of Historic Stone Structures. Report of Dahlem workshop, Berlin, 3-8 March 1996. Wiley, Chichester, New York, 7-24

Spence, R.D. 1992. *Chemistry and Microstructure of Solidified Waste Forms*. CRC Press.

Steiger, M., Asmussen, S., 2008. "Crystallization of Sodium Sulfate Phases in Porous Materials: The Phase Diagram Na_2SO_4–H_2O and the Generation of Stress." *Geochimica et Cosmochimica Acta* 72 (17): 4291–4306. doi:10.1016/j.gca.2008.05.053.

Steiger, M., Charola, A.E., Sterflinger, K., 2011. "Weathering and Deterioration." In *Stone in Architecture*, edited by S. Siegesmund and R. Snethlage, 227–316. Berlin, Heidelberg: Springer Berlin Heidelberg.

Steiger, M., Heritage, A., 2012. "Modelling the crystallisation behaviour of mixed salt systems: input data requirements." In *12th International Congress on the Deterioration and Conservation of Stone,* New York

Tate, M., Thomson, M., 2001. "Effect of air entrainment on freeze-thaw durability of type S Portland cement-lime masonry mortars." In *Proc. 9th Canadian masonry Symposium*. Canada

Taylor, H.F.W., 1997. *Cement Chemistry*. Thomas Telford.

Todorović, J., Janssen, H., 2014. "Numerical Simulation of Gypsum Transport and Crystallization." In *Proceedings of SWBSS 2014*, 133–49. Brussels, Belgium. doi:10.5165/hawk-hhg/273.

Todorović, J., Janssen, H., 2016. "Impact of Gypsum Pore Clogging on Moisture Transfer Properties of Bricks." In *Proceedings of the CESBP Central European Symposium on Building Physics and BauSIM 2016*. https://lirias.kuleuven.be/handle/123456789/550239.

Tsamatsoulis, D., Nikolakakos, N., 2013. "Optimizing the Sulphates Content of Cement Using Multivariable Modelling and Uncertainty Analysis." *Chemical and Biochemical Engineering Quarterly* 27 (2): 133–144.

Veran-Tissoires, S., Marcoux, M., Prat, M., 2012. "Discrete Salt Crystallization at the Surface of a Porous Medium." *Physical Review Letters* 108 (5): 054502-1–4. doi:10.1103/PhysRevLett.108.054502.

Vogt, R., Tatarin, A., 2013. "Lime Spalls and Efflorescence from Lime and Gypsum on Heavy Clay Products." *Ziegelindustrie International*, no. 7–8: 29–41.

Xiantuo, C., Ruizhen, Z., Xiaorong, C., 1994. "Kinetic Study of Ettringite Carbonation Reaction." *Cement and Concrete Research* 24 (7): 1383–89. doi:10.1016/0008-8846(94)90123-6.

Zhang, J., Scherer, G.W., 2011. "Comparison of Methods for Arresting Hydration of Cement." *Cement and Concrete Research* 41 (10): 1024–36. doi:10.1016/j.cemconres.2011.06.003.